NEXT-GENERATION HUMANIZED MOUSE MODELS OF HIV AND TB

DEVELOPING AND UTILIZING A NEXT-GENERATION HUMANIZED MOUSE MODEL FOR INVESTIGATING HIV AND TUBERCULOSIS

By MADELEINE LEPARD, B.Sc. (Hons)

A Thesis Submitted to the School of Graduate Studies in Partial Fulfilment of the Requirements for the Degree of Master of Sciences

McMaster University MASTER OF SCIENCES (2022) Hamilton, Ontario (Infection & Immunity)

TITLE: Developing and Utilizing a Next-Generation Humanized Mouse Model for Investigating HIV and Tuberculosis AUTHOR: Madeleine Lepard, B.Sc. (Hons) (McMaster University) SUPERVISOR: Dr. Amy Gillgrass NUMBER OF PAGES: xvii, 178

Lay abstract

Human immunodeficiency virus (HIV) and tuberculosis (TB) are infectious diseases that affect millions of people worldwide every year. The greatest cause of death in people living with HIV is co-infection with TB and HIV-positive individuals are much more likely to get TB. Humanized mouse (hu-mouse) models possess human immune cells for HIV to infect and are useful for studying HIV. Our goal is to create hu-mouse models of HIV, TB and HIV/TB co-infection that will allow us to study how these diseases interact. We are currently developing a traditional hu-mouse model (known as NRG), as well as an improved next-generation model (known as DRAG-A2) with a more functional immune system. Both models have been successfully infected with HIV or TB. Only DRAG-A2 mice were able to make antibodies against HIV. The improved DRAG-A2 model will enable future studies on HIV, TB and co-infection, which continue to be understudied global problems.

Abstract

Currently, there are 38 million people living with human immunodeficiency virus (HIV-1) worldwide and there were 680,000 HIV-related deaths in 2020 alone. The greatest cause of mortality in people living with HIV (PLHIV) is infection with opportunistic pathogens such as tuberculosis (TB), which accounts for one third of HIV-related deaths. PLHIV are 20 times more susceptible to TB and co-infection leads to significantly worsened outcomes in terms of both diseases. Humanized mouse (hu-mouse) models, which possess human immune cells for HIV to infect, have been useful for HIV research. Our aim is to create hu-mouse models of HIV, TB and co-infection to investigate disease progression, immune responses, therapeutics, prevention and vaccination. NOD-Rag1^{null}-IL2rg^{null} (NRG) mice are highly immunocompromised mice that are traditionally used to generate hu-mouse models. We are also developing NRG mice that are transgenic for human HLA-DR4 and HLA-A2 (DRAG-A2) and similar mice have been reported to have improved immune responses. NRG and DRAG-A2 mice were humanized with hematopoietic stem cells obtained from human umbilical cord blood. DRAG-A2 mice had significantly higher engraftment success rates (defined as the percentage of mice with >10% hCD45+) as well as higher overall CD45+ leukocyte, CD4+ T cell, CD19+ B cell and CD14+ monocyte reconstitution in the blood compared to huNRGs. huNRG mice were permissive to infection with JR-CSF or NL4.3-Bal-Env HIV-1 intravaginally or systemically. huDRAG-A2 mice were also infected intravaginally with NL4.3-Bal-Env HIV-1. huDRAG-A2 mice, but not huNRGs, produced HIV-specific IgG, indicating improved immune responses. huNRG mice were infected intranasally with mCherry-Erdman, YFP-H37Rv or H37Rv

Mtb. huDRAG-A2 mice were also infected with H37Rv. Human immune cell involvement and human-like granuloma formation was observed using flow cytometry and immunohistopathology. These findings show that the DRAG-A2 model may be optimal for investigating HIV, TB and co-infection, which continue to be serious global health concerns.

Acknowledgements

First and foremost, I would like to thank my supervisor, Dr. Amy Gillgrass, for all her guidance, mentorship and support throughout this process. I am very grateful for her dedication to the lab as a new investigator and her devotion to her students. I would also like to thank my supervisory committee, Drs. Charu Kaushic and Zhou Xing, for their advice, encouragement and expertise in their respective fields. I could not have asked for a better committee for this project. Thank you to Xiaozhi (Jack) Yang for being an amazing assistant in the lab and making day-to-day activities enjoyable. I would also like to thank all those who contributed their expertise to this project: Drs. Ali Ashkar and Fatemeh (Leila) Vahedi for their help optimizing the humanization protocols, Dr. Sam Afkhami for all his help and advice conducting the TB experiments, Dr. Aisha Nazli for all her help with containment level 2+ training and protocols, as well as Anna Zganiacz for her technical support in the containment level 3 facility. And finally, thank you to my family and friends who have supported me the past 2.5 years throughout this challenging process.

Table of Contents

List of Figures

List of Tables

List of Abbreviations

Abbreviation	Definition
A2	NRG transgenic HLA class I A2.1/A*0201
ACK	Ammonium, chloride and potassium
AFB	Acid fast bacillus
Ag	Antigen
AIDS	Acquired immunodeficiency syndrome
APC	Antigen-presenting cells
ART	Antiretroviral therapy
BAL	Bronchoalveolar lavage
BCG	Bacillus Calmette-Guérin
BLT	Bone marrow, liver and thymus
Bp	Base pair
BPaMZ	Bedaquiline, pretomanid, moxifloxacin and pyrazinamide
BPaZ	Bedaquiline, pretomanid and pyrazinamide
BSA	Bovine serum albumin
CCR5 (or R5)	C-C chemokine receptor type 5
CD4	Cluster of differentiation 4
cDNA	Complementary DNA
CFU	Colony forming units
cGy	Centigray
CXCR4 (or X4)	C-X-C chemokine receptor type 4
DEAE-dextran	Diethylaminoethyl dextran
DMEM	Dulbecco's Modified Eagle Medium
DMPA	Depot medroxyprogesterone acetate
DNA	Deoxyribonucleic acid
DRAG	NRG transgenic HLA class II DR4/DRB1*0401
ELISA	Enzyme-linked immunosorbent assay
F1	First generation
F2	Second generation
FBS	Fetal bovine serum
Fc	Fragment, crystallisable
FDA	Food and Drug Administration
FMO	Fluorescence minus one
Gag	Group-specific antigen
GM-CSF	Granulocyte-macrophage colony-stimulating factor
gp120/41	Envelope glycoprotein 120/41
GROα	Growth regulated protein alpha
GvHD	Graft-vs-host disease
H&E	Hematoxylin and eosin
HIV	Human immunodeficiency virus

HIV-1/2	Human immunodeficiency virus type 1/2
HLA	Human leukocyte antigen
HRZE	Isoniazid, rifampicin, pyrazinamide and ethambutol
HSC	Hematopoietic stem cell
huDRAG-A2	Humanized DRAG-A2
Hu-mice	Humanized mice
huNRG	Humanized NRG
IFNγ	Interferon gamma
Ig	Immunoglobulin
IH	Intrahepatic
IHC	Immunohistochemistry
IL-2	Interleukin-2
IP	Intraperitoneal
IP-10	Interferon gamma-induced protein-10
IV	Intravenous
IVAG	Intravaginally
kDa	Kilo-daltons
LTR	Long terminal repeat
MCP-1	Monocyte chemoattractant protein-1
M-CSF	Macrophage colony-stimulating factor
MDC	Macrophage-derived cytokine
MIG/CXCL9	Monokine induced by interferon gamma
MIP-1β	Macrophage inflammatory protein -1 alpha
mRNA	Messenger RNA
Mtb	Mycobacterium tuberculosis
M-tropic	Macrophage-tropic
NHP	Non-human primate
NNRTI	Non-nucleoside reverse transcriptase inhibitor
NO	Nitrous oxide
NOD	Non-obese diabetic
NOD-Scid	NOD-Prkdc-scid
NOG	NOD/Shi-scid IL2rγnull
NRG	NOD-Rag1null-IL2rγnull
NRTI	Nucleoside reverse transcriptase inhibitor
NSG	NOD-scid-IL2rγnull
NtRTI	Nucleotide reverse transcriptase inhibitor
OADC	Oleic acid-albumin-dextrose-catalase
OD	Optimal density
PAMP	Pathogen-associated patterns
PBMC	Peripheral mononuclear cells
PBS	Phosphate buffered saline
PCR	Polymerase chain reaction

PEP	Post-exposure prophylaxis
PFA	Paraformaldehyde
pH	Potential of hydrogen
PI	Positive index
PLHIV	People living with human immunodeficiency virus
Pol	DNA polymerase
PrEP	Pre-exposure prophylaxis
Prkdc	Protein kinase, DNA-activated, catalytic polypeptide
PRR	Pattern recognition receptor
Rag	Recombination-activating gene
RANTES	Regulated on activation, normal T cell expressed and secreted
RBC	Red blood cell
RNA	Ribonucleic acid
ROS	Reactive oxygen species
RPM	Rotations per minute
RPMI	Roswell Park Memorial Institute
RT	Reverse transcriptase
RT-qPCR	Quantitative reverse transcription polymerase chain reaction
sCD40L	Soluble CD40 ligand
Scid	Severe combined immunodeficiency
SHIV	Simian-human immunodeficiency virus
SIPR1α	Signal-regulatory protein alpha
SIV	Simian immunodeficiency virus
TB	Tuberculosis
TB-IRIS	Tuberculosis-associated immune reconstitution inflammatory syndrome
TCID50	Median tissue culture infectious dose
TGF-β	Transforming growth factor beta
Th1	T helper type 1
TNFα	Tumour necrosis factor alpha
T-tropic	T cell-tropic
V(D)J	Variability, diversity and joining
VEGF-A	Vascular endothelial growth factor A
YFP	Yellow fluorescent protein

Declaration of Academic Achievement

I declare that this thesis has been composed by myself and that the work has not be submitted for any other degree or academic qualification. This thesis dissertation was written entirely by myself, with editing input provided by my supervisor, Dr. Amy Gillgrass. I confirm that the work submitted is an accurate representation of the experiments and findings that I have contributed to during my time as a M.Sc. candidate. I confirm that the work is my own, except where work was conducted in collaboration with others, as listed below:

Madeleine Lepard	Mouse breeding, animal monitoring, cord blood processing, humanizing mice, TZMbl assays, HIV-1 infections, sample collection, flow cytometry, RT-qPCR, YFP-H37Rv tissue processing, data analysis, contributed to experimental design
Dr. Amy Gillgrass	Experimental design, initial procedure-specific training, DRAG-A2 TB tissue processing
Xiaozhi (Jack) Yang	Mouse breeding and genotyping, animal monitoring, cord blood processing, HLA typing, humanizing mice, assistance with sample collection, RT-qPCR and flow cytometry
Dr. Sam Afkhami	*Mtb* infections, initial TB tissue processing
Dr. Aisha Nazli	Assistance with RT-qPCR optimization and TZMbl assays
Rhea Jangra	Mouse genotyping

1. INTRODUCTION:

1.1. HIV/AIDS:

1.1.1. A brief introduction to HIV:

Human immunodeficiency virus (HIV), a lentivirus of the retroviridae family, is the cause of acquired immunodeficiency syndrome (AIDS) in humans. This disease is characterized by the deterioration of the immune system and an increased susceptibility to opportunistic infections and certain cancers (Barré-Sinoussi et al., 1983; Gallo et al., 1983). HIV continues to be a worldwide health problem, with an estimated 37.7 million people currently living with HIV (WHO, 2020a). Although the majority of these cases occur in Sub-Saharan Africa, HIV and AIDS heavily affect vulnerable people across the globe (WHO, 2020a). Since it was first observed in 1981 following an outbreak of rare Pneumocystis pneumonia and Kaposi's sarcoma in homosexual men in the United States, HIV has claimed the lives of an estimated 36 million people, with 680,000 deaths and 1.5 million new infections in 2020 alone (WHO, 2020a). In 1983, HIV (then known as human T-lymphotropic virus type 3 or lymphadenopathy-associated virus) was isolated from patients with AIDS and identified as the cause of AIDS by two independent research groups, led by Drs. Françoise Barré-Sinoussi and Luc Montagnier and Dr. Robert Gallo, respectively (Barré-Sinoussi et al., 1983; Gallo et al., 1983). In fact, Drs. Barré-Sinoussi and Montagnier were co-recipients of the 2008 Nobel Prize in Physiology or Medicine for their role in the discovery of HIV. Although there is currently no known cure for HIV, antiretroviral therapies (ART) have greatly extended the lifespan of people living with HIV

(PLHIV) since their first use as an effective treatment for HIV/AIDS in 1995 (Gulick et al., 1997; Hammer et al., 1997; Moore & Chaisson, 1999).

ART is able to control HIV replication effectively and has allowed PLHIV to have a relatively normal quality of life, although there are still significant medical and social impacts (Brechtl et al., 2001; Call et al., 2000; Hays et al., 2000). However, if left untreated, AIDS will usually develop within an average of 10 years from the time of initial infection, with death occurring generally within 2 years of progression to the AIDS stage of disease (eART-linc collaboration et al., 2008; Zwahlen & Egger, 2006). Unfortunately, only an estimated 67% of PLHIV worldwide currently have consistent access to ART (UNAIDS, 2020). The development of an effective vaccine against HIV has been unsuccessful so far for many reasons. Primarily, natural mechanisms for eradicating HIV infection are poorly understood and as such the optimal mechanisms by which vaccine-induced immunity can be generated are not known (Fourcade et al., 2018; Hsu & O'Connell, 2017; Johnston & Fauci, 2011). Findings from previous unsuccessful vaccine trials indicate generating both robust humoral and cellular responses will be important for protection (Fong et al., 2018; Mascola et al., 1996; Thongcharoen et al., 2007; West et al., 2011). Another limiting factor is the genetic variability seen in HIV caused by a high rate of mutations per replication cycle combined with a high replication rate (Korber et al., 2001). This leads to considerable variability between the amino acid composition of the envelope proteins of different strains and subtypes of HIV, resulting in difficulties in identifying an appropriate molecular target that would offer protection from all strains of the virus (Gaschen et al., 2002).

1.1.2 Transmission of HIV:

There are two strains of the HIV virus, HIV-1 and HIV-2, although HIV-1 is responsible for the vast majority of cases (>95%) of HIV infection and AIDS worldwide (Gilbert et al., 2003). HIV-2 is similar, but genetically distinct from HIV-1, and is more difficult to transmit and is thus primarily localized to certain regions in West Africa (Ingole et al., 2013; Andersson et al., 2000). For these reasons, HIV-1 is the focus of most HIV and AIDS research. Transmission of HIV can occur following contact with bodily fluids (blood, seminal/vaginal/rectal fluids, placental blood, etc.) of a PLHIV (Klimas et al., 2008). This primarily occurs through sexual transmission but may also occur following use of contaminated needles or receiving contaminated blood products. Male-to-female sexual transmission is more commonly seen in heterosexual intercourse compared to female-to-male transmission, due to physiological differences in the reproductive tract (increased target cells and reduced epithelial barrier integrity in the vaginal mucosa compared to the penis) and social disadvantages caused by gender inequality (Hladik & McElrath, 2008; Shaw & Hunter, 2012). As a result, women are disproportionally affected, with 53% of PLHIV being women and girls in 2020 (UNAIDS, 2020). Receptive anal intercourse has also been shown to have an increased risk for HIV transmission per individual act and as such, homosexual men also make up a significant portion of HIV infections worldwide (Hladik & McElrath, 2008).

1.1.3. Pathogenesis and replication cycle of HIV:

The primary stages of HIV-1 infection are usually asymptomatic but the virus is replicating rapidly as the virus disseminates throughout the blood and lymphoid tissues (Naif, 2013). If symptoms do appear, they are similar to a mild flu and can include fatigue/weakness, fever, weight loss, swelling of the lymph nodes, skin rashes and diarrhea lasting approximately 2 weeks (Klimas et al., 2008). HIV-1 targets CD4+ T cells primarily, but can also infect macrophages and dendritic cells as they can also express the HIV-1 co-receptors CCR5 or CXCR4 (Bleul et al., 1997; Dalgleish et al., 1984; Klatzmann et al., 1984; Naif, 2013). The HIV-1 virion enters the cell by using the gp120 envelope protein on its surface to bind to the CD4 receptor, and then undergoes a conformational change, allowing it to also bind to the co-receptor (CCR5 or CXCR4) on the surface of the target cell (Dragic et al., 1996; Feng et al., 1996; Mcdougal et al., 1986). In fact, the two major subtypes of HIV-1 can de differentiated based on whether they utilize the CXCR4 or the CCR5 co-receptor to gain entry to the cell for infection (Moore et al., 1997). X4-tropic strains of HIV-1 utilize the CXCR4 co-receptor found on T lymphocytes in various stages of activation and maturity and as such, they are known as T-tropic (Feng et al., 1996). Conversely, the CCR5 co-receptor is primarily found on activated T cells and macrophages and as such, are known as M-tropic (Alkhatib et al., 1996; Deng et al., 1996; Dragic et al., 1996). R5 variants are the predominant strains found in humans, encompassing between 60 and 80% of all strains sequenced (Ferrer et al., 2014; Moyle et al., 2005). X4 variants were identified in about 20% of the tested individuals and dual-tropic strains that can use either co-receptor for entry are also found in a portion of individuals although prevalence varies

between populations as R5 strains can acquired the ability to use the CXCR4 co-receptor as well over time (and vice-versa, although this is less common) (de Mendoza et al., 2007; Ferrer et al., 2014). Infection with an R5 strain is generally associated with lower viral loads and less severe T cell depletion compared to X4 strains, likely as the CCR5 co-receptor is expressed on only a small portion of all T cells, while CXCR4 is found on almost all T cells (Grivel & Margolis, 1999; Tersmette et al., 1989). Disease progression is often associated with the evolution of the virus' ability to use the CXCR4 co-receptor for infection, as these are expressed on a wider subset of T cells (Berkowitz, Alexander, et al., 1998; Berkowitz, Beckerman, et al., 1998; Scarlatti et al., 1997; Tersmette et al., 1989). These viruses can become dual-tropic (able to use either CCR5 or CXCR4) or progress to a predominantly X4-strain of HIV-1.

Following the binding of the co-receptor with the envelope protein, the transmembrane protein, gp41, is able to penetrate the plasma membrane of the target cell (Freed et al., 1990; Gomez & Hope, 2005). The extracellular portion of the gp41 protein then collapses into a hairpin loop, bringing the virus into close proximity with the target cell and initiating a process known as fusion (Muñoz-Barroso et al., 1998, 1999). The HIV-1 virion then injects its genetic material into the target cell, including single-stranded RNA, reverse transcriptase (RT), integrase, protease and various other enzymes (Gomez & Hope, 2005). Once inside the target cell, HIV-1's single-stranded RNA is converted by reverse transcriptase into double-stranded DNA, known as cDNA, which is then transported into the nucleus of the cell and integrated into the host's cellular DNA by the integrase enzyme (Ferguson et al., 2002; Hu & Seeger, 1996). HIV-1 uses the host cells' DNA replication machinery to

transcribe its own viral genome into mRNA, which is then translated into the Gag-Pol polyprotein (Gomez & Hope, 2005; Shehu-Xhilaga et al., 2001). These immature HIV-1 virions build up along the host's cellular membrane, where they are activated by the protease enzyme into mature virions (Zennou et al., 1998). This buildup of virions eventually results in lysis of the host cell and release of the virions into the surrounding environment; where they go on to infect and kill further CD4+ T cells (Ferguson et al., 2002; Gomez & Hope, 2005). Following several weeks of the acute phase of the infection, there is a period of clinical latency established where the virus can lay dormant for up to decade without the individual developing any symptoms of immunodeficiency. In most cases, the CD4+ T cell counts will eventually drop as the disease progresses and viral replication persists (Cary et al., 2016; Naif, 2013). Once the CD4+ T cell count is depleted to 200 cells/uL or less in the blood the individual in considered to have progressed to the AIDS stage of the disease (García et al., 2004; Naif, 2013). This stage is characterised by an increased susceptibility to various infections, such as tuberculosis, some forms of pneumonia and meningitis, and certain rare types of cancer, commonly Kaposi's sarcoma, aggressive forms of non-Hodgkin's lymphoma and cervical cancer and ultimately results in death (Moylett & Shearer, 2002).

Although CD4+ T cells are the primary target of HIV-1, infection of monocytes, macrophages and dendritic cells is also possible (Naif, 2013). Dendritic cells are potent antigen-presenting cells (APC) and may be among the cells infected by HIV-1 following initial mucosal exposure (Cunningham et al., 2013). The infection of dendritic cells themselves is likely non-productive, but is thought to be contribute to the dissemination of

the virus from the mucosa into the periphery (Wu & KewalRamani, 2006). The infected dendritic cells travel to the lymph nodes, where they interact with and infect CD4+ T cells, thereby spreading the virus (Manches et al., 2013; Wu & KewalRamani, 2006). The antigen-presenting ability of HIV-infected dendritic cells is also thought to be impaired, which likely further contributes to the inefficient expansion of T cell responses observed following HIV infection (Loré & Larsson, 2003). Macrophages are long-lived cells that infiltrate almost every tissue in the body and as such HIV-1 infection is able to persist in these cells in the form of integrated proviral DNA without causing rapid cell death (Carter & Ehrlich, 2008; Castellano et al., 2019). This is thought to contribute to the chronic, life-long nature of the infection, as well as the long periods of clinical latency following infection, as these macrophages act as a persistent viral reservoir for HIV within the host (Baxter et al., 2014; Carter & Ehrlich, 2008). Infection of macrophages is thought to occur primarily as a result of engulfing HIV-infected T cells, which allows the virus entry into the macrophages cell wall (Baxter et al., 2014). However, using a myeloid-only humanized mouse model, tissue macrophages have been shown to sustain HIV-1 infection in the absence of T cells, indicating macrophages can be directly infected by either cell-free HIV or other cell-to-cell spread (Honeycutt et al., 2016, 2017). Infection of various macrophage populations has been associated with increased inflammation and immune activation, as well as the impairment of phagocytic clearance of pathogens resulting in increased susceptibility to co-infection (Booiman et al., 2017; Corleis et al., 2019; Cribbs et al., 2015).

1.1.4. Current treatment for HIV:

The ability to control HIV replication with ART has contributed to the dramatic increase in lifespan and improvement in quality of life of PLHIV in recent years. There are four major classes of ART drugs, often used in combination, that function by blocking viral replication at different stages of the virus replication cycle. The first class includes entry inhibitors such as CD4 or CCR5 binding inhibitors or fusion inhibitors which prevent the virus from gaining entry to the cell and thus blocking replication as the cell's host machinery is required for viral replication (Briz et al., 2006; Reeves et al., 2002). The second class includes nucleoside and non-nucleoside reverse-transcriptase inhibitors (NRTI and NNRTI), as well as nucleotide reverse-transcriptase inhibitors (NtRTI), which all act as inhibitors of reverse transcriptase, preventing the essential transcription of viral RNA into DNA (Akanbi et al., 2012; Feng et al., 2009; Grobler et al., 2007). Thirdly, integrase inhibitors act to block the integration of viral DNA into the host DNA and effectively block further spread of the infection (Kessl et al., 2012; Messiaen et al., 2013). Finally, protease inhibitors block the activity of the virus' protease enzyme and thus inhibit the cleavage of precursor proteins and virion maturation (Cígler et al., 2005). Current medical recommendations are for all patients to be prescribed an ART regiment immediately following diagnosis and then maintained for the duration of their lifetime to prevent relapse (WHO, 2019). Approved regimens generally include an integrase inhibitor and up to two nucleoside reverse transcriptase inhibitors, which have been shown to reduced viral load to below detectable levels within 6-12 months of treatment initiation in approximately 80% of patients when taken as prescribed (Bonora et al., 2009; Currie et al.,

2009; Ocheretyaner et al., 2019; Ottop et al., 2020; Wolff et al., 2017). There are currently almost 30 FDA-approved ART drugs and as such therapies are often customized based on individual medical history, drug susceptibility and adverse events. Currently, the mostly commonly recommended initial ART regimens generally include either tenofovir (a NtRTI) plus emtricitabine or lamivudine (both NRTIs), or abacavir (also a NRTI) plus lamivudine, with either efavirenz (a NNRTI), ritonavir-boosted atazanavir (a protease inhibitor), raltegravir or dolutegravir (both integrase inhibitors) as the third agent (De Clercq, 2006; Deeks & Perry, 2010; Gallant et al., 2017; Gallant et al., 2006; Montaner et al., 2015; Trottier et al., 2017). Each drug may be prescribed separately, or in single-pill combinations, such as Truvada (tenofovir/ emtricitabine), Triumeq (abacavir/dolutegravir/lamivudine) and Atripla (tenofovir/emtricitabine/efavirenz), for convenience. ART has also been successfully used as an HIV prophylaxis to prevent the establishment of the infection either pre- or post- exposure (PrEP and PEP, respectively) (Grant et al., 2010; Okwundu et al., 2012). When taken as prescribed, these drugs can effectively reduce the risk of contracting HIV by up to 80% following a suspected exposure (Bosco et al., 2019; Celum et al., 2019; Choopanya et al., 2013; Fonner et al., 2016; Janes et al., 2018; Johnson et al., 2019; Pinto & Carvalho, 2018; Pinto et al., 2019).

1.2 Tuberculosis:

1.2.1 A brief introduction to TB:

Tuberculosis (TB) is the leading cause of communicable disease and death worldwide, with an approximate 10 million new cases of active disease and 1.5 million deaths each year

(WHO, 2020b). TB is an infectious disease caused by *Mycobacterium tuberculosis* (*Mtb*) bacteria. Globally, one quarter of the world's population is thought to be infected with *Mtb* (WHO, 2020b). A small percentage of infected individuals are able to clear the infection completely without developing either active or latent TB, however these mechanisms are poorly understood as this phenomenon is difficult to identify and study in humans as they never display symptoms of TB (Morrison et al., 2008; Verrall et al., 2020). Approximately 90% of all cases do not go on to develop active pulmonary TB. Instead, the infection becomes latent and is not symptomatic or transmissible during this stage. About 5-10% of latent TB cases will reactivate at some point during the individual's life and cause disease, which is characterized by cough, bloody mucus, weight loss, fatigue and fever (WHO, 2020b). If left untreated, active TB results in death in approximately 50% of cases (Bozzano et al., 2014). Unfortunately, treatment can be difficult to access for particularly impoverished populations as it involves long-term administration of multiple antibiotics that are known to have high toxicities and can cause severe side effects, which results in reduce treatment compliance. Additionally, the only vaccine currently commercially available is the BCG vaccine, which has shown variable efficacy at reducing the risk of pulmonary and disseminated TB during childhood and into adult age (Mantilla-Beniers & Gomes, 2009; WHO, 2018).

BCG is a live attenuated form of *Mycobacterium bovis* (the causative agent of TB in cows) and was first used as a vaccine against TB in humans in 1921, although its use wasn't adopted on a large scale until after World War II (Fine, 1989). Efficacy has been reported as ranging from 30 to 80% protection against pulmonary TB in children and variability

between different geographical regions is high (Colditz et al., 1994; Hart, 1967; Ponnighaus et al., 1992; Sutherland & Springett, 1987). Although, the BCG vaccine is not commonly used in adult populations due to significantly lower efficacy rates, it may be considered in select populations at high-risk of exposure (healthcare workers, prison workers, those living in the same household as someone with active TB) in regions where drug-resistant strain are prevalent (Brett & Severn, 2020; Faust et al., 2019). Traditionally, the BCG vaccine is given intradermally. However some recent non-human primate (NHP) studies have indicated that intravenous (IV) or mucosal administration may offer enhanced protection against pulmonary TB in macaques following *Mtb* challenge (Darrah et al., 2020; Vierboom et al., 2021). The mechanisms by which these improved responses are generated are not well understood but are thought to be a result of improved trained innate immunity and mucosal responses compared to intradermal administration, which likely results in improved early clearance of the infection (Darrah et al., 2020; Vierboom et al., 2021).

1.2.2 Current struggles in developing TB vaccines:

There are currently several novel vaccine candidates currently in various stages of development, with 14 candidates currently being investigated in clinical trials (WHO, 2021). One of the major limiting factors in the development of new vaccines has been a lack of reliable correlates of protection (Bhatt et al., 2015). In the case of most pathogens that have had successful vaccines developed against them, serum levels of circulating neutralising antigen (Ag)-specific antibodies can be used as an accurate measure of protection against subsequent infection as these antibodies play an important role in

fighting the infection (Plotkin, 2010). Conversely, the role of antibodies in protection against *Mtb* infection is unclear as B cell-deficient mouse and NHP models of TB show only modest susceptibility to *Mtb* infection compared to the dramatic impairment seen in T cell-deficient models (Chan et al., 2014; Green et al., 2013; Maglione et al., 2007; Phuah et al., 2016; Vordermeier et al., 1996). However, B cells have been found within the granulomatous tissues, are thought to contribute to the inflammatory milieu of the granuloma and *Mtb*-specific antibodies have been detected in the blood and lungs of latently infected individuals, indicating their role is not unimportant (Li et al., 2017; Maglione et al., 2007). As a result, T cell-specific correlates of protection are generally preferred for TB, although they are more difficult to quantify compared to antibody responses and the differences in inflammatory cytokine profiles between exposed and uninfected individuals are poorly characterised (Day et al., 2011, 2013; Kagina et al., 2010). Other potential correlates of protection are currently being explored but remain in experimental use due to limitations in feasibility and reliability, including differences in gene expression within granulomatous tissues of a NHP model of TB that was associated with improved BCG-induced protection following infection (Mehra et al., 2013).

1.2.3 Mtb evades phagocytosis and replicates within macrophages:

Mtb is transmitted by aerosols generated by individuals with active TB disease, usually by coughing, sneezing, speaking or spitting. The necessary dose of *Mtb* bacteria for infection is very low, which facilitates spread of the disease (Nicas et al., 2005). Following exposure, the *Mtb* bacteria travels along the airway until it reaches the alveolar sacs, there they infect

alveolar macrophages and begin to replicate within the endosome of the macrophages (Bozzano et al., 2014). Although alveolar macrophages are the primary target of *Mtb* infection, the bacterium is also able to infect interstitial and other macrophage populations, T and B lymphocytes, alveolar epithelial cells, lymphatic endothelial cells, neutrophils, dendritic cells, pneumocytes, fibroblasts, adipocytes and bone marrow-derived stem cells among others (Beigier-Bompadre et al., 2017; Hernández-Pando et al., 2000; Lerner et al., 2017; Mayito et al., 2019). Following endocytosis, the alveolar macrophage is able to recognize the *Mtb* bacteria as foreign and attempts to mount an immune response by initiating phagocytosis. However, *Mtb* are particularly adept at resisting host killing mechanisms due in part to their thick plasma membrane rich in mycolic acid and other lipids, and thus the *Mtb* bacteria continue to replicate within the cells, eventually killing them.

In normal phagocytic processes, macrophages possess many pattern recognition receptors (PRR) that are able to recognize pathogen-associated molecular patterns (PAMP) on the surface of pathogens (Stafford et al., 2002). In order to initiate phagocytosis, macrophages also require binding by various receptors (Aderem & Underhill, 1999). Pathogens are then engulfed following binding with PPRs located along the macrophage's plasma membrane. The receptor-pathogen complex is then internalized and transported into the phagosomes. Transport vesicles mediate the translocation of phagocytic compartments and microtubules allow bidirectional flow between compartments (Berón et al., 1995). As a result, the phagosome fuses with lysosomes (organelles containing hydrolytic enzymes) and accumulates proton pumps along the phagosomal membrane, resulting in gradual

acidification of the phagosomes in a process known as phagolysosome maturation (Chua et al., 2004; Kinchen & Ravichandran, 2008; Sun-Wada et al., 2009). There are various mechanisms by which intracellular killing of pathogens can occur, including acidification of the phagolysosome and the release of reactive oxygen species (ROS) or nitrous oxide (NO) which directly attack the bacterium (Stafford et al., 2002). *Mtb* has evolved to evade these mechanisms of early bacterial clearance by preventing lysosomal fusion and phagolysosome maturation and allowing the bacteria to continue replicating within the phagocytic compartments (Chua et al., 2004).

1.2.4 Mtb delays the adaptive immune system:

In addition to the suppression of the phagocytic ability of the cells of the innate branch of the immune system, *Mtb* is able to evade killing by delaying the initiation of the adaptive immune response, of which T cells are crucial for controlling *Mtb* infection (Chackerian et al., 2001; Chackerian et al., 2002; Lin et al., 2006; Wolf et al., 2008). Since early stages of infection are difficult to study in humans since this usually occurs before diagnosis is made, NHP and mouse models are important tools to understanding this phenomenon. In most other types of infection, the adaptive immune system is engaged within 1 week post infection through antigen presentation by dendritic cells and other APCs to naïve T cells in the draining lymph nodes, resulting in the generation of Ag-specific helper and cytotoxic T cells, as well as B cells that secrete Ag-specific antibodies once activated into plasma cells, all of which are critical for clearing pathogens and establishing long lasting memory responses to prevent reinfection (Schenten & Medzhitov, 2011). The entirety of this process

can last until about 10 to 14 days post infection, during which time the T and B lymphocyte populations undergo clonal expansion, specific antigen receptors are generated and differentiation into effector cells occurs (Janeway et al., 2001; Chua et al., 2015; Schenten & Medzhitov, 2011). *Mtb* is able to delay the initiation of the adaptive immune responses until 2-3 weeks post-infection in mouse models (Chackerian et al., 2001; 2002; Wolf et al., 2008) and 4 weeks in NHPs (Lin et al., 2006). Bacterial replication and dissemination occurs mostly unhindered during this time due to the suppression of phagocytic ability of innate cells by *Mtb* before T cell responses can be generated and contribute to controlling the infection (Chackerian et al., 2002; Chua et al., 2004; Wolf et al., 2008).

In latent tuberculosis, other macrophages, T and B lymphocytes, as well as fibroblasts, surround the infected macrophages and form a granuloma that contains the infection (Bozzano et al., 2014). Over time, the centre of the granuloma becomes necrotic as the immune cells attack the bacteria within the infected macrophages, although over time scarring and fibrotic tissue replace the necrotic core. The formation of granulomas is thought to prevent dissemination into the bloodstream and peripheral tissues during latent infection. While the exact causes of latent TB reactivation are unknown, immunosuppression via the impairment of the function of any of the above mentioned cell types can accelerate this process, leading to the development of active pulmonary, disseminated or miliary TB (Bozzano et al., 2014). T cell depletion has been associated with reactivation of latent TB, increased bacterial replication and dissemination and significantly worsened outcomes compared to wildtype controls in various mouse and NHP models, highlighting their importance in controlling the infection and maintaining latency

(Corleis et al., 2019; Diedrich et al., 2020; Diedrich et al., 2010; Green et al., 2013; Klein & Flynn, 1999; Lin et al., 2012; Scanga et al., 2000). Macrophages are also considered crucial for early clearance of the bacteria and maintaining the integrity of the ring of immune cells surrounding granulomas in latent TB (Huang et al., 2015; Marino et al., 2015; Shi et al., 2019). Several types of immune cells are involved in establishing latent TB and preventing immediate progression to active infection, but CD4+ and CD8+ T cells and macrophages are critical. CD4+ T cells secrete many important cytokines such as interferon (IFN)-γ, tumour necrosis factor (TNF)-α and interleukin (IL)-2, which are necessary for proper activation and function of several immune cells involved in anti-mycobacterial responses (Cozmei et al., 2007). IFNγ and TNFα are important for macrophage activation, which then in turn release reactive oxygen and nitrogen species that directly inactivate phagocytosed bacteria by inducing irreparable DNA damage (Dharmaraja et al., 2012; Fang, 2004). IL-2 is important for the differentiation and activation of effector cells, including cytotoxic CD8+ T cells, which are also involved in controlling the infection (Liao et al., 2011; Lin & Flynn, 2015). CD8+ T cells and other cytotoxic cells release perforin, granulysin and granzymes to lyse and destroy *Mtb*-infected cells (Hudig et al., 1993; Podack et al., 1985).

1.2.5 Current treatment for TB:

The discovery of streptomycin, the first antibiotic identified to be effective for the treatment of *Mtb*, by Drs. Albert Schatz and Selman Abraham Waksman in 1943 revolutionized the treatment of TB. In fact, Dr. Waksman was awarded the 1952 Nobel Prize in Physiology

or Medicine for his contribution to its discovery. Several other antibiotics have been developed since that time and the standard drug regiment for TB includes a 2 month course of four antibiotics (isoniazid, rifampin, pyrazinamide and ethambutol, known as HRZE) at which time the patient is confirmed to be culture negative in the sputum, before continuing another 4 month course of just rifampin and isoniazid to eliminate the bacterial reservoir entirely (Via et al., 2015). Although lengthy, this regiment is quite effective in most patients with drug-susceptible TB. In the case of drug-resistant TB, more aggressive antibiotics, such as bedaquiline, pretomanid, moxifloxacin or ciprofloxacin, may need to be added to the drug regiment to prevent relapse (Borisov et al., 2017; Dawson et al., 2015; Gillespie, 2016). Some of these drugs are also currently being evaluated as potentially treatment shortening alternatives to the traditionally used HRZE regimen as they show enhanced sterilising activity (Via et al., 2015; Walter et al., 2021). Novel regimens that are currently being investigated include BPaZ (bedaquiline/ pretomanid/pyrazinamide) and BPaMZ (bedaquiline/pretomanid/moxifloxacin/pyrazinamide) (Dawson et al., 2017; Salinger et al., 2019; Tweed et al., 2019; Walter et al., 2021).

1.3 HIV and TB co-infection:

1.3.1 A brief introduction to HIV and TB co-infection:

The greatest risk factor for developing active TB is co-infection with HIV-1. In fact, PLHIV are approx. 20 times more susceptible to developing active TB compared to HIV-negative people, as well as significantly more likely to progress immediately to active disease following initial infection (Corbett et al., 2003; Gelaw et al., 2019). Co-infection with both

HIV and TB leads to significantly worsened outcomes in terms of both diseases, as well as complications in diagnosis and therapeutic intervention (Bell & Noursadeghi, 2018; McShane, 2005; Pawlowski et al., 2012). TB accounts for approximately 25% of AIDS-related deaths worldwide, with an estimated 215,000 deaths occurring in 2020 alone (Corbett et al., 2003; Gelaw et al., 2019; WHO, 2020b). Interestingly, increased susceptibility to TB is not entirely eliminated even in virally-suppressed PLHIV treated with ART although reactivation, mortality and relapse rates are greatly decreased as viral loads are supressed and CD4+ T cell counts return to normal (Chelkeba et al., 2020; Kaplan et al., 2018; Lawn et al., 2011; Manosuthi et al., 2006). HIV and TB offer many similarities in terms of epidemiology. Both HIV and TB primarily target vulnerable populations, with the majority of those affected living in third-world countries in Sub-Saharan Africa, Asia or South America where both HIV and TB are endemic (WHO, 2020b, 2020a). Due to poor sanitation, crowded living conditions, poverty and lack of education in preventative measures, these populations are prone to vulnerability and exposure to opportunistic infections (Coope et al., 2004). In areas where resources are limited, the lengthy and expensive treatments for either HIV and TB are difficult to obtain consistently, have significant toxicities and thus, compliance can be low (WHO, 2020b, 2020a).

In North America, there is an elevated incidence of both HIV and TB found in marginalized populations, namely immigrants, indigenous communities, as well as incarcerated and homeless populations (Essien et al., 2019; Harris et al., 2006; Long & Boffa, 2010). There were an estimated 62,000 Canadians living with HIV in 2018, with about 50% being men who have sex with men, 10% being indigenous people, 15% being people who inject drugs

and 2% being new immigrants (PHAC, 2018). The provinces with the highest rates of HIV are Saskatchewan, Manitoba, Quebec and Alberta (PHAC, 2018). Although TB is not endemic in Canada, there were still an estimated 1,800 active cases reported in 2017 (PHAC, 2017). Approx. 70% of these cases were in new immigrants (usually screened and diagnosed during immigration proceedings) and another 20% were in Indigenous peoples (PHAC, 2017). In fact, the rate of active TB is more than 4 times higher in indigenous populations compared to other Canadians (PHAC, 2017). Due to overcrowding and poor sanitation, homeless and incarcerated populations make up a significant portion of non-Indigenous Canadian-born individuals with either HIV or TB (PHAC, 2017, 2018).

1.3.2 HIV-infected macrophages are less equipped to clear Mtb:

The immunosuppressive nature of HIV-1 infection, in combination with the ubiquitous nature of *Mtb*, increases the risk for co-infection. HIV-1 targets primarily CD4+ T cells but also various types of macrophages (Naif, 2013). *Mtb* primarily targets alveolar macrophages and essential *Mtb*-specific immune responses are heavily T cell dependent, which results in complex immune interactions between the two pathogens (McShane, 2005). All types of macrophages, including alveolar macrophages, are also targeted directly by HIV-1. Phagocytosis is particularly affected, which is thought to result in reduced early clearance of the bacteria and increased risk of new primary TB infection following exposure (Mwandumba et al., 2004). Macrophages are dependent on CD4+ T cells for activation and proper function, which further impairs the phagocytic and inflammatory activity as the disease progresses (Booiman et al., 2017; Singh et al., 2019). The infection

of alveolar macrophages by HIV-1 is thought to occur by dissemination of virus from infected peripheral blood cells across the alveolocapillary membrane into the alveolar space (Agostini et al., 1993). This has been shown to occur during the early stages of acute infection in both humans and NHP models (Barber et al., 2006; Corleis et al., 2019). Alveolar macrophages are thought to be the primary reservoir of HIV-1 in the lung (Charles & Shellito, 2016). Approximately 4-5% of alveolar macrophages isolated from whole BAL were infected when collected from asymptomatic ART-naïve HIV-infected patients (Jambo et al., 2014). Infection of alveolar macrophages with HIV-1 impairs their antimicrobial responses to respiratory infections and results in both increased susceptibility to lower respiratory infection and worsened outcomes compared to non-infected individuals (Cribbs et al., 2015). The primary mechanism by which HIV-infected alveolar macrophages show impaired immune responses in by inhibition of phagocytosis (Cribbs et al., 2015; Koziel et al., 1998; Lê-Bury & Niedergang, 2018). In fact, phagocytosis was reduced in both ART-treated (Cribbs et al., 2015) and ART-naïve (Jambo et al., 2014) HIV-infected individuals. The phagocytic ability of HIV-1 infected alveolar macrophages was reduced by 50% in some studies (Da Glória Bonecini-Almeida et al., 1998). This is thought to occur by both the downregulation of cell surface receptors used to initiate phagocytosis, as well as the inhibition of intracellular killing mechanisms (Koziel et al., 1998; Lê-Bury & Niedergang, 2018).

Due to their thick mycolic acid cell wall and natural inhibition of phagolysosome maturation, *Mtb* bacilli are already extremely adept at withstanding normal phagocytic killing mechanisms such as phagolysosome acidification or the release of ROS and NO

(Warner & Mizrahi, 2007). The combination of HIV-1 impaired macrophage activation and *Mtb*'s resistance to killing by phagocytosis likely results in uncontrolled *Mtb* growth within the alveolar macrophage. *Mtb* bacilli have been found in un-acidified phagosomes in alveolar macrophages isolated from the bronchoalveolar lavage (BAL) of PLHIV with TB, suggesting that HIV-1 infection may impair the ability of the phagosome to fuse with a lysosome which is an integral part of phagocytosis (Mwandumba et al., 2004). *Mtb*-containing vacuoles of primary HIV-infected alveolar macrophages were reported to have a high pH and failed to fuse with lysosomes *in vitro* (Mwandumba et al., 2004). Although the mechanism by which lysosome acidification is impaired is poorly understood, it is thought to involve dysregulation of the lysosomal proton pumps (Lê-Bury & Niedergang, 2018; Sun-Wada et al., 2009). Intracellular killing mechanisms like phagosome acidification and the release of reactive oxygen or nitrogen intermediates is also impaired in PLHIV, resulting in uncontrolled intracellular *Mtb* growth within the macrophage (Hirsch et al., 1994). The mechanism by which this occurs is poorly understood but is thought to involve dysregulation of key cytokines and chemokines necessary for macrophage activation and phagocytosis (Hirsch et al., 1994; Weiss et al., 2004).

1.3.3 HIV-mediated T cell depletion and dysfunction threatens the containment of Mtb within the granulomas:

Although TB infection commonly occurs following HIV-1 infection due its immunosuppressive effects, this is not always the case considering that a quarter of the world's population is thought to be latently infected with *Mtb* (WHO, 2019). Latent TB

infection is often reactivated by co-infection with HIV-1, which results in worsened outcomes in terms of both diseases (Bell & Noursadeghi, 2018). HIV promotes the progression of *Mtb* infection, while TB exacerbates the course of HIV infection. In fact, both clinical and NHP studies have shown that the incidence of active TB in PLHIV is directly correlated with CD4+ T cell depletion (Antonucci, 1995; Bunjun et al., 2017; Lin et al., 2012). In those with latent TB, granulomas are able to contain the infection with the help of T and B cells, macrophages and fibroblasts to keep it latent. Although what occurs in the lungs of co-infected individuals has been challenging to investigate, it is thought that co-infected individuals are less equipped to mount an efficient immune response as T cells and macrophages are depleted from the granulomas periphery by HIV-1 (Caruso et al., 1999; Lin et al., 2012; Scanga et al., 2000). It is well understood that HIV-1 infection causes impaired immune function and this may result in poor containment of the *Mtb* growth within the granuloma and dissemination of *Mtb* bacilli (Bucşan et al., 2019; Chetty et al., 2015). As the HIV infection progression, the macrophages and CD4+ T cells making up the granuloma cuff are thought to become dysfunctional or die, which increases the risk of the granuloma breaking down and releasing *Mtb* bacilli into the surrounding lung tissues (Bezuidenhout et al., 2009; Lawn et al., 2002). TNFα production is also impaired in co-infected individuals, which is important for the normal formation of granulomas and controlling *Mtb* growth (de Noronha et al., 2008). TNFα may also play a role in promoting HIV replication, which then leads to greater CD4+ T cell depletion and IFNγ impairment, further disrupting granuloma containment (Laurence, 1992). Lung tissue collected from HIV-1 and TB co-infected individuals showed poorly contained granulomas with areas of

necrosis and a heterogeneous immune cell population composed primarily of granulocytes and very few lymphocytes, as well as significantly higher bacterial loads compared to granulomas from HIV-negative *Mtb*-infected individuals (de Noronha et al., 2008). Traditionally, CD4+ T cells have been thought to be primarily involved in mediating anti-mycobacterial responses within the granuloma, however some recent studies have shown that other immune cells are involved (Diedrich et al., 2020). In this study, rhesus macaques with latent TB were treated with anti-CD4 antibodies to deplete CD4+ T cells within the granuloma. Surprisingly, there was not a significant change in *Mtb* burden or amount of granulomatous tissue compared to untreated macaques, indicating the involvement of other immune cells such as macrophages, CD8+ T cells and B cells (Diedrich et al., 2020). Granulomas from HIV and TB co-infected individuals are also characterized by high levels of TGF-β, which is known to suppress both T cell and macrophage responses (Toossi & Ellner, 1998).

1.3.4 HIV-induced inflammation and dysfunctional cytokine production impairs anti-TB immune responses:

Additionally, IFNγ and IL-2 secretion are reduced and Th1 responses are impaired in the blood of PLHIV, which are known to be important for mounting robust anti-mycobacterial responses (Murray et al., 2018). HIV infection is thought to induce preferential differentiation of regulatory macrophages of an anti-inflammatory phenotype (Chihara et al., 2012). This likely results in macrophages that are unable to contain the *Mtb* infection without the support of CD4+ T cells and dissemination of the infection occurs (Cassol et

al., 2010; Chihara et al., 2012). HIV infection is also thought to impair the functionality of the dendritic cell - T cell axis, the pathway through which antigen-presenting dendritic cells activate and trigger proliferation of *Mtb*-specific CD4+ T cells. This results in suboptimal activation of immune cells and a dysfunctional tolerogenic phenotype (Singh et al., 2019). In the blood, HIV and TB co-infected individuals show a depletion and impairment of *Mtb*-specific CD4+ T cell responses, particularly their Th1 and IFNγ responses which are crucial for mounting a robust immune response against *Mtb* infection (Esmail et al., 2018; Geldmacher et al., 2010). Interestingly, this function is not entirely recovered even when an individual is successfully treated with ART, has an undetectable viral load and normal CD4+ T cell counts. Although this phenomenon is still poorly understood, it is likely HIV infection does permanent damage to the T cell repertoire (Lawn et al., 2011). NHP models have also shown that *Mtb*-specific activated and memory CD4+ T cells are preferentially depleted in the blood and lungs of NHPs co-infected with SIV and *Mtb* (Cheynier et al., 1998; Corleis et al., 2019). This is likely in part due to the high expression of the CCR5-coreceptor on these CD4+ T cell subsets which increases their susceptibility to infection (Meditz et al., 2011). Differences in inflammatory profiles, such as increased IL-2 and reduced IFNγ and MIP-1β production, are also thought to contribute to preferential infection and depletion of these cells (Geldmacher et al., 2010; Riou et al., 2016).

In fact, PLHIV have been shown to have elevated levels of a variety of surface markers and cytokines that are associated with T cell and monocyte/macrophage activation (Fahey et al., 1998; Giorgi et al., 1999, 2002; Gottlieb et al., 1981). As previously discussed, activated immune cells are more readily targeted by R5-strains of HIV-1 due to their increased

expression of the CCR5 co-receptor and are associated with more severe disease progression, target cell depletion and elevated viral load (Meditz et al., 2011). This immune dysfunction is likely also exacerbated in PLHIV due to an irreversible depletion of the T cell repertoire during the early stages of infection which results in weakened adaptive and memory immune responses (Heather et al., 2016; Turner et al., 2021). Although ART acts very quickly to reduce viral load and boost CD4+ T cell count, it is not able to restore the T cell repertoire to its pre-infection state. Over time, as the individual is exposed to various microbes, their T cell repertoire may begin to repopulate itself (Heather et al., 2016). ART is also unable to completely restore the inflammatory profiles of PLHIV to their pre-infection state, and thus even virally-suppressed PLHIV are prone to developing inflammation-associated co-morbidities (Abad-Fernández et al., 2013; Bosho et al., 2018; Gootenberg et al., 2017). Although the mechanisms involved are not well understood, several processes are thought to contribute to this dysfunction through a combination of chronic antigen stimulation, disruption of intestinal epithelial barrier integrity resulting in microbial translocation and even as a result of chronic ART toxicities (Dillon et al., 2017; Zevin et al., 2016; Zicari et al., 2019). All these factors result in a significantly increased risk for developing active pulmonary TB immediately following exposure, as well as reactivation of latent TB (McShane, 2005; Pawlowski et al., 2012). PLHIV are also at increased risk of developing disseminated TB as their immune system is unable to contain the infection within the lungs, with about 50% of PLHIV co-infected with TB showing extrapulmonary involvement (Golden & Vikram, 2005).

1.3.5 Outstanding questions in HIV/TB:

HIV-1 and TB co-infection has been extremely difficult to investigate due to a lack of affordable animal models. There are currently several underlying questions that have not been resolved in the field of HIV and TB co-infection. A significant concern is the vaccination of PLHIV against *Mtb* infection, as these individuals are known to be extremely susceptible to TB infection. Additionally, most TB vaccine candidates often rely on the generation of *Mtb*-specific T cell responses for protection against TB infection, which is impaired in PLHIV. All novel vaccine formulations against *Mtb* infection will need to be evaluated in the context of PLHIV's immune responses. Humanized mice (hu-mice) can be an important tool for measuring vaccine safety and efficacy in pre-clinical studies. There are also questions about the effectiveness and tolerability of ART and anti-TB drugs when taken in conjunction by co-infected individuals. Particularly, the phenomenon of tuberculosis-associated immune reconstitution inflammatory syndrome (TB-IRIS) in HIV-infected individuals is poorly understood. TB-IRIS can occur in some co-infected individuals following the initiation of ART in order to treat the HIV infection. Following the recovery of some of the CD4+ T cell count, the immune system may become over-activated, resulting in detrimental non-specific systemic inflammation (Namale et al., 2015). The cause of TB-IRIS is poorly understood, as not all co-infected people treated with ART develop it, and as such humanized mouse models may be helpful in studying this topic as hu-mice possess human immune systems. Another major area of interest is the HIV- and *Mtb*-specific immune responses in the lung of co-infected individuals. Lung tissue in particular is difficult to study in humans as it requires painful and invasive

procedures to extract the required tissue samples. For these reasons, there is an urgent need for small animal models of HIV/TB co-infection in which we can explore these questions fully.

1.4 Humanized mouse models:

1.4.1 A brief introduction to humanized mice:

Humanized mouse models are extremely useful for the preclinical stages of research where traditional animal models may not be able to reliably reproduce clinical aspects of the human disease. During the preclinical stages of research, it is not possible to use human subjects for obvious ethical and moral reasons. This is problematic especially in the field of immunology, where immune responses are mediated by specific cells whose function is not always homologous with humans (Shultz et al., 2012). For example, HIV-1 is a human tropic disease and is not able to infect normal small animal models, like mice or rats as the human CD4 receptor and CCR5/CXCR4 co-receptors are required for viral entry into the cell and subsequent viral replication (Naif, 2013). As a solution to this issue, researchers have developed humanized mouse models in which immunocompromised mice are reconstituted with human immune cells so that they can be infected by certain human tropic pathogens and better recapitulate certain immune responses seen in humans and thus are useful in revealing how the human immune system may respond to various stimuli when traditional small animal models may not be appropriate. In order to create humanized mouse models, severely immunocompromised strains, such as non-obese diabetic (NOD), NOD/Shi-scid IL2rγ^{null} (NOG), NOD-Prkdc^{scid} (NOD-Scid), NOD-scid-IL2rγ^{null} (NSG) or

NOD-Rag1^{null}-IL2rγ^{null} (NRG), are commonly used as they offer a "blank slate" for the engrafted human stem cells and are less able to recognize these cells as foreign and mount immune responses to eliminate them (Skelton et al., 2018). Although these mice are already severely immunocompromised, non-functional and dysfunctional immune cells may remain and as such, these mice require irradiation conditioning to clear the few remaining murine immune cells and create a niche in the bone marrow matrix for the engrafted human stem cells. Following irradiation, the mice will then be engrafted with CD34+ hematopoietic stem cells (HSC) that can be obtained from umbilical cord blood, bone marrow, fetal liver and/or mobilized peripheral blood, although umbilical cord blood and fetal tissues are preferred sources as they contain a higher frequency of progenitor HSCs (Skelton et al., 2018).

1.4.2 Immunocompromised strains are commonly used for humanized mice:

One of the most promising and widely used background strains is the NRG, which reconstitutes significant lymphoid and myeloid cell lineages following engraftment with human HSCs, express diverse T and B cell repertoires and are able to secrete various human cytokines (Cheng et al., 2017; Harris et al., 2013; Volk et al., 2016). The NRG mouse is on the NOD background, which has a severely defective innate immune system and has dysfunction complement activation, resulting in non-functional macrophages and dendritic cells, which are important antigen-presenting cells and responsible for initiating murine immune responses (Bosma et al., 1983). The NOD background is also characterised by overexpression of the SIRPα allele, which binds to CD47 on immune cells and triggers a

"don't eat me" signal and prevents the phagocytosis of human cells by mouse macrophages following engraftment, reducing graft-vs-host disease and improving the degree of reconstitution of donor HSCs (Skelton et al, 2018). The NRG mouse also has a non-functional mutation in either the Rag 1 or Rag 2 genes instead of the Prkdc-scid mutation that was traditionally used in older models (ex: NSG and NOD-scid) (Mombaerts et al., 1992). The Rag knockout is functionally similar to the scid mutation in that they both result in an entirely non-functional adaptive immune system that is characterized by a lack of mature T and B cells and no antibody production. This is accomplished by blocking the activity of V(D)J recombinase which is essential for creating the single-stranded nick in the DNA during V(D)J recombination (Mombaerts et al., 1992). Although the NRG and NSG mice share similar immunocompromised phenotypes, the NRG is superior for use for hu-mice models as they are less radiation sensitive. NRG mice lack the Prkdc-scid mutation and are therefore better at repairing the DNA damage that occurs during radiation conditioning, which is an essential part of generating humanized mice (Skelton et al., 2018).

1.4.3 Next-generation humanized mouse models offer advantages in immune reconstitution and function:

However, only around 40% of NRG mice showed significant engraftment with human immune cells following engraftment with human cord blood-derived HSCs (Danner et al., 2011; Dykstra et al., 2016). Although huNRG mice are able to generate modest Ag-specific T cell responses and can secrete low levels of some inflammatory cytokines under certain conditions, these levels are generally quite low and significant differences may be difficult

to observe due to high variability (Cheng, Yu, et al., 2017; Sonntag et al., 2015; Yao et al., 2017). This limitation can be dramatically improved by engrafting NRG mice that are transgenic for human HLA complexes. These mice are genetically engineered to express human HLA on their cells, which allows engrafted human immune cells to interact with human HLA located on the surface of murine thymocytes during T cell education and maturation (Bevan, 1981). NRG mice transgenic for the human HLA class II allele HLA DR4/DRB1*0401, known as DRAG mice, have been shown to greatly improve the rate of human T cell reconstitution to approximately 90% and had significantly higher T cell levels in the blood compared to non-transgenic controls (Danner et al., 2011). These mice have been successfully used for studying the immune system in the context of antimicrobial responses (adenovirus, *Francisella tularensis* and dengue virus) and autoimmunity (rheumatoid arthritis) as they are able to generate more robust Ag-specific T cells with a diverse T cell repertoire targeted against both foreign and self-antigens, have improved pro- and anti-inflammatory cytokine profiles and better B cell function compared to traditionally used non-transgenic controls (Allam et al., 2015; Behrens et al., 2010; Billerbeck et al., 2013; Majji et al., 2016, 2018; Shultz et al., 2010; Szántó et al., 2004; Taneja & David, 2010). Previous studies have shown that these T and B cell-mediated responses generated in these mice occur in the context of HLA-restricted peptide presentation, which is an important feature for accurately recapitulating the human immune system and is not seen in non-transgenic hu-mouse models (Behrens et al., 2010; Shultz et al., 2010; Yu et al., 2010). The generation of HLA-restricted T cells also results in enhanced immune cell function, such as improved secretion of T cell-associated cytokines (IFNγ, TNFα and IL-

2), which results in improved interactions between helper T cells and other immune cells its environment (Danner et al., 2011). This facilitates B cell function, including the ability to undergo isotype switching and a significant improvement in all IgG and IgA antibody responses, which are not present in humanized NRG mice (Danner et al., 2011). There are also NRG mice transgenic for the human HLA class I allele HLA-A2.1/A*0201 (A2) that show enhanced immune cell function but the addition of this HLA does not significantly improve T cell reconstitution, which suggests that the HLA class I molecule is less important for human immune cell engraftment that the HLA class II molecule (Majji et al., 2016). Interestingly, the addition of the HLA class I molecule does offer some advantages in terms of improvements in antigen-specific cytotoxic CD8+ T cell responses (Billerbeck et al., 2013; Majji et al., 2016). Hu-mice transgenic for HLA class I have been similarly shown to generate HLA-restricted T cell responses following infection with dengue virus or Epstein-Barr virus (Jaiswal et al., 2012; Shultz et al., 2010). Utilizing hu-mice transgenic for both HLA class I and II offers even greater immune function as the benefits of both transgenes are present (Brumeanu et al., 2020; Majji et al., 2018; Mendoza et al., 2020). Although transgenic models of hu-mice offer many benefits in terms of improving engraftment and generating more robust immune responses, there is the added requirement of using HLA-matched CD34+ HSCs for engraftment to allow T cell education to occur under the context of human HLA complexes (Majji et al., 2016). Theoretically, there is an expectation that mice transgenic for human HLA will have lower rates of graft-vs-host disease (GvHD), although this has not been published in the literature.

1.4.4 Cord blood as a source for progenitor cells:

Following childbirth and the subsequent delivery of the placenta, the remaining blood within the placenta and umbilical cord is known as cord blood. Although cord blood contains the same components (erythrocytes, leukocytes, plasma and platelets) as peripheral blood obtained from adults, there is a higher incidence of immature cell phenotypes and progenitor cells (Lee et al., 2010). For example, cord blood is known to contain nucleated RBCs, higher levels of immature T cells and is rich in various hematopoietic and non-hematopoietic progenitor stem cells (Lee et al., 2010). Cord blood-derived stem cells are quite useful as a therapeutic as they can be used to reconstitute the immune system following conditioning therapy in order to treat a variety of hematopoietic, autoimmune and genetic disorders, as well as various forms of cancer (Gluckman et al., 1989; Lee et al., 2010). CD34 is cell surface marker found primarily on the surface of progenitor HSCs and plays a role in mediating cell adhesion. CD34 is thought to play an important role in mediating the attachment of HSCs to the extracellular matrix of the bone marrow (Lee et al., 2010). For these reasons, CD34 is commonly used as a marker for HSCs. Unprocessed cord blood has a CD34+ HSC frequency of approximately 0.1-1% of the total nucleated cells (Kinniburgh & Russell, 1993). To be used for experimentation, cord blood is enriched by either positive or negative selection. In negative selection, a cocktail of antibodies is used to target and remove other cell markers, leaving only CD34+ HSCs behind. Although this method generally results in lower purity, it is often preferred since it leaves the CD34+ HSCs untouched by antibodies that may interfere with its function (Beliakova-Bethell et al., 2014).

CD34+ HSCs obtained from cord blood or fetal liver are the preferred source of progenitor stem cells due to the higher frequency of undifferentiated progenitor stem cells compared to cells recovered from bone marrow or mobilized peripheral blood obtained from adults (Drake et al., 2012). However, fetal tissues are much more difficult to obtain due to restrictions in sample availability and legal implications. Once isolated, CD34+ HSCs are engrafted into immunocompromised mice pre-conditioned with irradiation, which allows for the development of a functional human immune system. There are several methods of engraftment that may be used to generate hu-mice. The most commonly used method is by IV infusion of HSCs which has successfully been used in adult mice of various backgrounds (Ito et al., 2002; Pearson et al., 2008; Shultz et al., 2005; Verma & Wesa, 2020). However other methods of engraftment are also being explored, such as intrahepatic (IH) injections in newborns pups or surgical implantation of tissue fragments. IH engraftment of HSCs has also recently shown to be an equally effective, if not slightly superior, method for generating hu-mice (Dykstra et al., 2016; Reddy et al., 2020; Shultz et al., 2005; Song et al., 2020). Previous studies have shown that the liver is an important site for extramedullary hematopoiesis in newborns, as HSCs and other progenitor cells are thought to migrate from the liver into the bone marrow in the early stages of hematopoiesis and as such other a promising location for HSC engraftment for optimal immune cell reconstitution in hu-mice (Clapp et al., 1995; Keller et al., 1999; Wolber et al., 2002).

1.4.5 Previous use of humanized mice for HIV-1:

Hu-mouse models are extremely useful in the study of human-tropic infectious diseases, such as HIV-1, where normal mouse models are not a viable model for the study of the disease. Murine immune cells are not infected with HIV and normal mice do not develop HIV infection or AIDS (Marsden & Zack, 2017). NHP models of simian immunodeficiency virus (SIV) infection have been useful in studying the development of simian AIDS, but there are some marked differences between SIV infection in NHPs and HIV infection in humans as they are two genetically distinct viruses (Pollom et al., 2013). HIV-1 is not able to infected NHPs as human CD4, CCR5 and/or CXCR4 are essential for viral entry and replication. Some studies have found variability of up to 50% between the RNA sequences of SIV and HIV, resulting in significant differences in the secondary structure of the Env and Gag-Pol polyproteins during viral entry, replication and virion release (Pollom et al., 2013). In particular, this is problematic when evaluating the efficacy of vaccine candidates and immunotherapies targeted against specific HIV-1 antigens, as these antigens are not homologous between the two viruses (Joag et al., 1997; Stephens et al., 1996). In an attempt to address this problem, chimeric simian-human immunodeficiency viruses (SHIV) were developed as they are able to infect NHPs while expressing important HIV-1 antigens (Joag et al., 1996; Reimann et al., 1996). Strains of SHIV are often comprised of an SIV backbone and genetically engineered to expressed HIV-1 genetic material, typically the Env protein, followed by serial passaging in NHPs until virulence was observed (Joag et al., 1996; Reimann et al., 1996). Although NHP models are permissive to infection with most strains of SHIV, the HIV-1 Env protein may still show reduced affinity for simian CD4 in certain

strains of SHIV, which results in important difference in disease progression compared to either virus in their natural host (Bar et al., 2019; Joag et al., 1996; Reimann et al., 1996, 1999). For these reasons, humanized mouse models have been particularly useful in recent years as they are permissive to HIV-1 as target cells expressing human CD4 and CCR5/CXCR4 are developed in these models. There are also important ethical considerations when using NHP models that are significantly more stringent than what is required for mouse models, which can further limit experimental design.

Traditionally, hu-mouse models of HIV-1 infection have used either NSG or NRG mice engrafted with CD34+ HSCs and/or fetal tissues. These mice have been shown to be permissive to productive infection following either systemic (via IV or intraperitoneal (IP) delivery) or mucosal (vaginal and rectal) routes to simulate exposure through contaminated needles/blood products or sexual transmission, respectively (Balazs et al., 2014; Kim et al., 2017; Sun et al., 2007). Currently, the vast majority of HIV infections are transmitted through sexual intercourse, with 53% of new infections occurring in women and girls, and as such mucosal routes of infection, particularly intravaginally, need to be investigated further (UNAIDS, 2020; WHO, 2020a). These models have shown that HIV-1 infection in hu-mice is dependent on the frequency of target human immune cells in the blood and tissues (Nguyen et al., 2017). There is a significant correlation between HIV-1 susceptibility and the frequency of target human immune cells in the blood of hu-mice, with a frequency of 10% human CD45+ of the total blood leukocyte population being adequate to sustain infection (Nguyen et al., 2017). These models are characterised by detectable HIV-1 RNA, as well as depletion of CD4+ T cells, in the blood and tissues

following mucosal or systemic infection (Berges et al., 2008a, 2010; Denton et al., 2008, 2012; Gorantla et al., 2007; Honeycutt et al., 2017; Marsden & Zack, 2017; Nguyen et al., 2017; Quispe Calla et al., 2018; Sun et al., 2007). Since the transgenic DRAG mice show significantly higher T cell reconstitution and function, it's likely this model is a superior model for HIV-1 infection. In fact, humanized DRAG mice have also been successfully used to study HIV-1 infection in previous literature (Allam et al., 2015; Kim et al., 2017). Viral RNA was detected in the blood plasma starting at 1 week post-infection, peaked around 2 weeks post-infection, and was then maintained for 4 months indicating chronic infection was achieved (Kim et al., 2017). These mice also showed high levels of viral RNA in the bone marrow and spleen by 3 weeks post-infection (Kim et al., 2017). Since this model has also been shown to have improved T cell-specific cytokine and antibody production, this model may be useful to develop and investigate immunotherapies or vaccines against HIV-1 (Danner et al., 2011; Majji et al., 2016).

1.4.6 Previous use of humanized mice for TB:

Normal mouse strains are susceptible to *Mtb* infection and are commonly used to investigate TB. Although these models have been helpful in elucidating the mechanisms of disease progression, most normal strains of mice are more resistant to TB compared to humans due to differences in key genes involved in mediating defenses against *Mtb* and show important differences in inflammatory responses. Thus, normal mouse models of TB do not develop the same pathology but are still unable to effectively control the disease and will eventually succumb to infection (Apt & Kramnik, 2009; Franco et al., 2012; Kramnik

et al., 2000; Singh & Gupta, 2018). The major limitations of mouse models of TB are their low susceptibility to *Mtb* infection and the lack of development of necrotic lung tissue, caseation and cavitation within the granulomas, which are all hallmarks of pulmonary TB in humans (Singh & Gupta, 2018). Other animal models of TB, such as NHPs, are a more reliable reproduction of human TB but their high cost and major ethical consideration limit their usefulness.

The implementation of hu-mouse models for use in *Mtb* experiments offers several advantages over normal mouse models. In particular, hu-mouse models of TB develop caseating necrotic cores within their granulomas, a feature of human TB that is not well recapitulated in normal mouse models of TB (Apt & Kramnik, 2009; Arrey et al., 2019; Calderon et al., 2013). NSG mice humanized with CD34+ HSCs infected with *Mtb* develop necrotic lesions, bronchial obstruction and cholesterol crystals in the lung tissues that are very similar to what is observed in humans (Arrey et al., 2019; Calderon et al., 2013). Bacterial dissemination was observed from the primary infection site to the spleen and liver within a few weeks after infection (Arrey et al., 2019; Calderon et al., 2013). Human T cells were recruited to sites of bacterial replication and inflammation throughout the lung, liver and spleen, as well as at the periphery of granulomas (Calderon et al., 2013). huNRG mice were able to generate modest *Mtb*-specific T cell cytokine secretion (IFNγ, TNFα and IL-2) following immunization with an adenoviral-based vaccine expressing the *Mtb* antigen Ag85A (Yao et al., 2017). These features are not observed in non-humanized mouse models, demonstrating the benefits of using hu-mice to study TB despite the existence of well-established small animal models. Although these models look promising, they have

only been used sparingly in traditional hu-mouse models and never before used in next-generation transgenic models (Arrey et al., 2019; Calderon et al., 2013; Zhao et al., 2015).

1.4.7 Humanized mice are feasible small animal models of HIV/TB co-infection:

There are currently very few humanized mouse models of HIV-1 and TB co-infection. Up until recently, NHP models were the primary method of studying SHIV or SIV and TB co-infection. Not only is SIV genetically distinct from HIV, but NHP models are expensive and subject to ethical debate. In the first ever reported model of HIV/TB co-infection in hu-mice, Nusbaum et al. (2016) showed that co-infected NSG mice humanized with fetal bone marrow, liver and thymus (BLT) had more severe CD4+ T cell depletion and increased viral and bacterial loads compared to HIV-1 or TB only groups. There was a significant correlation between increased viral load and *Mtb* bacterial load in co-infected mice. Co-infected mice also showed increased granuloma dissemination and necrotic caseation compared to *Mtb* only controls (Nusbaum et al., 2016).

HIV-1 and TB co-infected mice showed lesion pathology in the lung that is similar to lesion pathology of co-infected humans (Nusbaum et al., 2015; Nusbaum et al., 2016). Not only did co-infection exacerbate TB disease in humanized mice, but HIV-infected cells were primarily localized within TB lesions in the lung tissue (Nusbaum et al., 2016). HIV-1 and TB co-infection has also been associated with neutrophil accumulation in the lung tissue of co-infected mice and was linked to an increased *Mtb* burden and tissue necrosis (Nusbaum et al., 2015). Others studies have shown that HIV-1 infection in BLT-NSG mice leads to a severe depletion of CD4+ T cells in the lung interstitial space, which is a feature that is

associated with increased risk of dissemination (Corleis et al., 2019). More severe CD4+ T cell depletion was also associated with increased bacterial dissemination in similar NHP models of TB reactivation in macaques following co-infection with SIV (Corleis et al., 2019; Diedrich et al., 2010). In a similar BLT-NSG model of HIV-induced TB relapse following chemotherapy-induced latency, HIV-1 infection was shown to significantly increase the rate of TB reactivation, as well as bacterial load and dissemination and viral load following the completion of an 8 week course of rifampin and isoniazid (Huante et al., 2020). This is the first known use of a hu-mouse model of co-infection where HIV-1 was administered subsequent to a primary latent TB infection resulting in reactivation of the TB. This is an important advancement in hu-mouse models of co-infection as reactivation of latent TB with a subsequent HIV-1 infection commonly occurs in humans with almost a quarter of the world's population latently infected with *Mtb* (WHO, 2020b). In preliminary data, Naqvi et al. (2018) also showed that HIV-1 and TB co-infection may have been associated with uncontrolled inflammation in the lung tissue and exacerbations in lung pathology of humanized Balb/c mice. Since HIV-1 and *Mtb* can both infect macrophages, it is thought that co-infection leads to an increase in inflammatory activity that is likely detrimental to the host (Naqvi et al., 2018). Hu-mouse models are ideal for investigating HIV-1 and TB co-infection as they recapitulate many features of disease in humans and they offer improvements over traditional mouse models that are inadequate in reproducing the clinical manifestations of HIV and TB co-infection in humans. Hu-mouse models are also less expensive and less ethically complex than NHP models of SIV/TB co-infection and thus are often more feasible.

1.5 Rationale and Hypothesis:

The use of next-generation hu-mice that are transgenic for human HLA is a novel approach that has resulted in the development of more robust immune systems compared to traditional hu-mouse models (Fig. 1) (Allam et al., 2015; Danner et al., 2011; Kim et al., 2017; Majji et al., 2016, 2018; Mendoza et al., 2020). There are currently some important barriers and limitations to the use of small animal models for HIV and TB studies. The vast majority of research currently being done on HIV is either in *in vitro* settings, in NHP models of SIV/SHIV or in observational, clinical or epidemiological data. Although normal mouse models of TB are used extensively, there are important difference in pathology compared to human manifestations of TB (Arrey et al., 2019; Calderon et al., 2013). Due to the high global incidence of HIV and TB, as well as the complex interactions between these pathogens and the immune system, there is an urgent need for the development of updated humanized mouse models of HIV-1 and TB that will enable us to further investigate these pathogens, separately or during co-infection. We hypothesize that an HLA class I and II transgenic humanized mouse model (DRAG-A2) will be superior to the traditional humanized NRG mouse model in terms of generating human immune responses in the context of HIV-1 and TB infections, laying the groundwork for this model to be used for co-infection studies. huDRAG-A2 mice have been shown to have improved leukocyte and T cell reconstitution compared to huNRG mice and also produce significantly improved cytokine and isotype-switched immunoglobulin (Ig) responses (Danner et al., 2011; Majji et al., 2016) (Fig. 1). All of these factors should contribute to the creation of models of HIV-1 and TB that are clinically relevant and will allow us to further investigate

HIV-1 and TB disease progression, vaccination, treatment, prophylaxis and transmission in the context of human immune responses. These advantages will likely also render the DRAG-A2 model a promising candidate for investigating HIV/TB co-infection.

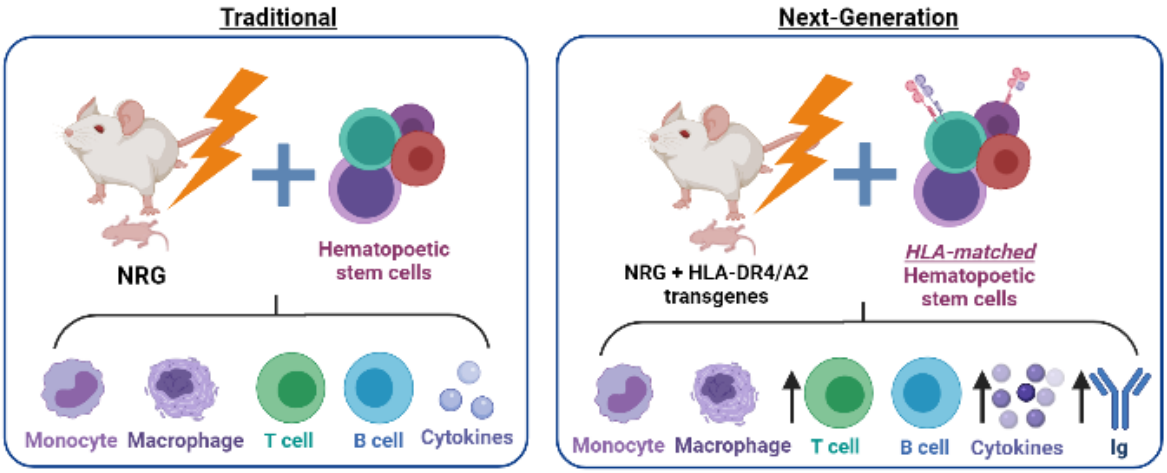

Fig. 1. *Comparison between traditional huNRG (left) and next-generation HLA-transgenic DR4/A2 (right) hu-mouse models (Danner et al., 2011; Majji et al., 2016) (created with BioRender).*

1.6 Specific Aims:

AIM 1: Determining the best method for humanizing NRG and DRAG-A2 mice.

AIM 2: Establishing and validating clinically relevant models of intravaginal and systemic HIV-1 infection in huNRG and huDRAG-A2 mice.

AIM 3: Establishing and validating a clinically relevant model of TB in huNRG and huDRAG-A2 mice.

2. METHODS:

2.1. AIM 1: Determining the best method for humanization in NRG and DRAG-A2 mice.

As discussed in Chapter 1, the humanized NRG and DR4/A2 transgenic models show promise as small animal models of HIV-1, TB and HIV/TB co-infection due to their ability to develop a human immune system once engrafted with progenitor HSCs, including robust populations of all major immune cell subsets involved in mediating these infectious diseases (Danner et al., 2011; Dykstra et al., 2016; Majji et al., 2016). A similar next-generation huDRAG-A2 model offers significant improvements in terms of T cell, cytokine and antibody responses compared to the more commonly used huNRG mice (Danner et al., 2011; Majji et al., 2016). huNRG mice have successfully been generated following infusions of cord blood-derived CD34+ HSCs in both adult and neonate mice via IV or IH injection, respectively (Cheng et al., 2018; Dykstra et al., 2016; Pearson et al., 2008; Vanshylla et al., 2021). To date in the literature, huDRAG-A2 mice have only been generated using the adult method of engraftment and the effectiveness of the IH neonate engraftment needed to be confirmed (Allam et al., 2015; Brumeanu et al., 2020; Danner et al., 2011; Majji et al., 2016, 2018). The liver is thought to be an important site for early extramedullary hematopoiesis in neonates and may offer advantages over more commonly used methods (Clapp et al., 1995; Keller et al., 1999; Wolber et al., 2002). Newborn engraftment also offers some practical advantages as mice are available for experiments at a younger age and thus have fewer health problems.

2.1.1 Breeding NRG and DRAG-A2 mice for engraftment:

NRG mice (JAX, stock# 007799), as well as NRG mice with a transgene for human HLA-DR4/DRB1*0401 (JAX, stock# 017914) (DRAG) were obtained from the Jackson laboratories. NRG mice homozygous for the transgene for human HLA-A2.1/A*0201 (A2) were obtained as a generous gift from Dr. Ali Ashkar and Dr. Yonghong Wan (McMaster University) following 12 generation of back-crossing of the HLA-A2 transgene from the NSG-A2 strain (JAX, stock # 009617) onto an NRG background. One founder DRAG breeding pair was obtained as heterozygotes and produced several litters of pups (F1). Pups were weaned at 3 weeks of age and ear tagged. DNA was extracted from small samples of ear tissue using the DNeasy Blood & Tissue Kit (QIAGEN, cat# 69506) and was polymerase chain reaction (PCR) genotyping was performed using the Platinum II Hot-Start PCR Master Mix (Invitrogen, cat# 14000011) using primers specific for the DRAG allele (Forward primer: 5'-GTTTCTTGAGCAGGTTAAAC-3'; Reverse primer: 5'-CTGCACTGTGAAGCTCTCAC-3'; Forward internal control: 5'-CAAATGTTGCTTGTCTGGTG-3'; Reverse internal control: 5'-GTCAGTCGAGTGCACAGTTT-3') and ran on a 1.5% agarose gel (Invitrogen, cat#16500-500) combined 6:1 with EZ VISION loading dye (VWR, cat# 97064-190) to visualize the DNA. Double-banded wells are DRAG-positive and single-banded wells are DRAG-negative, as negative wells only contain the internal control (~271 bp) and not the transgene (~324 bp). Female and male DRAG-positive mice (F1) were identified and then bred with DRAG-negative NRGs to determine their zygosity. The resulting pups (F2) were also genotyped for the DRAG allele. F1 DRAG-positive mice that produced only DRAG-

positive pups (F2) were identified as DRAG homozygotes after at least 15 DRAG-positive progeny, while F1 DRAG-positive mice that produced any DRAG-negative pups (F2) were identified as DRAG heterozygotes. The DRAG homozygous mice were then bred together to establish a DRAG homozygous breeding colony. In contrast, the A2 mice were obtained as homozygotes and did not need to be homozygoused. However, A2 mice were genotyped occasionally to confirm the presence of the A2 allele. DNA was extracted as previously described and PCR genotyping was performed using the MyTaq HS Red Mix (Bioline, cat# BIO-25047) using primers specific for the A2 allele (Forward primer: 5'-TTCTCCCTCTCCCAACCTATGTAG-3'; Reverse primer: 5'-CGACGACACTGATTGGCTTCT-3') and gel electrophoresis as previously described. Wells with DNA bands of approximately 130bp are A2-positive and wells with DNA bands of around 220bp bands are A2-negative. DRAG homozygotes were cross-bred with A2 homozygous mice to create NRG mice with both the HLA-DR4 and HLA-A2 transgenes (DRAG-A2) and genotyped to confirm the presence of these transgenes. While using DRAG homozygous is more effective for generating DRAG-A2 pups (100% of the pups will be DRAG positive), the homozygousing process is very time consuming and we have also been crossing DRAG-positive mice that have not yet been identified as heterozygotes or homozygotes with A2 homozygotes in order to produce DRAG-A2 mice more rapidly. The pups were genotyped at 3 weeks of age to identify the DRAG-A2 double-positive pups for subsequent humanization at 6-10 weeks of age.

2.1.2 Optimizing panels for flow cytometry:

Human peripheral mononuclear cells (PBMC) and/or murine splenocytes (obtained from C57Bl/6 mice) were treated with human Fc block (eBiosciences, cat# 14-9161-73) and/or murine Fc block (eBiosciences, cat# 14-0161-82). Then stained with various antibodies (as described in Table 1) in order to determine the optimal quantity for use in future experiments, followed by fixation with a 2% paraformaldehyde (PFA) solution in PBS. Fluorescence minus one (FMO) and isotype controls were used to determine accurate positive and negative populations for each antibody. Cells were acquired using the CytoFlex LX cytometer (Beckman Coulter) and analyzed using Flow Jo software.

Table 1. *Summary of optimization strategy for flow cytometry antibody panels.*

Panel	Marker	Indicator Of	Clone	Fluorochrome	Suggested quantity	Optimal quantity	Manufacturer	Catalog #
All	Dead cells	Viability	-	eFluor 780	1:100	1:1000	eBiosciences	65-0865-14
Cord Blood	hCD34	Progenitor HSCs	4H11	APC	5 uL	5 uL	eBiosciences	17-0349-42
	A2	HLA-A2	BB7.2	PE	5 uL	5 uL	eBiosciences	12-9876-42
Humanized mice	hCD45	Human leukocytes	H130	Pacific Blue	5 uL	5 uL	eBiosciences	MHCD4528
	mCD45	Murine leukocytes	30-F11	Alexa Fluor 700	2.5 uL	2 uL	eBiosciences	56-0451-82
	hCD3e	T cells	UCHT1	Qdot 605	1 uL	1 uL	eBiosciences	Q10054
	hCD4	Helper T cells	RPA-T4	PerCP-Cy5.5	5 uL	5 uL	eBiosciences	45-0049-42
	hCD8a	Killer T cells	RPA-T8	PE-Cy7	5 uL	5 uL	eBiosciences	25-0088-42
	hCD19	B cells	HIB19	PE	5 uL	5 uL	eBiosciences	12-0199-42
	hCD14	Monocytes/ macrophages	Tuk4	Alexa Fluor 647	5 uL	5 uL	eBiosciences	A51013
	hCD16	NK cells/ monocytes	3G8	FITC	5 uL	2.5 uL	BioLegend	302006
	hCD11b	Monocytes/ macrophages	CBRM1/ 5	PerCP-Cy5.5	5 uL	5 uL	BioLegend	301418
	hCD14	Monocytes/ macrophages	M5E2	BV785	5 uL	4 uL	BioLegend	301840
	hCD169 (Siglec-1)	Alveolar macrophages	7-239	PE	5 uL	2 uL	BioLegend	346004
	hCD206	Monocytes/ macrophages	15-2	APC	5 uL	10 uL	BioLegend	321110
	IFNγ	T cell associated cytokines	4S.B3	PE	5 uL	5 uL	eBiosciences	12-7319-42
	TNFα		MAb11	FITC	2 uL	2 uL	eBiosciences	11-7349-81
	IL-2		MQ1-17H12	APC	1.25 uL	1.25 uL	eBiosciences	17-7029-82

Fixable viability dye-eFluor 780 were optimized by the Ashkar lab; hCD11b-PerCP-Cy5.5, hCD14-BV785, hCD169-PE and hCD206-APC were optimized by the Xing lab

2.1.3 Obtaining and characterizing CD34+ HSCs:

Mice were humanized with CD34+ HSCs isolated from human umbilical cord blood as described in previous literature (Kwant-Mitchell, Ashkar, et al., 2009; Kwant-Mitchell, Pek, et al., 2009). Since we have begun collecting cord blood samples, we have processed and frozen down 75 samples. The cord blood samples were depleted of red blood cells (RBC) using a 6% hetastarch solution (HetaSep, StemCell, cat# 07906) as an erythrocyte aggregation agent. CD34+ HSCs were enriched from the remaining nucleated cells using a CD34 negative selection kit containing markers against CD2, CD3, CD14, CD16, CD19, CD24, CD56, CD61, CD66b on various mature immune cells and glycophorin A on RBCs (Human Cord Blood Progenitor Enrichment Kit, StemCell, cat# 15026). CD34+ HSCs were then separated using density gradient centrifugation (Lymphoprep, StemCell, cat# 07851) and frozen for storage in liquid nitrogen in a serum-free freezing media (CryoStor CS10, StemCell, cat# 07930). A small aliquot of the CD34+ HSCs were collected and compared to a sample of the non-selected cord blood-derived cells from the same sample using flow cytometry. This will allow us to confirm the efficacy of the CD34 negative selection kit in use. Cells were treated with human Fc block and stained with fixable viability dye (eFluor 780) and anti-human CD34-APC antibodies, and then analyzed using Flow Jo software. Some samples were also stained for CD3 (hCD3e-Qdot 605) as a measure of T cell depletion using the CD34 negative selection kit. Cord blood samples were also screened for HLA-DR4/DRB1*0401 using MicroSSP Allele Specific HLA-typing class II DNA typing trays - DRB1*0401 (OneLambda, cat# SSPR2-104), then for HLA-A2.1/A*0201 using MicroSSP Allele Specific HLA-typing class I DNA typing trays

- A*02 (OneLambda, cat# SSPR1-A2) and ran on a 2.5% agarose gel supplemented with GelRed nucleic acid stain (1uL per 10mL gel) (Biotium, cat# 41001) in order to visualize the DNA. Gels were analysed using the HLA Fusion Software to identify possible allele pairs, then cross-referenced with the Allele Frequencies Database to determine HLA type (www.allelefrequencies.net). Cord blood samples identified as both DRB1*0401 and A*0201 positive will be used to humanize DRAG-A2 mice, while DR4 and A2 negative samples will be used to humanize NRG mice. DNA extraction, PCR, gel electrophoresis and analysis were performed by Jack Yang.

2.1.4 Creating humanized NRG and DRAG-A2 mice:

NRG and DRAG-A2 mice were engrafted with human CD34+ HSCs in both the neonate (24-72 hours) and adult (6-10 weeks) stages of life. DRAG-A2 mice are engrafted with HLA-matched CD34+ HSCs, while NRG mice were not HLA-matched. Newborn pups were irradiated with 3 cGy twice; once three hours before engraftment and again immediately prior to engraftment. The irradiated pups were injected IH with $1x10^5$ - $1x10^6$ CD34+ HSCs in 30 uL phosphate buffered saline (PBS) (McMaster Media Stores). Pups were then returned to their mother until ready to wean at 4 weeks of age. Adult mice were irradiated with 550 cGy then injected IV with $5x10^5$ - $1x10^6$ CD34+ HSCs in 200 uL PBS. Adult mice were monitored regularly for signs of radiation poisoning or infection post-engraftment. At 12 and 16 weeks post-engraftment, approximately 50uL of blood was collected from the facial vein of all mice in order to measure the degree of human immune reconstitution using flow cytometry. Erythrocytes were lysed using an ACK lysis buffer (Quality Biological, cat# 10128-802) and the remaining cells were treated with both human

and mouse Fc block. Cells were then stained with fixable viability dye (eFluor 780), followed by a cocktail of antibodies (mCD45-AlexaFluor 700, hCD45-Pacific Blue, hCD3e-Qdot 605, hCD4-PerCP-Cy5.5, hCD8a-PE-Cy7, hCD19-PE, hCD14-AlexaFluor 647), and then ran on the CytoFlex LX cytometer equipped with a flow rate calibrator and analysed using Flow Jo software (Version 7 or 8) utilizing the gating strategy described below (Fig. 2). Briefly, the frequency of human CD45+ leukocytes was calculated as the portion of the total blood leukocytes (mouse and human) and the absolute count was calculated using the total number of positive cells extracted from a known volume of whole blood. Mice were assessed for GvHD based on symptomology (rapid weight loss, scabby skin and diarrhea) for the duration of their lifespan.

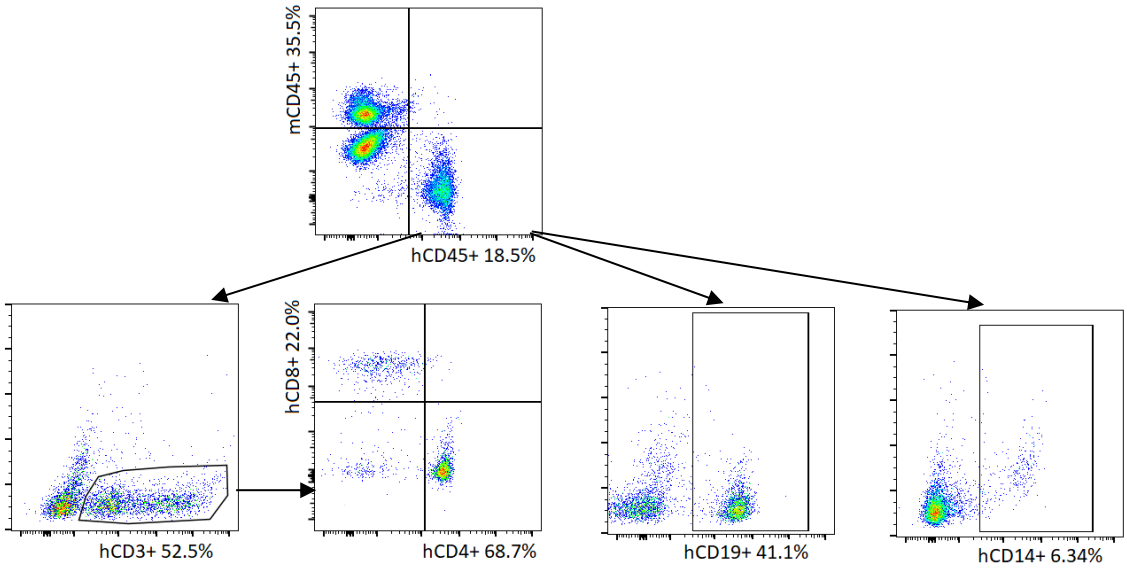

Fig. 2. *Gating strategy used for the flow cytometric analysis of the blood of humanized mice.* Shown here is an example of a successfully engrafted huDRAG-A2 mouse at 12 weeks post-engraftment.

2.2. AIM 2: Establishing and validating a clinically relevant model of HIV-1 infection in humanized NRG and DRAG-A2 mice.

2.2.1. Measuring the titre of HIV-1 stocks:

R5-trophic strains of HIV-1, NL4.3-Bal-Env and JR-CSF, were obtained as a generous gift from Dr. Charu Kaushic (McMaster University) and Dr. Andrés Finzi (Université de Montréal), respectively. Infectious titre was measured in both strains using TZMbl assays. TZMbl cells (generously provided by Dr. Charu Kaushic, originally obtained from the NIH AIDS Research and Reference Reagent Program, cat# 8129) are a HeLa cell line genetically engineered to express HIV-1's target receptors (CD4, CCR5 and CXCR4), as well as luciferase and β-galactosidase indicator genes. This allows simple and quantitative analysis of HIV infectivity as HIV-infected TZMbl cells turn blue. This assay is an accurate measure of infectious virus only and is not able to reliably detect non-infectious viral particles (Sarzotti-Kelsoe et al., 2014). TZMbl cells were plated in a 24-well plate at a concentration of $6x10^4$ cells per well and left to incubate at 37°C and 5% CO_2 for overnight. The media was then removed, and the cells were treated with DEAE-dextran (Pharmacia, cat# 17-0350-01) to a final concentration of 20 μg/mL to promote viral infection. HIV-1 stocks were then diluted in a 10-fold serial dilution using DMEM (McMaster Media Stores) as a diluent and 180 uL of pre-diluted HIV-1 was added to the cells and incubated for 2 hours at 37°C and 5% CO_2, then topped up with DMEM supplemented with 20% FBS (Gibco, cat# LS10082147) and incubated for another 48 hours. Duplicates for each dilution were included. Cells were then fixed with a 1% formaldehyde (Sigma, cat# F1635) and

0.2% glutaraldehyde PBS solution (Sigma, cat# G6257) and stained with an X-gal staining solution (0.4 mg/mL X-gal (Promega, cat# V394A), 0.004M potassium ferrocyanide (Sigma, cat# P-3289), 0.004M potassium ferricyanide (Sigma, cat# 24402-3) and 0.02M magnesium chloride (EM Science, cat# B10149-34) in PBS). The viral stocks infectious titres were calculated as the number of blue HIV-infected TZMbl cells divided by the total volume of virus corrected to account for the dilution factor and expressed as infectious units per mL (IU/mL).

2.2.2. Intravaginal infection of huNRG and huDRAG-A2 mice using NL4.3-Bal-Env:

Highly engrafted (%hCD45 of total leukocytes > 10%) female huNRG (N = 2) and huDRAG-A2 (N = 2) mice were infected intravaginally with NL4.3-Bal-Env HIV-1 to confirm susceptibility to infection (Fig. 3). huNRG mice with similar immune reconstitution levels as the huDRAG-A2 mice were selected as controls to prevent variability between the groups due to number of immune cells alone. One week prior to infection, the mice were treated subcutaneously with 2mg depot medroxyprogesterone acetate (DMPA) (McMaster Hospital Pharmacy, DIN# 00585092), an injectable synthetic progestin-based female contraceptive used in humans, in order to ensure the mice are in diestrus at the time of infection. In mice, the thickening of the epithelial barrier that occurs during estrus blocks migration of the virus into the mucosa and reduces the rate of successful infection, and thus diestrus is desired for intravaginal HIV-1 infection in order to minimize failed infections (Wessels et al., 2021). A vaginal lavage (2 x 30 uL sterile PBS pipetted in and out of the vaginal canal 8-10 times) was performed 5 days post-DMPA

and examined microscopically to confirm diestrus. The presence of many leukocytes but very few cornified epithelial cells in the vaginal lavage indicates the mice are in diestrus and are receptive to intravaginal infection (Wessels et al., 2021). Mice were anesthetized with 72 mg/kg ketamine (McMaster Hospital Pharmacy, DIN# 00224405) and 4.8 mg/kg xylazine (McMaster Hospital Pharmacy, DIN# 02169592) diluted in sterile saline (Hospira #04888010) via IP injection. The vagina was swabbed gently and $3.6x10^5$ TCID50 ($7.5x10^5$ IU) of NL4.3-Bal-Env HIV-1 in a 25 uL volume was pipetted into the vaginal canal. The mice were placed in a supine position with their tails elevated slightly until recovered from anesthesia (approx. 30-45 minutes).

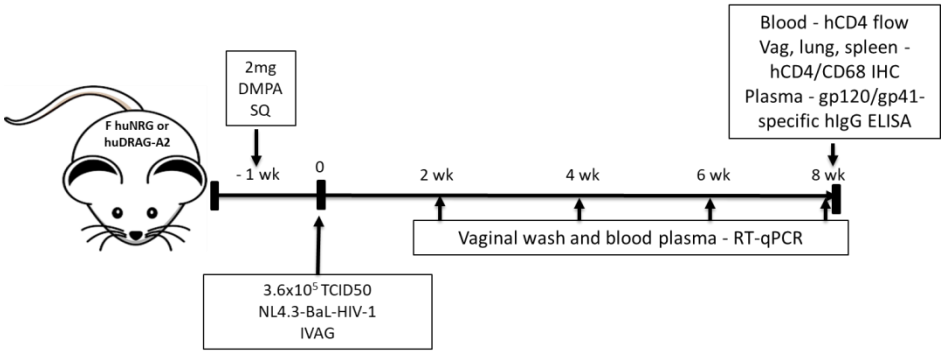

Fig. 3. *Experimental timeline for intravaginal HIV-1 infection in female huNRG and huDRAG-A2 mice.*

2.2.3. Quantification of viral load in the plasma and vaginal wash:

Vaginal lavage and blood plasma were collected at 2, 4, 6 and 8 weeks post-infection for viral load quantification using an in-house RT-qPCR assay. Whole blood was collected in EDTA-coated blood tubes (VWR, cat# CABD365974L) via facial or retro-orbital bleed and then centrifuged at 14,000 RPM for 5 minutes to remove cells, before collecting the plasma supernatant. Vaginal wash was collected as previously described. Samples were

stored frozen at -80°C. RNA was extracted from 50uL of plasma or vaginal wash using the QIAamp MinElute Virus Spin Kit (QIAGEN, cat# 57704) and RT-qPCR was performed using the SensiFAST Probe Hi-ROX One-Step Kit (FroggaBio, BIO-77005) using primers and a Taqman probe (ThermoFisher) specific for the HIV-1 long terminal repeat (LTR) promoter (Forward primer: 5′-GCCTCAATAAAGCTTGCCTTGA-3’; Reverse primer 5′-GGCGCCACTGCTAGAGATTTT-3’; Reporter probe: 5′-AAGTAGTGTGTGCCCGTCTGTTRTKTGACT-3’, 5′ reporter 6-FAM and 3′ quencher TAMRA). Vaginal wash and plasma from previously successfully infected humanized mice were obtained as a generous gift from Dr. Charu Kaushic and used as positive controls. Vaginal wash and plasma from non-infected mice was used as negative controls. No template and no reverse transcriptase controls were also included to detect contamination. RT-qPCR was performed using an in-house assay and Ct values were quantified using a standard curve extrapolated using samples quantified by the Mount Sinai Department of Microbiology (Toronto, Ontario).

2.2.4. Quantification of target cell depletion:

Whole blood was also collected at 8 weeks post-infection to measure target cell depletion in the blood using flow cytometric analysis, as previously described. Briefly, cells were stained with an antibody cocktail (hCD45-PacBlue, mCD45-Alexa Fluor 700, hCD3e-Qdot 605 and hCD4-PerCP-Cy5.5) and analysed to measure human CD4+ T cell depletion following infection. The lung and vaginal tissues were also collected at 8 weeks post-infection and fixed in 10% formalin (McMaster Histology Core Facility) for 1 week to

measure target cell depletion in the tissues using human CD4+ T cell, CD68+ macrophage immunohistochemistry (IHC). Briefly, sections were deparaffinized and boiled in Tris/EDTA (pH=9) for 20 minutes in a microwave. After blocking with 5% bovine serum albumin (BSA), sections were incubated with 1:50 mouse anti-human CD4 monoclonal antibodies (clone 4B12, Leica Biosystems, cat# PA0371) or mouse anti-human CD68 monoclonal antibodies (clone PG-M1, Dako, cat# GA61361-2) for 1 hour at room temperature, followed by visualization using the Bond Polymer Refine Red Detection kit (Leica BioSystems, cat# DS9390) on an automated Leica Bond RX autostainer (Leica Biosystems). Human tonsil and non-humanized NRG mouse lung sections were used as positive and negative controls, respectively (Fig. 4).

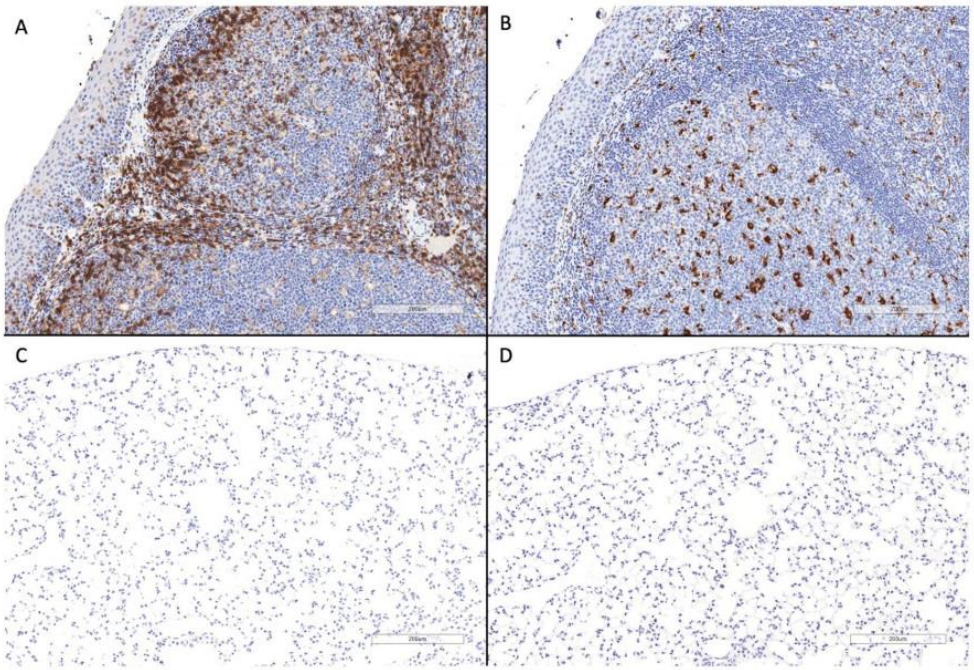

Fig. 4. *Immunohistochemistry positive and negative controls.* Top: Human tonsil **(a)** hCD4+ and **(b)** hCD68+ IHC positive controls. Bottom: Non-humanized NRG mouse lung **(c)** hCD4+ and **(d)** hCD68+ IHC negative controls (all 20x, scale bar = 200μm).

2.2.5. Quantification of cytokine profile and antibody production:

To measure cytokine production in our humanized mice following HIV-1 infection, inactivated blood plasma samples were analysed using the Human Cytokine Array/Chemokine Array 48-plex assay (Eve Technologies Corp., Calgary, Alberta, cat# HD48). Cytokine levels were initially reported as pg per mL of blood plasma and corrected to account for dilution with inactivation buffer (4 parts sample to 1 part inactivation buffer, then diluted further with sterile PBS to a final dilution of 1:2). Although IFNγ, TNFα and IL-2 can be produced by a wide variety of immune cells, T cells are thought to be the major producers of these cytokines in many similar hu-mice models (Shultz et al., 2012; Skelton et al., 2018). Since considerable T cell depletion was observed in these mice following chronic infection with HIV-1, cytokine secretion was also quantified as the amount of cytokines (pg/mL) in the blood plasma divided by the total number of human CD3+ T cells per mL of whole blood collected at the same time-point, as determined by flow cytometry. Blood plasma was also collected at 8 weeks post-infection and analysed for the presence of HIV-specific human IgG antibodies using the Human Anti-HIV-1 gp120/gp41 IgG ELISA Kit (Alpha Diagnostics, cat# HIV-060). Non-humanized NRG controls were included to detect any cross-reaction with mouse IgG antibodies. Plasma samples were diluted 1:100 and analysed as per the manufacturer's guidelines. Experimental sample values were expressed relative to the values of negative control and blank wells as suggested by the manufacturer. Net optical density (OD) was calculated as the difference between the final and initial OD readout. A positive index (PI) was calculated as the net OD mean of negative control wells + 2 standard deviations. The net OD of each tested sample was divided by the

positive index (net OD/PI). Sample values with net OD/PI greater or less than 1.0 are considered positive or negative for antibody activity, respectively.

2.2.6. Validation of systemic and intravaginal infection of huNRG mice using JR-CSF:

Highly-engrafted (%hCD45 of total leukocytes > 10%) male and female huNRG mice were infected either systemically (N=5) or intravaginally (N=2) with JR-CSF to confirm susceptibility to infection with this strain of HIV-1 (Fig. 5). For systemic infection, male mice were anesthetized briefly with gaseous isoflurane and $1x10^5$ (N=2) or $1x10^6$ (N=3) IU of JR-CSF HIV-1 in 100 uL PBS was injected IP. For intravaginal infection, female mice (N=2) were infected with $1x10^6$ IU JR-CSF as previously described. Blood plasma was collected at 1, 2, 4, 6 and 8 weeks post-infection for viral load quantification using RT-qPCR, as previously described. The low dose IP mice were followed up until 18 weeks post-infection in order to capture both the acute and chronic phases of the infection. Whole blood was also collected from all mice at 4, 6 and 8 weeks post-infection for flow cytometric analysis to measure human CD4+ T cell frequency post-infection, as previously described. The low dose mice IP were also tested at 16 weeks post-infection to measure chronic T cell depletion in the blood.

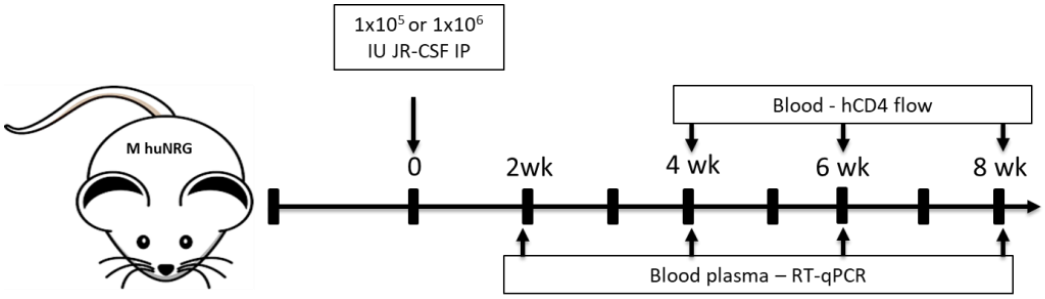

Fig. 5. *Experimental timeline for systemic HIV-1 infection in male huNRG mice.*

2.3. AIM 3: Establishing and validating a clinically relevant model of TB in humanized NRG and DRAG-A2 mice.

2.3.1. Intranasal infection in huNRG and huDRAG-A2 mice with various strains of Mtb:

Highly-engrafted (%hCD45 of total leukocytes > 10%) huNRG and huDRAG-A2 mice were infected intranasally with 25 uL of *Mtb* and we aimed for a dose of $1x10^4$ CFU (Fig. 6). Mice were anesthetized briefly with gaseous isoflurane and infected intranasally with confirmed titres of either $6.1x10^3$ CFU of mCherry-Erdman (N = 2 huNRG), $1.0x10^4$ CFU of YFP-tagged H37Rv (N = 2 huNRG) or $1.9x10^4$ CFU of normal H37Rv (N = 3 huNRG and 3 huDRAG-A2) obtained as a generous gift from Drs. Samuel Behar and Rocky Lai (University of Massachusetts) (fluorescently-tagged *Mtb*) and Dr. Zhou Xing (McMaster University), respectively. At 3-4 weeks post-infection, the lung and spleen were collected for pathological scoring and bacterial load quantification using CFU enumeration.

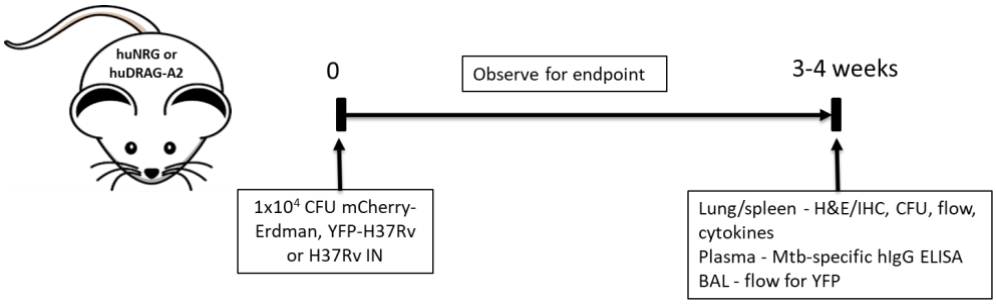

Fig. 6. *Experimental timeline for intranasal TB infection in huNRG and huDRAG-A2 mice.*

2.3.2. Quantification of bacterial load in the lung and spleen:

Briefly, the right lobe of the lung and a third of the spleen were homogenized mechanically in 2mL of PBS supplemented with 10% glycerol (Fisher Scientific, cat# FLBP2291) and

0.1% Tween 80 (Fisher Scientific, cat# T164500) and 10-fold serial dilutions were plated on Middlebrook 7H10 agar plates (Fisher Scientific, cat#DF0627174) containing 10% Middlebrook oleic acid-albumin-dextrose-catalase (OADC) enrichment (Fisher Scientific, cat# B11886) and supplemented with 0.5% glycerol, 5 μg/mL ampicillin (Sigma, cat# A5354) and 50 μg/mL cycloheximide (Sigma, cat# C7698). Plates were incubated for 3 weeks at 37°C and the colonies were counted to quantify the bacterial load. The left lobe of the lung and another third of the spleen were also collected and fixed in 10% formalin for 1 week, then stained with Hematoxylin and Eosin (H&E), acid-fast bacilli (AFB) staining (McMaster Histology Core Facility), as well as human CD4+ T cell and CD68+ macrophage immunohistochemistry, to visualise granulomas, as previously described.

2.3.3. Preparation of tissues for flow cytometry:

A small portion of the lung (auxiliary lobes) was also analysed using flow cytometry as previously described (Yu et al., 2016). Briefly, lung tissue was digested in a type 1 collagenase solution for 1 hour (10U/mL) (Fisher Scientific, cat# 17100017) and stained with an antibody cocktail (hCD45-Pacific Blue, hCD3e-Qdot 605, hCD14-BV 785, hCD11b-PerCP-Cy5.5, hCD16-FITC or Alexa Fluor 700, hCD169-PE and hCD206-APC) to measure human macrophages populations in the lung post-infection. When using the fluorescently-tagged strains of *Mtb*, the frequency of mCherry or YFP-positive *Mtb*-infected alveolar macrophages was also measured. For the mice infected with YFP-H37Rv, this analysis was performed in the BAL instead of the lung. Briefly, mice were euthanized by isoflurane overdose and exsanguination before the chest cavity was opened and the lung-

heart complex was removed intact. The trachea was cannulated with a 23G needle threaded with plastic tubing to blunt the tip and tied into placed using sutures. An exhausting lavage (250uL, 200uL, 300uLx3 for a total of 1.35mL RPMI 1640 media (McMaster Media Stores)) was performed using a 1mL syringe and collected. The BAL fluid was passed through a 40μm cell strainer (VWR, cat# 352340) to ensure a single cell suspension and then stained with the lung macrophage antibody panel described previously for flow analysis. Splenocytes were mechanically extracted from the remaining spleen by crushing through a 100μm filter (VWR, cat# 352360) and lysed with ACK lysing buffer before staining with an antibody cocktail to measure T cell frequency (mCD45-AlexaFluor 700, hCD45-Pacific Blue, hCD3e-Qdot 605, hCD4-PerCP-Cy5.5, hCD8-PE-Cy7, hCD19-PE) and analysed using FlowJo software.

2.3.4. Quantification of cytokine profile and antibody production:

Blood plasma was also collected at 4 weeks post-infection from the H37Rv-infected huDRAG-A2 and huNRG mice and was analysed for the presence of *Mtb*-specific human IgG antibodies using the *Mycobacterium tuberculosis* IgG ELISA kit (antigens: 18, 36 and 40 kDa) (GenWay BioTech, cat# GWB-FFE4D4). Non-humanized NRG controls were included to detect any cross-reaction with mouse IgG antibodies. Plasma samples were diluted 1:50 and analysed as per the manufacturer's guidelines. Lung homogenates were also collected for multiplex human cytokine quantification, as previously described. To quantify the total cytokine levels in the whole lung, the concentration of cytokines in the

lung homogenate (pg/mL) was multiplied by the total volume of lung homogenate (2mL) and tissue factor (1 lobe = tissue factor of 2).

2.4. Statistical analysis:

Data were analyzed using FlowJo software Version 10.7.1, 10.8.0 or 10.8.1 (flow cytometry), HLA Fusion software Version 4.2.0 (HLA-typing gels) or GraphPad Prism 6 software. Data were considered significant if the p-values obtained using an unpaired t-test was < 0.05. Significant differences are noted as $*p<0.05$, $**p<0.01$, $***p<0.001$, $****p<0.0001$ or n.s. (not significant). Data were expressed as mean +/- SEM.

3. RESULTS:

3.1 AIM 1: Determining the best method for humanization in NRG and DRAG-A2 mice.

3.1.1 Characterizing human cord blood-derived CD34+ HSCs for engraftment:

To date we have processed a total of 75 cord blood samples for cryostorage (see methods section 2.1.3). In order to validate the efficacy of the CD34 negative selection kit used, CD34+ HSC purity was measured in pre- and post- CD34 negative selection. The mean CD34+ HSC purity observed pre-enrichment was 1.00 ± 0.30% (N = 16), while the mean post-enrichment purity was 6.31 ± 2.14% (N = 23) (Fig. 7a). This data confirms that the CD34 negative selection kit being used is effective at increasing the mean CD34+ HSC purity by a mean of 6-fold. As GvHD is a particular concern when engrafting immune cells, samples were analyzed pre- and post-enrichment with the CD34 negative selection kit to confirm CD3 depletion. The mean CD3+ T cell percentage pre-depletion was 38.71 ± 7.01%, while it was reduced to 6.36 ± 1.74% post-depletion (Fig. 7b). It's important to note that the FMO for CD3 was relatively high (2.51%), while the mean post-depletion CD3+ T cell level was 6.36%. An FMO value of above 1% can be indicative of background signal (usually caused by spillover or autofluorescence) that may result in a inaccurately high measurement (Maecker & Trotter, 2006). This means that the true mean CD3+ T cell level is likely lower, approximately 4%, indicating further CD3 depletion may still be necessary to prevent the development of GvHD following engraftment as even the smallest mature CD3+ T cell contamination can trigger GvHD over time (Greenblatt et al., 2012). All mice

were assessed for GvHD based on symptomology (rapid weight loss, scabby skin, diarrhea) for the duration of their lifespan and we have observed a very low incidence of GvHD symptoms in our successfully engrafted mice (16.5%) using this cord blood processing method and these symptoms do not usually occur until at least 6 months post-engraftment, although this was variable. In fact, more than half of these cases were in mice engrafted with the same donor cord blood samples, which may indicate these particular samples had an especially high quantity of CD3+ T cells (Table 2). Cord blood samples were then HLA-typed as only DR4+A2+ positive samples can be used for engrafting DRAG-A2 mice and approximately 10% of samples were DR4+A2+ positive (data generated by Jack Yang).

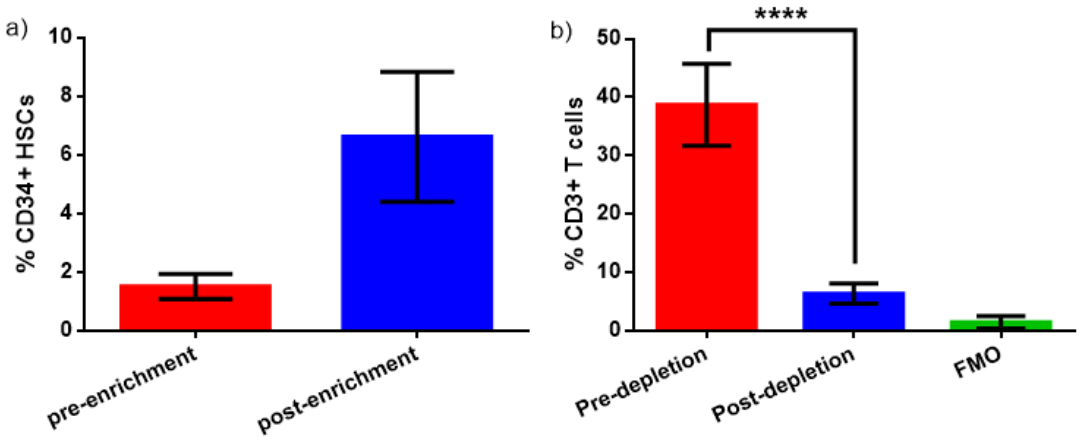

Fig. 7. *CD34 negative selection is effective in significantly enriching CD34+ HSCs and depleting CD3+ T cells.* **(a)** Percentage of CD34+ HSCs in cord blood samples before (N = 16) and following (N = 23) CD34 negative selection; **(b)** Percentage of CD3+ T cells in cord blood samples before (N = 14) and following (N = 15) CD34 negative selection. Data were expressed as mean ± SEM, p-value **** = <0.0001.

Table 2. *Summary of all cord blood samples used for humanizing NRG and DRAG-A2 mice to date.*

Cord blood sample #	HLA type	Mouse strain engrafted	Success rate (>10% hCD45+)	Engraftment method	GvHD rate (of >10% hCD45+ only)
1	DR4+A2+	DRAG-A2	6/6 (100%)	IH	1/6 (16.7%)
2	DR4-	NRG	9/9 (100%)	IH	5/9 (55.5%)
3	DR4-	NRG	4/8 (50%)	IH	1/4 (25%)
4	DR4-	NRG	9/9 (100%)	IH	1/9 (11.1%)
5	DR4-	NRG	3/7 (42.8%)	IH	0/3 (0%)
6	DR4-	NRG	6/7 (85.7%)	IH	0/6 (0%)
7	DR4-	NRG	9/10 (100%)	IH	1/9 (11.1%)
8	DR4-	NRG	6/7 (85.7%)	IH	0/6 (0%)
9	DR4-	NRG	7/7 (100%)	IH	2/7 (28.6%)
10	DR4-	NRG	3/6 (50%)	IV	0/3 (0%)
11	DR4-	NRG	0/6 (0%)	IH	0/0 (0%)
12	DR4-	NRG	6/8 (75%)	IV	1/6 (16.7%)
13	DR4-	NRG	1/9 (11.1%)	IV	0/1 (0%)
14	DR4-	NRG	8/8 (100%)	IV	4/8 (50%)
15	DR4-	NRG	9/9 (100%)	IH	3/9 (33.3%)
16	DR4-	NRG	9/9 (100%)	IH	1/9 (11.1%)
17	DR4-	NRG	7/7 (100%)	IH	0/7 (0%)
18	DR4-	NRG	1/7 (14.3%)	IH	0/1 (0%)
19	DR4-	NRG	8/8 (100%)	IH	3/8 (37.5%)
20	DR4-	NRG	8/10 (80%)	IH	0/8 (0%)
21	DR4-	NRG	4/8 (50%)	IH	0/4 (0%)
22	DR4-	NRG	0/5 (0%)	IH	0/0 (0%)
23	DR4-	NRG	0/7 (0%)	IH	0/0 (0%)
24	DR4-	NRG	3/7 (42.8%)	IH	0/3 (0%)
25	DR4-	NRG	9/12 (75%)	IH	0/9 (0%)
26	DR4-	NRG	4/6 (66.7%)	IH	0/4 (0%)

Abbreviations: GvHD = graft-vs-host disease; HLA = human leukocyte antigen; IH = intrahepatic; IV = intravenous.

3.1.2 Creating and characterizing huNRG and huDRAG-A2 mice:

NRG and DRAG-A2 mice were engrafted with human CD34+ HSCs as previously described (see methods section 2.1.4). To date, a total of 188 NRG mice and 6 DRAG-A2 mice have been engrafted (Table 3). The production of huDRAG-A2 mice has unfortunately been limited severely by breeding problems. Recently, we have successfully been able to re-establish our breeding colony and have been able to produce and engraft several more DRAG-A2 mice. These mice are still in the process of reconstituting and will be evaluated at 12 weeks post-engraftment.

Table 3. *Summary of human CD45+ leukocyte reconstitution in the blood of all huNRG and huDRAG-A2 mice generated to date at 12 weeks post-engraftment.*

Strain	Total # generated	% of mice >10% hCD45+	Mean % hCD45+ / Total Leukocytes	Mean # hCD45+ /mL blood
huNRG IH	157	64.33	24.85±1.81	84,289±8,575*
huNRG IV	31	61.29	22.62±3.47	90,163±17,441**
huDRAG-A2 IH	6	100.00	53.98±10.24	234,113±60,503

*hCD45+ absolute count data was only available for 133 huNRG mice engrafted as neonates IH.

**hCD45+ absolute count data was only available for 25 huNRG mice engrafted as adults IV.

At approximately 12, 16 and 20 weeks post-engraftment, whole blood was collected and human immune cell reconstitution was measured. The percentage and total number of human leukocytes (hCD45+) of the total blood leukocyte population was calculated and mice were considered successfully humanized if the percentage of human leukocytes was 10% or greater (Nguyen et al., 2017). Our engraftment data suggests that both methods of engraftment are effective in the NRG model but that the newborn method offers slightly higher engraftment (although the actual mean may be not significant) compared to the adult

method (Fig. 8). The mean human immune cell engraftment was 31.63% or $1.1x10^5$ hCD45+/mL using the newborn IH method (N = 81) and 22.62% or $9.0x10^4$ hCD45+/mL using the adult IV method (N = 31) which are both well above the 10% hCD45+ leukocyte cut-off required for engraftment to be considered successful enough for our experiments.

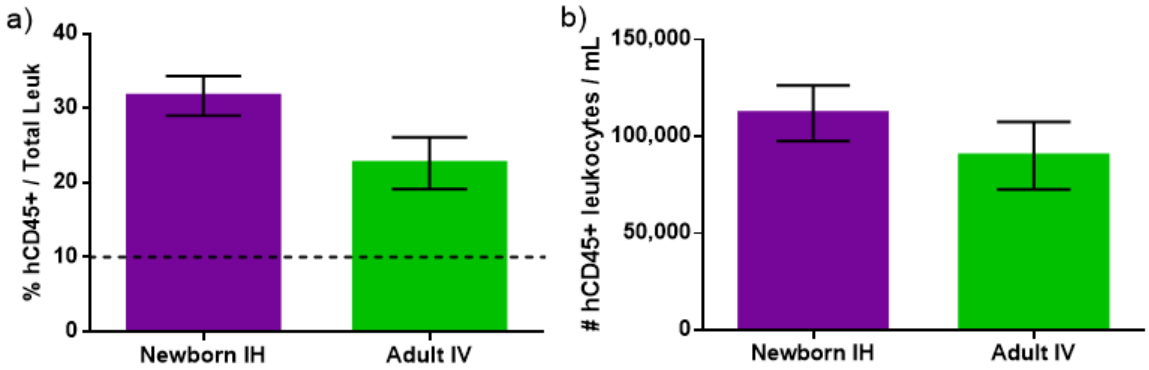

Fig. 8. *Both methods of engraftment are effective in generating huNRG mice with 10% or greater human leukocytes.* Mean hCD45+ leukocyte **(a)** frequency (%) and **(b)** absolute count in huNRG mice humanized via newborn IH (N=81) and adult IV (N=31) at 12 weeks post-engraftment. Dashed line indicates the 10% hCD45+ cut-off for engraftment to be considered successful. Data are expressed as mean +/- SEM.

In an early subset of hu-mice, the human immune cell subset breakdown was measured in a group of huNRG (N=18) and huDRAG-A2 (N=6) mice in order to compare the reconstitution levels of the different types of immune cells in both models (Fig. 9). All of these mice developed a measureable human immune system but of these mice, 72.2% (13 of 18) of the huNRG mice generated were successfully engrafted to 10% or greater hCD45, while 100% (6 of 6) of the huDRAG-A2 mice were successfully engrafted (Fig. 9a). At 12 and 20 weeks post-engraftment, the mean human leukocyte reconstitution was significantly higher in the huDRAG-A2 mice compared to the huNRGs (Fig. 9b & c). The mean human CD4+ T cell, CD19+ B cell and CD14+ monocyte reconstitution was also significantly

higher in the huDRAG-A2 mice compared to the huNRGs (Fig. 9d &e). In preliminary experiments in a small group of mice, both models were found to produce low levels (above cut-off) of a wide variety of human cytokines/chemokines in the blood plasma and/or lung homogenate under either healthy or diseased conditions. Human cytokines/chemokines that were detected above background levels (determined using non-humanized controls) included sCD40L, eotaxin, fractalkine, GM-CSF, GROα, IFNα2, IFNγ, IL-1α, IL-1RA, IL-2, IL-3, IL-4, IL-5, IL-6, IL-7, IL-10, IL-12p40, IL-12p70, IL-13, IL-15, IL-17A, IL-17F, IL-18, IL-27, IP-10, MCP-1, MCP-3, M-CSF, MDC, MIG/CXCL9, MIP-1α, MIP-1β, RANTES, TGF-α, TNFα and VEGF-A (data not shown).

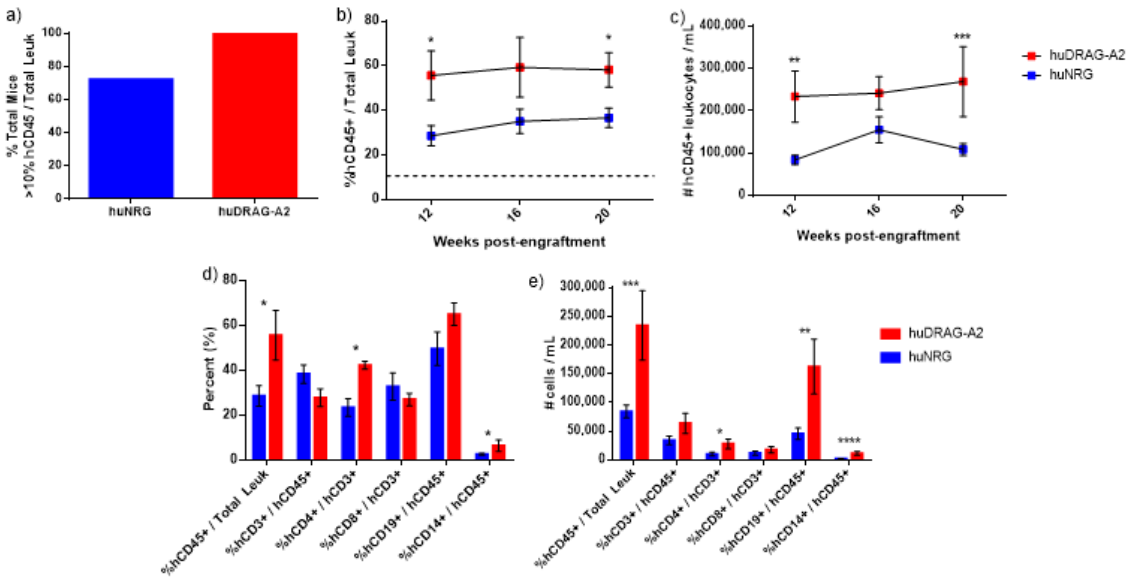

Fig. 9. *huDRAG-A2 mice show significantly improved human immune cell reconstitution compared to huNRG.* **(a)** Percentage of huNRG (N = 18) and huDRAG-A2 (N = 6) mice that were successfully engrafted to 10% or greater hCD45+ of the total blood leukocytes at 12 weeks post-engraftment; **(b)** Mean percentage hCD45+ of total blood leukocytes (dashed line indicates the 10% hCD45+ cut-off for engraftment to be considered successful) and **(c)** absolute hCD45+ leukocyte count per mL of whole blood of all huNRG (N = 18) and huDRAG-A2 (12 weeks N = 6, 16-20 weeks N = 5) mice at 12, 16 and 20 weeks post-engraftment; **(d)** Mean reconstitution (%) and **(e)** absolute count per mL of human immune cells in the blood of huNRG (N = 18) and huDRAG-A2 (N = 6) at 12 weeks

post-engraftment. Data are expressed as mean +/- SEM, p value = * <0.05, ** <0.01, *** <0.001, **** <0.0001.

3.2. AIM 2: Establishing and validating a clinically relevant model of HIV-1 infection in humanized NRG and DRAG-A2 mice.

3.2.1. Quantifying viral stocks for use in humanized mouse experiments:

Two R5-tropic strains of HIV-1, NL4.3-Bal-Env and JR-CSF, have been obtained for use in humanized mouse experiments. Viral titre was measured using a TZMbl assay to allow for precise dosage during infection (see methods section 2.2.1). The NL4.3-Bal-Env stock viral titre was measured as $10^{7.87}$ IU/mL, while the titre for the JR-CSF stock was measured as $10^{8.48}$ IU/mL. High titre virus is essential for mucosal HIV-1 infection as the infectious dose must be concentrated into a small volume (25 uL) and both these stocks are at a high enough concentration that they will useful for these infections. Both of these strains have been used successfully in similar hu-mouse models in previous studies (Jamieson et al., 1995; Mariani et al., 2001; Münk et al., 2002; Nguyen et al., 2017; Schiff et al., 2021; Schweighardt et al., 2004; Wessels et al., 2021). To date, we have successfully infected hu-mice using the NL4.3-Bal-Env and JR-CSF strains of HIV-1 intravaginally, as well as systemically using JR-CSF, and we are currently validating systemic infection using NL4.3-Bal-Env.

3.2.2. Intravaginal infection of huNRG and huDRAG-A2 mice using NL4.3-Bal-Env:

To compare the feasibility of the huNRG and huDRAG-A2 models for HIV-1 infection, highly-engrafted (>10 %hCD45+) female mice were infected intravaginally with NL4.3-Bal-Env to confirm susceptibility to infection with this strain of HIV-1 (Fig. 3) (see methods section 2.2.2). The mice were randomized based on overall human CD45+ leukocyte and CD4+ T cell engraftment to prevent variability in results based on differences in reconstitution alone (Table 4). At 2 weeks post-infection, both huNRG and huDRAG-A2 mice had an elevated viral load in the vaginal wash as measured by an in-house RT-qPCR assay (see methods section 2.2.3), which is expected following intravaginal infection (Fig. 10b). Moderate viral load was detected in the plasma at 2 weeks post-infection and increased over the subsequent weeks as the virus continued to replicate and disseminated throughout the periphery (Fig. 10a). Although the frequency of HIV-1 target cells was depleted in the blood and tissues of both models, the CD4+ T cells may have been more severely reduced in the blood of huDRAG-A2 mice compared to the huNRG mice at 8 weeks post-infection (Fig. 10c & d). Human CD4+ T cell and CD68+ macrophage IHC of the vaginal mucosa and the lung tissue of these mice confirm target cell depletion also occurs at the site of infection (vaginal mucosa) and in known early dissemination sites in humans (lung) as well as the blood (Fig. 11 & 12).

Table 4. *Baseline pre-infection human immune cell reconstitution in the blood of humanized mice used for HIV-1 infections.*

Exp.	Mouse #	Sample #	Strain	Sex	%hCD45+ of Total Leuk	#hCD45+/ mL	%hCD3+ / hCD45+	#hCD3+/ mL	%hCD4+ / hCD3+	#hCD4+/mL
NL4.3-Bal-Env IVAG	1	1	huDRAG-A2	Female	79.56	449.300	26.5	119.065	55.1	65.605
	2	1	huDRAG-A2	Female	62.82	272.901	25.0	68.225	57.4	39.161
	3	2	huNRG	Female	55.45	294.968	33.0	97.339	44.4	43.219
	4	2	huNRG	Female	71.11	237.307	38.7	91.838	55.0	50.511
High dose JR-CSF IP	5	8	huNRG	Male	57.5	82.667	94.5	78.120	69.9	54.606
	6	8	huNRG	Male	16.52	12.925	81.0	10.469	86.4	9.045
	7	8	huNRG	Male	30.81	35.171	88.1	30,986	69.2	21.442
Low dose JR-CSF IP	8	8	huNRG	Male	12.27	3.675	78.2	2.874	92.2	2.650
	9	9	huNRG	Male	32.38	124.500	66.1	8.2295	46.1	37.938
	10	9	huNRG	Male	32.7	71.100	60.0	42.660	48.3	20.604
High dose JR-CSF IVAG	11	4	huNRG	Female	74.85	460.320	17.7	81.477	35.8	29.169
	12	4	huNRG	Female	25.03	231,911	15.3	35,482	25.0	8,871

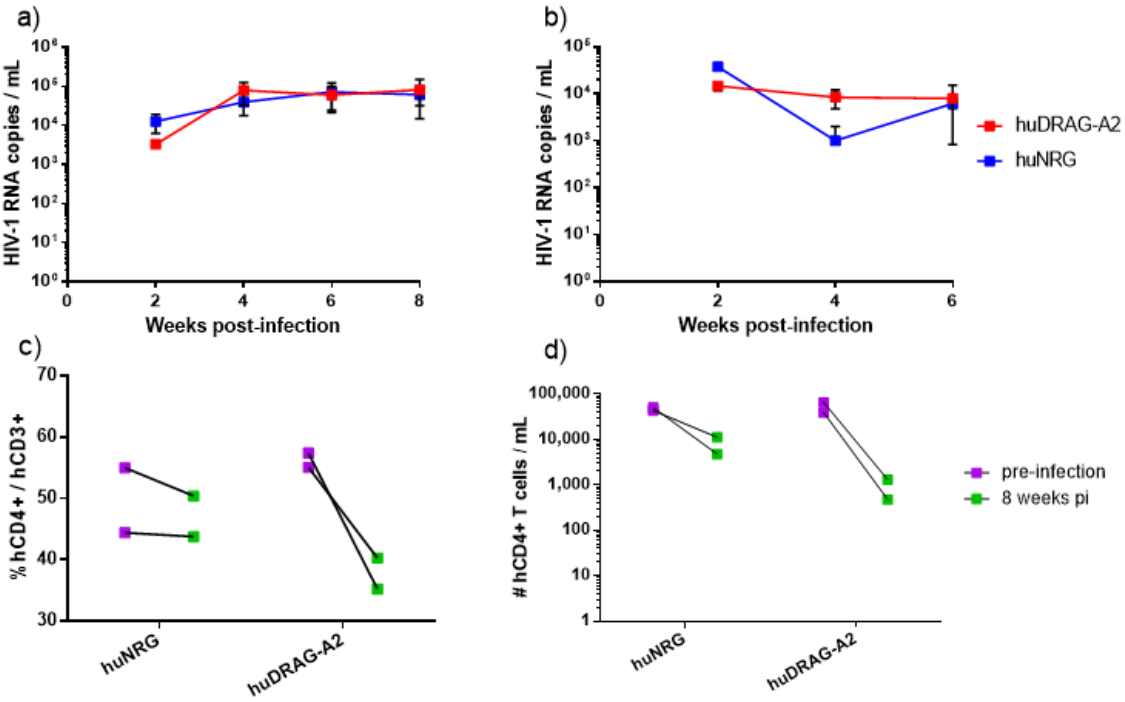

Fig. 10. *Both huNRG and huDRAG-A2 mice can sustain HIV-1 infection via intravaginal inoculation but huDRAG-A2 mice show a trend towards more severe CD4+ T cell depletion compared to huNRGs.* Viral load in the **(a)** blood plasma and **(b)** vaginal wash of huNRG (N = 2) and huDRAG-A2 (N = 2) mice at 2, 4, 6 and 8 weeks post-intravaginal HIV-1 infection; **(c)** Percent and **(d)** absolute human CD4+ T cell frequency pre- and 8 weeks post-infection in the blood of huNRG (N = 2) and huDRAG-A2 (N = 2). Data are expressed as mean +/- SEM.

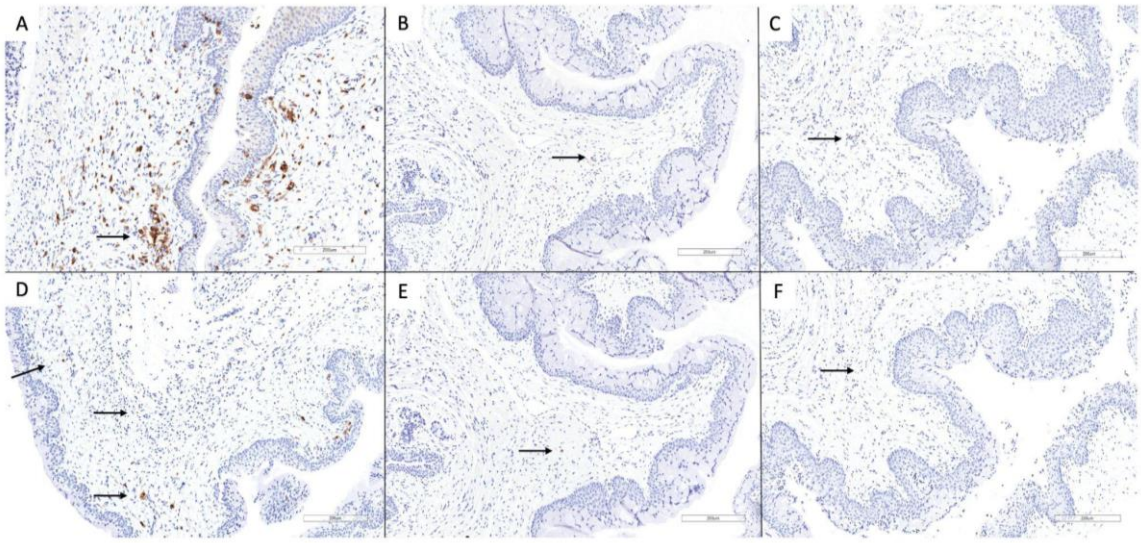

Fig. 11. *Intravaginal HIV-1 infection results in depletion of target cells at the site of infection in huNRG and huDRAG-A2 mice.* Left: Uninfected huNRG vaginal mucosa stained with human **(a)** CD4+ and **(d)** CD68+ IHC. Middle: huNRG vaginal mucosa at 8 weeks post-infection stained with human **(b)** CD4+ and **(e)** CD68+ IHC. Right: huDRAG-A2 vaginal mucosa at 8 weeks post-infection stained with human **(c)** CD4+ and **(f)** CD68+ IHC (all 10x, scale bar = 100μm). Uninfected huDRAG-A2 control was not available due to limited number of these mice generated.

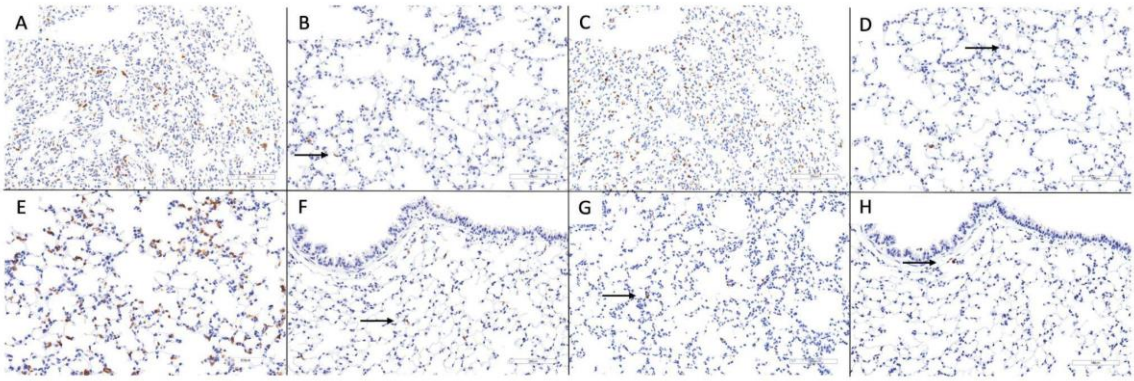

Fig. 12. *HIV-1 target cells are depleted in the lung of huNRG and huDRAG-A2 mice at 8 weeks post-infection, indicating viral dissemination.* Top: Uninfected huDRAG-A2 lung stained with human **(a)** CD4+ and **(c)** CD68+ IHC. huDRAG-A2 lung at 8 weeks post-infection stained with human **(b)** CD4+ and **(d)** CD68+ IHC. Bottom: Uninfected huNRG lung stained with human **(e)** CD4+ and **(g)** CD68+ IHC. huNRG lung at 8 weeks post-infection stained with human **(f)** CD4+ and **(h)** CD68+ IHC (all 20x, scale bar = 100μm).

3.2.3. Preliminary data indicates antibody and cytokine responses may be improved in huDRAG-A2 mice:

Lastly, cytokine and antibody production was evaluated in these mice at 8 weeks post-infection to elucidate the differences in the functionality of the immune systems of these models (see methods section 2.2.5). Both huNRG and huDRAG-A2 mice were found to secrete a wide variety of human cytokines (although levels were much lower that seen in humans) but cytokines typically associated with T cell functionality are of particular interest. This data is preliminary as there were only 2 mice per group and variability was quite high between some samples. For these reasons, we will be interested in looking at cytokine responses in future experiments as well to further characterize the cytokine profiles of these mice. The absolute human IFNγ, TNFα and IL-2 levels in the blood plasma were found to be at a quite low level at 8 weeks following HIV-1 infection, especially in the huDRAG-A2 mice (Fig. 13a,b,c). Flow data from the blood of these mice collected at the same time-point showed that these mice had particularly low levels of T cells compared to the pre-infection values (Fig. 10c,d). Since T cells are thought to be major producers of IFNγ, TNFα and IL-2 in these models, we normalized cytokine levels using the number of T cells, revealing a trend towards being slightly elevated cytokine levels in the blood of the huDRAG-A2 mice (Fig. 13d,e,f). huDRAG-A2 mice, but not huNRGs, were also found to produce human IgG antibodies against the HIV-1 antigen gp120, indicating improved B cell function in these mice as well (Fig. 14) (see methods section 2.2.5).

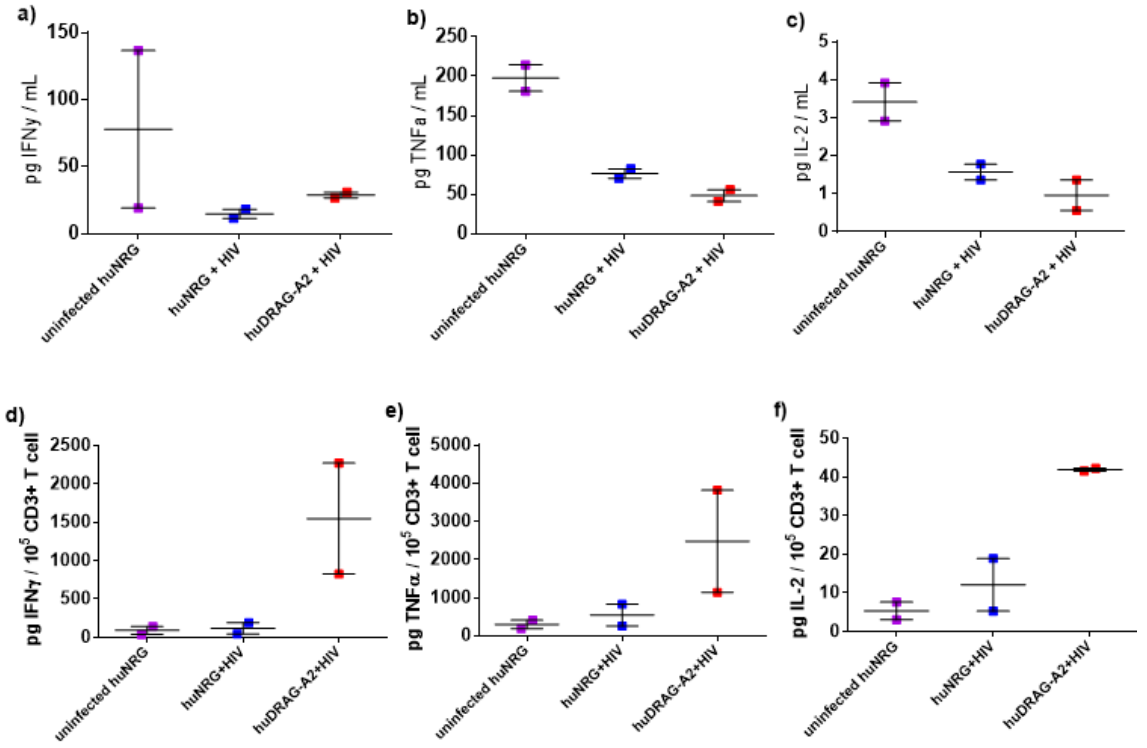

Fig. 13. *T cell associated cytokines were detected in the blood of both huNRG and huDRAG-A2 mice following HIV-1 infection.* Absolute **(a)** IFNγ, **(b)** TNFα and **(c)** IL-2 secretion in the blood plasma; and **(d)** IFNγ, **(e)** TNFα and **(f)** IL-2 secretion corrected to account for T cell depletion in the blood of uninfected huNRG (N = 2), and huNRG (N = 2) and huDRAG-A2 (N = 2) mice at 8 weeks post-infection. For T cell corrected data **(d, e & f)**, the amount of cytokine detected in the blood plasma (pg/mL) was divided by the absolute CD3+ T cell count in the whole blood (#CD3+ T cell/mL) at the same time-point to account for HIV-induced T cell depletion (see methods section 2.2.5). Data are expressed as mean +/- SEM.

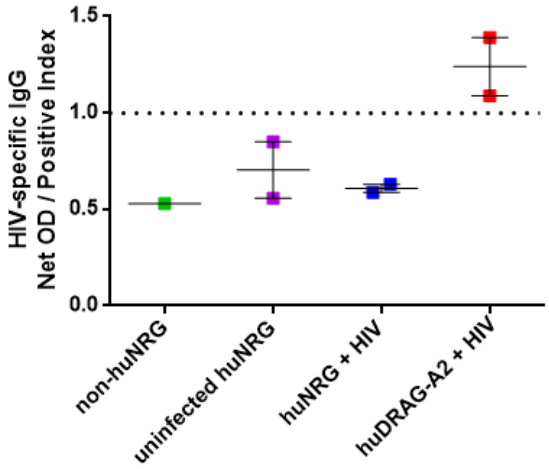

Fig. 14. *HIV-specific human IgG antibodies were detected in the blood plasma of huDRAG-A2 mice, but not huNRGs.* Non-humanized NRG (N = 1), uninfected huNRG (N = 2), and huNRG (N = 2) and huDRAG-A2 (N = 2) at 8 weeks post-infection. Net OD/Positive index expresses sample OD values relative to the OD values of negative controls (see methods section 2.2.5). Data are expressed as mean +/- SEM.

3.2.4. Validation of systemic and intravaginal infection of huNRG mice using JR-CSF:

The JR-CSF strain of HIV-1 has also been successfully used in the huNRG model via both intravaginal and systemic infection (see methods section 2.2.6). Viral RNA as detected in the blood plasma starting at 1 week post-systemic infection and at 2 weeks post-intravaginal infection (Fig. 15a). CD4+ T cells trended towards being depleted (not significant) in the blood of these mice, although there was a lot of variability between some time-points (Fig. 15b & c). One mouse in the low dose systemic group was not successfully infected (removed from dataset). Notably, this was the mouse with the lowest human immune reconstitution. Another mouse in the low dose systemic group was found to have elevated T cells at 16 weeks post-infection compared to its pre-infection T cell reconstitution as

determined by flow cytometry (Fig. 15b & c - green X). However this mouse showed symptoms of GvHD at this time (severely scabby skin, enlarged spleen) and given that uncontrolled cytotoxic T cell proliferation is a known feature of this condition in hu-mouse models, this may account for the increased T cell numbers observed in this mouse (Zheng et al., 2013).

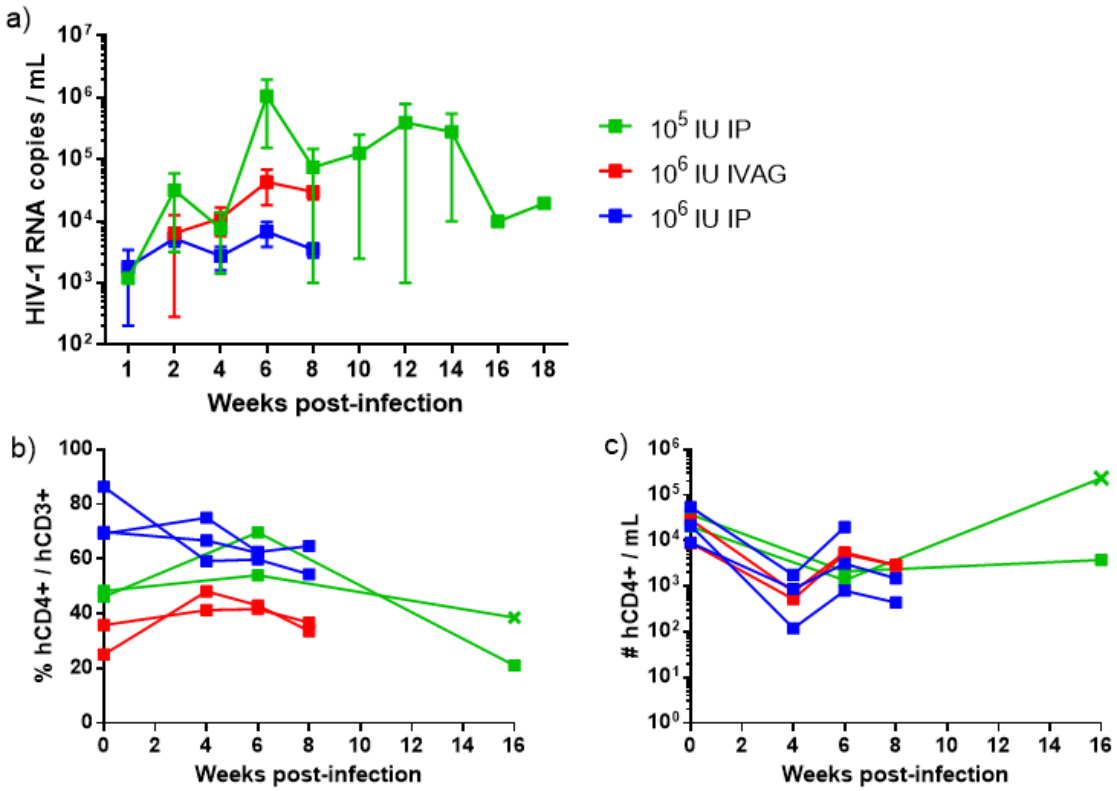

Fig. 15. *huNRG mice can also sustain infection via systemic or intravaginal inoculation using the JR-CSF strain of HIV-1*. **(a)** Mean viral load in the blood plasma, and **(b)** percent and **(c)** absolute CD4+ T cell frequency at various time-points following high dose (10^6 IU) systemic (N=3) and intravaginal (N=2), and low dose (10^5 IU) systemic (N=2) infection in huNRG mice. Green X indicates mouse with severe GvHD at endpoint.

3.3. AIM 3: Establishing and validating a clinically relevant model of TB in humanized NRG and DRAG-A2 mice.

3.3.1. Preliminary data indicates human target cells are permissive to Mtb infection in hu-mice models:

Preliminary *Mtb* infection in the hu-mouse models was conducted in huNRG mice prior to having huDRAG-A2 mice available (Table 5) (see methods section 2.3.1). Two highly-engrafted (%hCD45 of total leukocytes > 10%) male huNRG mice were infected intranasally with $6.1x10^3$ CFU of fluorescently-tagged (mCherry) Erdman *Mtb* (Fig. 6). At 3 weeks post-infection, the lung and spleen were collected for pathological scoring and bacterial load quantification using CFU enumeration (see methods section 2.3.2). Lung was also analysed using flow cytometry (see methods section 2.3.3). A high bacterial load was detected in the lung and spleen of huNRG mice at 3 weeks post-infection indicating the successful development of pulmonary TB as well as bacterial dissemination (Fig. 16a). One of the mice reached the humane weight loss endpoint (20% of original weight) by 3 weeks post-infection so this time-point was selected to conclude this experiment. Using mCherry-tagged *Mtb*, 79.1% of the human CD206+CD169+ alveolar macrophages in the lung tissue of huNRG mice were determined to be infected with *Mtb* using molecular markers for alveolar macrophages (Yu et al., 2016) (Fig. 16b). A portion of the CD206+CD14+CD169- interstitial macrophage and CD3+ T cell populations were also found to be infected with the *Mtb*. Histopathology performed on lung tissue from *Mtb*-infected huNRG mice revealed an abundance of granulomatous tissue in these mice 3 weeks following infection, characterised by immune cell infiltration and caseous necrosis within the cores of the

granulomas were also observed (Fig. 17). A significant number of *Mtb* bacilli were visualised in a diffuse pattern throughout the lung tissue using AFB staining (Fig. 17e & f). This may indicate that the virulent Erdman strain of *Mtb* may be poorly contained within the granulomas of these mice.

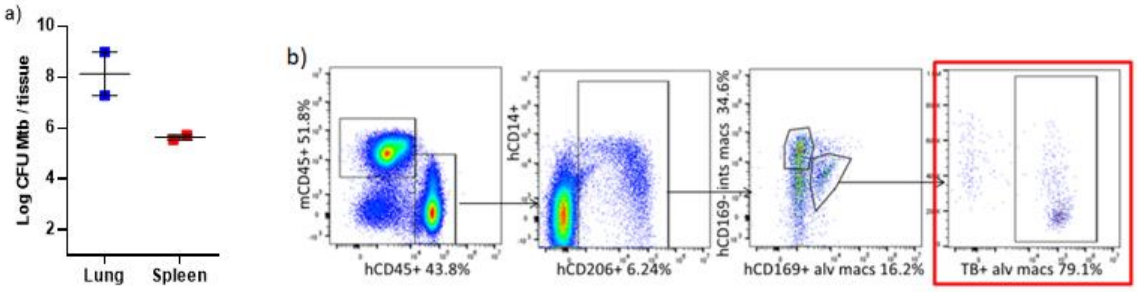

Fig. 16. *Erdman Mtb successfully infects human alveolar macrophages in the huNRG model of TB.* **(a)** Bacterial load in the lung and spleen of huNRG (N =2) mice and **(b)** flow cytometric analysis of the lung of huNRG mice (N = 1) at 3 weeks post-infection with mCherry-tagged Erdman *Mtb*. Data are expressed as mean +/- SEM. Red panel indicates *Mtb*-infected (mCherry+) hCD206+CD169+ alveolar macrophages.

Table 5. *Baseline pre-infection human immune cell reconstitution in the blood of humanized mice used for Mtb infections.*

Exp.	Mouse #	Sample #	Strain	Sex	%hCD45 + of Total Leuk	#hCD45+ /mL	%hCD3+ / hCD45+	#hCD3+ /mL	%hCD4+ / hCD3+	#hCD4+ /mL	%hCD8+ / hCD3+	#hCD8+ /mL	%hCD14+ / hCD45+	#hCD14+ /mL
mCherry -Erdman	13	3	huNRG	Male	48.48	-	26.5	-	13.9	-	1.06	-	8.11	-
	14	3	huNRG	Male	10.96	-	35.1	-	21.3	-	2.13	-	6.74	-
H37Rv	15	1	huDRAG-A2	Male	65.65	87,224	68.4	59,662	77.7	46,357	16.8	10,023	2.06	1,797
	16	1	huDRAG-A2	Female	48.50	106,400	27.6	29,366	65.0	19,088	17.9	5,257	13.0	13,832
	17	1	huDRAG-A2	Female	34.23	110,800	52.4	58,059	68.7	39,887	22.0	12,773	6.34	7,025
	18	4	huNRG	Male	29.70	127,660	21.3	27,192	51.9	14,112	9.64	2,621	6.20	7,915
	19	4	huNRG	Male	39.00	119,760	31.5	37,724	64.4	24,295	11.9	4,489	2.71	3,245
	20	4	huNRG	Male	19.97	196,940	20.0	39,388	51.9	20,442	8.49	3,344	3.58	7,050
YFP-H37Rv	21	7	huNRG	Female	62.33	98,480	57.5	56,626	65.6	37,147	22.9	12,967	-	-
	22	7	huNRG	Female	65.99	48,040	80.0	38,432	68.2	26,211	24.7	9,493	-	-

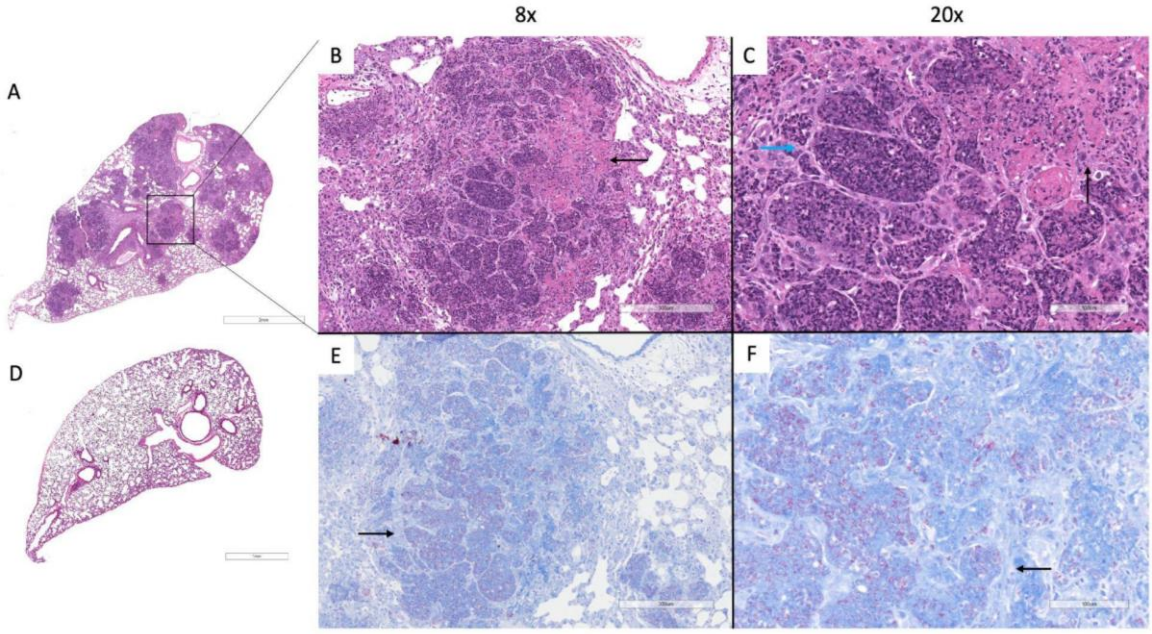

Fig. 17. *huNRG mice develop caseating granulomas in the lung at 3 weeks post-infection with highly virulent Erdman Mtb.* **(a)** whole lung section H&E (2x), **(b)** H&E (8x) arrow indicate caseating necrosis, **(c)** H&E (20x) blue arrow indicate immune cell infiltration and black arrow indicate caseating necrosis, **(e)** AFB (8x) and **(f)** AFB (20x) black arrow indicate *Mtb* bacilli stained red; **(d)** whole lung section H&E (2x) of healthy lung tissue control (scale bar for 2x = 2mm; 8x =300μm; 20x = 100μm).

Although the molecular markers used for flow analysis of the lung tissue in the previous mCherry-Erdman experiment are commonly used in other literature to identify alveolar macrophage populations (Yu et al., 2016), alveolar macrophages are more commonly collected from the airway lumen by BAL. This results in a much cleaner sample of the immune cells present within the airways and alveolar sacs of the lung, as other types lung-resident macrophages, immune cells and debris found within the lung tissues will not be collected by BAL. In order to confirm our findings in the lung tissue using the mCherry-tagged *Mtb*, we repeated the experiment using YFP-tagged H37Rv with the goal of collecting BAL as a primary outcome and confirming the presence of *Mtb* within the human

target cells. Unfortunately, once harvested, the lungs of these mice were found to be severely hemorrhaged and the collected BAL was mostly composed of CD3+ T cells, likely from blood contamination, and few target macrophages. For these reasons, we were unable to accurately measure the frequency of *Mtb*-infected alveolar macrophages using the YFP-tagged *Mtb*. CFU quantification of the lung and spleen of the mice indicated the bacterial burden was elevated (mean of $10^{7.82}$ and $10^{5.79}$ CFU in the lung and spleen, respectively). Histopathology of the lungs of these mice are not yet available, but may still be useful for understanding the lung damage caused by the YFP-H37Rv strain used in this experiment.

3.3.2. Comparison of huNRG and huDRAG-A2 models of TB:

In our next experiment, three highly-engrafted (%hCD45 of total leukocytes > 10%) huNRG and huDRAG-A2 mice were infected intranasally with $1.9x10^4$ CFU of non-tagged H37Rv *Mtb* (Fig. 6). At 4 weeks post-infection, an elevated bacterial burden was measured in the lung and spleen of both models, indicating pulmonary infection and bacterial dissemination was successful (Fig. 18a). None of the mice reached their humane weight loss endpoint during this time. The lung and spleen were also analysed using flow cytometry (see methods section 2.3.3). Despite the fact that the overall human leukocyte and CD3+ T cell frequency was higher in the blood of the huDRAG-A2 mice pre-infection (Table 5), there may have been a trend towards a slightly reduced frequency of human CD3+ T cells, as well as CD4:CD8 ratio, in the lungs and spleen of huDRAG-A2 mice compared to the huNRG mice at endpoint (not significant) (Fig. 18b, d & e). Although we cannot directly compare data from the blood, the lung and the spleen of these mice, this

would suggest T cell reconstitution was likely reduced following *Mtb* infection. The frequency of certain macrophage phenotypes (hCD206+, hCD169+ alveolar macrophages and hCD169- interstitial macrophages) was not significantly different in the huDRAG-A2 mice following *Mtb* infection (Fig. 18c). At the time of harvest, one huNRG mouse was showing symptoms of severe GvHD (Fig. 18 - blue triangle), a common complication of immune cell engraftment that causes immune cell dysfunction and inflammation and as such, may not be an accurate representation of the T cell responses that would normally occur in these mice. Additionally, one of the huDRAG-A2 mice had extremely low quantity of CD206+ macrophages in the lung (3.97% of hCD45 vs 28.6% and 32.8% in the 2 remaining huDRAG-A2 mice, Fig. 18c - red circle). This mouse also completely lacked hCD169- interstitial macrophages although there were no signs of any health issues during the course of this experiment. There were no other abnormalities seen in the frequency of any other immune cell population in this mouse.

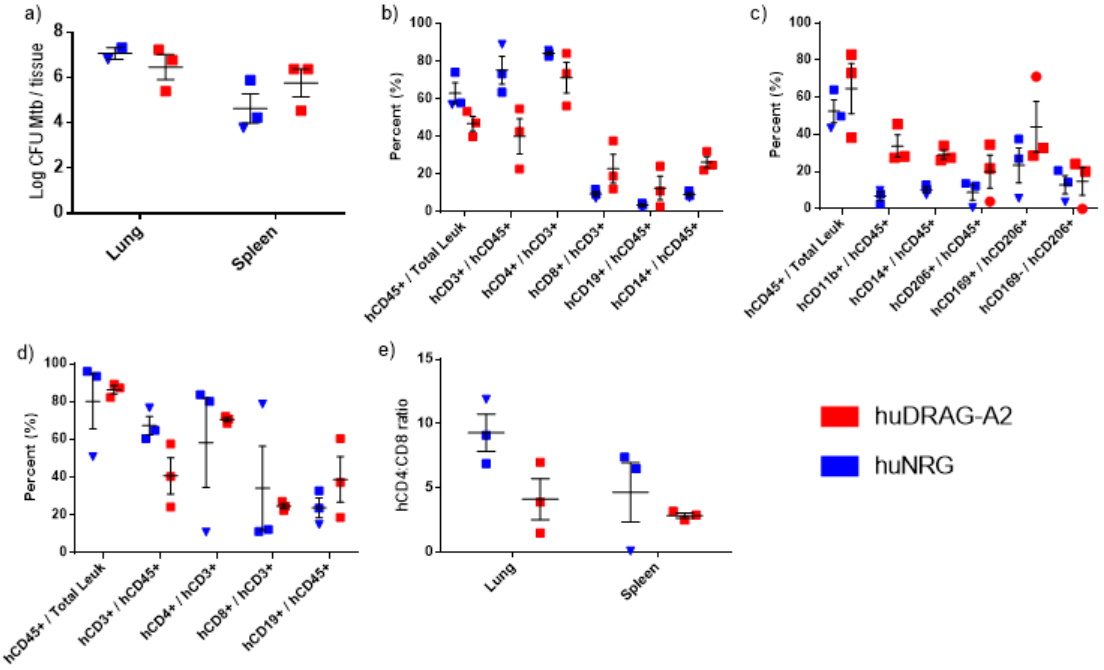

Fig. 18. *Mtb (H37Rv) infected huDRAG-A2 and huNRG mice have similar bacterial loads and immune distribution in the lung and spleen, but there may be a trend of reduced CD4/CD8 ratio in the lungs of huDRAG-A2 mice.* **(a)** Bacterial load in the lung and spleen of huNRG (N = 2 only as a sample was not plated in error) and huDRAG-A2 (N = 3) mice; **(b)** the frequency of human CD45+ leukocytes, T and B cells, and monocytes/macrophages in the lung and **(d)** spleen; **(c)** the frequency of human macrophages populations in the lung; and **(e)** the ratio of human CD4+ to CD8+ T cells in the lung and spleen of huNRG (N = 3) and huDRAG-A2 (N = 3) mice; at 4 weeks post-infection with H37Rv *Mtb*. Data are expressed as mean +/- SEM. Blue triangle indicates huNRG with clinical signs of severe GvHD. Red circle indicates huDRAG-A2 with abnormal lung macrophage populations.

3.3.3. Humanized mice develop human-like organized caseating granulomas:

Histopathology was also conducted on the lungs of these mice to visualize differences in granuloma structure and containment between the huNRG and huDRAG-A2 mice. Both models developed well organized granulomas following infection with *Mtb*, although the huDRAG-A2 mice showed a more classical granuloma structure compared to the huNRGs

(Fig. 19 & 20). This was characterized by a ring of CD4+ T cells surrounding the granuloma, with CD68+ macrophages located within the core of the granuloma, confirming the involvement of human immune cells in the containment and control of the *Mtb* infection (Fig. 19d & e). H&E staining revealed more caseating necrosis within the cores of the huDRAG-A2 granulomas compared to the huNRGs (Fig. 19a,b & 20a,b), which is a hallmark characteristic of TB in humans and the lack of caseating necrosis within the granuloma is a limitation of most normal mouse models of TB. The *Mtb* bacilli were also visualized using AFB staining and were found to be mostly localized within the core of the granulomas in both models, with very little bacteria located within the healthy lung tissue. Although AFB staining is difficult to quantify, the huDRAG-A2 mice appeared to have less *Mtb* within the granuloma core, which may indicate improved anti-mycobacterial responses and enhanced containment of the infection (Fig. 19c & 20c).

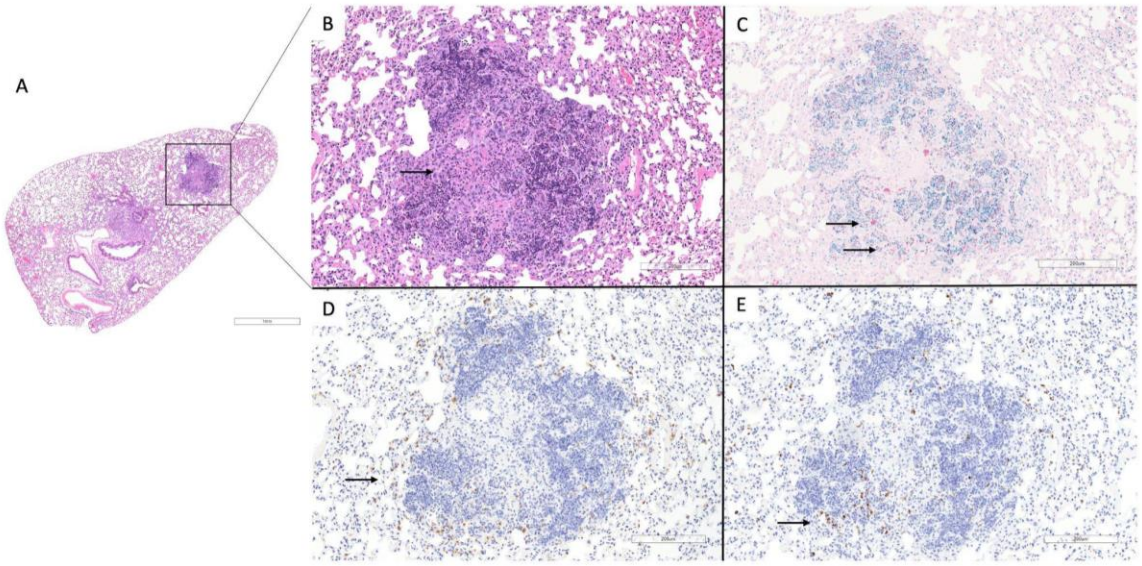

Fig. 19. *huDRAG-A2 mice show classically organized granuloma formation with human immune cell involvement at 4 weeks post-infected with H37Rv Mtb.* **(a)** Whole lung section H&E (2x), **(b)** granuloma H&E (10x), arrow indicates central caseating necrosis, **(c)** granuloma AFB (10x), arrows indicate *Mtb* bacilli stained red, **(d)** human CD4+ IHC (10x), arrow indicates human CD4+ T cells stained brown, **(e)** human CD68+ IHC (10x), arrow indicates human CD68+ macrophages stained brown (scale bars for 2x = 1mm; 10x = 200µm).

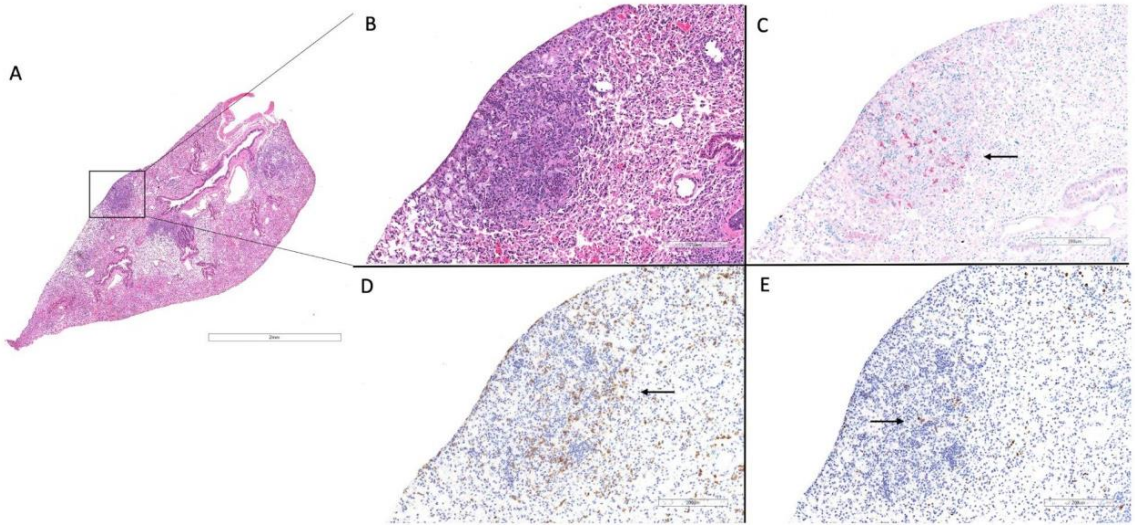

Fig. 20. *Histopathology of the lung of a huNRG mouse at 4 weeks post-infection with H37Rv Mtb indicates significant granuloma formation.* **(a)** whole lung section H&E (2x), **(b)** granuloma H&E (10x) **(c)** granuloma AFB (10x), arrow indicate *Mtb* bacilli stained red, **(d)** human CD4+ IHC (10x), arrow indicates human CD4+ T cells stained brown, **(e)**

human CD68+ IHC (10x), arrow indicates human CD68+ macrophages stained brown (scale bars for 2x = 1mm; 10x = 200µm).

3.3.4. Preliminary data indicates huDRAG-A2 mice may have improved pro-inflammatory cytokine responses:

In order to elucidate differences in immune cell functionality, the presence of certain pro-inflammatory cytokines and *Mtb*-specific human IgG was measured in the lung homogenates and blood plasma, respectively, of huNRG and huDRAG-A2 mice (see methods section 2.3.4). We were unable to detect any *Mtb*-specific IgG in the plasma of either model at the 4 week post-infection time-point. Low levels of human pro-inflammatory cytokines (IFNγ and TNFα) were detected in the lung homogenates of both huNRG and huDRAG-A2 mice. Although the huDRAG-A2 mice trended towards a slightly higher level of these cytokines on average compared to infected huNRGs (not significant), there was a lot of variability between mice resulting in significant spread (Fig. 21).

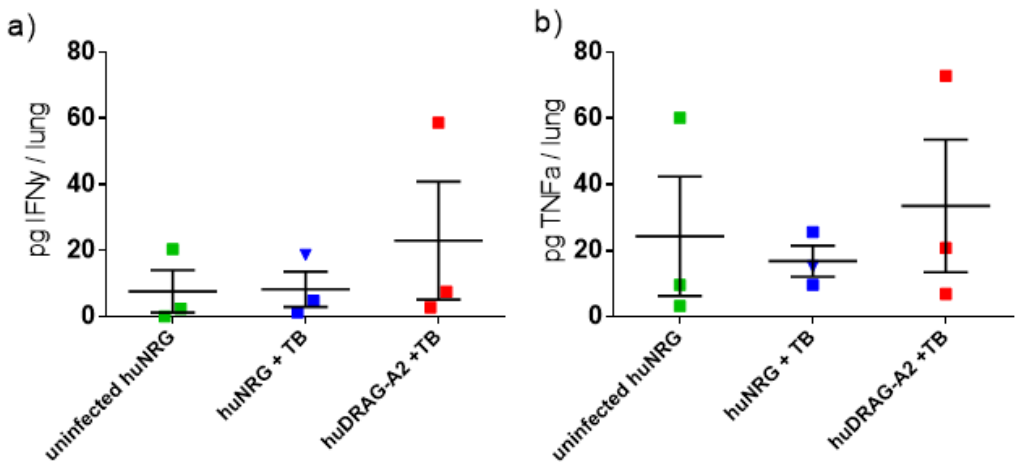

Fig. 21. *Both huNRG and huDRAG-A2 mice secrete pro-inflammatory cytokines in the lung homogenate following Mtb infection.* **(a)** IFNγ and **(b)** TNFα secretion in the lung homogenate of uninfected huNRG (N = 3), and huNRG (N = 3) and huDRAG-A2 (N = 3) mice at 4 weeks post-infection. Data are expressed as mean +/- SEM. Blue triangle indicates huNRG with severe GvHD.

4. DISCUSSION:

There are several essential components required to generate hu-mice; an appropriate immunocompromised background strain, radiation pre-conditioning and a source of CD34+ progenitor HSCs. Our choice to utilize the transgenic DRAG-A2 model adds the extra complication of crossbreeding the DRAG and the A2 lines and the requirement of HLA-matching the engrafted CD34+ HSCs. Unfortunately, we have had difficulty producing DRAG-A2 mice for humanization due to serious breeding problems when initially generating homozygous DRAG mice. The process of homozygousing a previously heterozygous mouse line requires several generations of selective inbreeding that ultimately reduces the genetic diversity of the line which is generally associated with reduced fitness and loss of reproductive ability (Ralls et al., 2013; Taft et al., 2006). We believe this is what occurred the first time we attempted this process, resulting in the colony dying out within 2 generations. New heterozygous mouse stock had to be acquired and the process repeated on a larger scale to account for potential fertility issues. So far this process has been successful, as several homozygous DRAG litters and DRAG-A2 mice have been produced. We utilize umbilical cord blood as a source of CD34+ HSCs as it is a convenient source rich in progenitor cells (Lee et al., 2010). Although we have reported relatively low CD34% purity levels compared to some of the literature (Fig. 7) (Bernard et al., 2008; Choi et al., 2011; Danner et al., 2011; Majji et al., 2016), we have successfully been able to generate both huNRG and huDRAG-A2 mice using our CD34+ HSC enrichment and isolation protocol, with the mice developing complications of the engraftment such as GvHD at a low rate (Table 2). The majority of cases of GvHD were seen in mice engrafted

with the same cord blood sample, which would suggest these particular samples may have had high T cell contamination. However we cannot be sure of this as these were older samples that had not been screened for T cell contamination using flow cytometry. Due to our high engraftment success rate and low rates of GvHD, we plan on continuing with this method of CD34 enrichment in the future. Another considerations for the production of huDRAG-A2 mice is the limited availability of HLA-matched cord blood samples. These samples come to us from the Hamilton community and surrounding areas, and we must genotype each sample to identify HLA type. So far around 10% have had the DRB1*0401- and A*0201-positive alleles and thus are suitable for use with DRAG-A2 mice, which is in line with the expected frequencies previously reported in North American populations (Chen et al., 2002; Ellis et al., 2000) (http://www.allelefrequencies.net/).

To date, we have successfully generated a total of 120 huNRG (63.8% success rate) and 6 huDRAG-A2 (100% success rate) mice to 10% hCD45+ leukocytes or greater (Table 3). This threshold value was selected as previous studies have shown that an adequate frequency of human target cells is an important factor for establishing HIV-1 infection and that engraftment of 10% or greater is adequate for intravaginal infection (Nguyen et al., 2017). Although it has been common practice to quantify the degree of immune reconstitution in hu-mice solely based on the frequency of human CD45+ leukocytes, these values are somewhat arbitrary as the number of murine leukocytes remaining can vary greatly between mice and even within the same mouse over time and thus influence the accuracy of our evaluation of successful human reconstitution. In order to account for this variability, it is becoming more common to include absolute count measurements alongside

the usual frequency reporting since advancements in technology now allow for simpler quantification (Coughlan et al., 2016; Labarthe et al., 2020). We have found that our previously established threshold of 10% generally correlates to about 50,000 hCD45+ leukocytes per mL of whole blood in our mice, although certain mice have had higher or lower absolute counts than expected based on the percentage measured (i.e. low %hCD45+ but high absolute count due to elevated levels of murine leukocytes in the blood artificially lowering the percentage of human cells).

In initial experiments comparing the immune cell breakdown of huNRG and huDRAG-A2 mice, a sample of blood was collected from a subset of mice to quantify human CD45+ leukocyte, CD3+, CD4+ and CD8+ T cell, CD19+ B cell and CD14+ monocyte reconstitution levels (Fig. 9). These mice were all humanized using the newborn IH method of engraftment and all mice were found to develop a measurable human immune system including all immune cell subsets of interests. In these mice, 72.2% of the huNRG mice (N=18) and 100% of the huDRAG-A2s (N=6) were successfully engraftment to 10% leukocytes or greater, which is significantly higher than the success rates previously reported in the huNRG model and similar to what has been reported in the huDRAG-A2 model (40% vs 90% respectively) (Danner et al., 2011). The huDRAG-A2 mice had a significantly higher overall human CD45+ leukocyte reconstitution in the blood at 12 and 20 weeks post-engraftment, as well as significantly higher CD4+ T cell and CD14+ monocyte levels at 12 weeks post-engraftment compared to huNRGs (Fig. 8). These immune cell subsets are especially important for models of HIV-1 and TB as CD4+ T cells and macrophages are the primary target cells for infection and are also heavily involved in

mediating immune responses following infection (Nusbaum et al., 2016; Pawlowski et al., 2012). Both models were also found to be capable of secreting a wide variety of human cytokines, including the pro-inflammatory cytokines, IFNγ, TNFα and IL-2, which are essential for proper T cell function and heavily involved in mediating both HIV and TB infection. However, the levels of the cytokines detected are much lower compared to what is seen in humans and it is not yet clear the physiological relevance of the cytokines when detected in these low amounts (Danner et al., 2011). Although further studies are required to elucidate the cytokine profiles developed in these mice, especially in different disease contexts and time-points, these findings indicate that both models develop robust human immune systems, high levels of important immune cell subsets and will likely be useful for investigating immune responses. However, the huDRAG-A2 model may offer some advantages for models of HIV-1 and/or TB in particular due to reported improvements in T cell function, cytokine and antibody secretion (Danner et al., 2011; Majji et al., 2016).

Overall leukocyte engraftment was also measured in a larger subset of huNRG mice humanized either by the newborn IH or adult IV methods of engraftment in order to determine if one method offers any improvements in reconstitution (see methods section 2.1.4). A previous study in huNRGs found that the methods of engraftment were both effective and comparable in terms of overall leukocyte engraftment over time but that the newborn IH method may offer improved T cell responses in certain tissues (Dykstra et al., 2016). We found that the mean hCD45+ leukocyte reconstitution was 31.63% or $1.1x10^5$ hCD45+/mL using the newborn IH method (N = 81) and 22.62% or $9.0x10^4$ hCD45+/mL using the adult IV method (N = 31), which are both well above the 10% hCD45+ leukocyte

cut-off required for engraftment to be considered successful enough for our experiments (Fig. 8). This difference was not significant. However the newborn engraftment method does offers a few practical advantages as the mice are ready for experiments at a younger age which leads to fewer health problems. For this reason, we primarily use the newborn method of engraftment but we can successfully use either method depending on genotyping or other experimental requirements.

huNRG mice have been successfully infected with both the NL4.3-Bal-Env and the JR-CSF strains of HIV-1, while the huDRAG-A2 mice have only been infected intravaginally with NL4.3-Bal-Env to date. Both of these strains are R5-tropic, which are typically used for HIV-1 studies as about 80% of wildtype strains are thought to be R5-tropic (Ferrer et al., 2014; Moyle et al., 2005). In addition, R5-tropic strains are generally used for mucosal infections as X4-tropic strains of HIV-1 are less successful at penetrating the vaginal/rectal mucosa and disseminating into the periphery to establish productive infection (Berges et al., 2008b). CCR5-expressing Langerhans cells (a type of highly susceptible tissue-resident antigen-presenting dendritic cell that does not express CXCR4) located in the vaginal/rectal mucosa are thought to be important in the early stages of establishing mucosal HIV-1 infection (Hladik et al., 2007; Jinjie Hu et al., 2000). The NL4.3-Bal-Env strain is a genetically modified strain of HIV-1 comprised of the X4-tropic NL4.3 backbone and the Env protein of the R5-tropic Bal strain, rendering it functionally R5-tropic. Infection with this strain is effective in generating infectious virus in cell lines and viremia in the blood of hu-mice, although it is less commonly used in the literature (Mariani et al., 2001; Skelton et al., 2019). In contrast, the JR-CSF strain of HIV-1 is much more commonly used in the

literature and has been shown to effectively infect CD4+ T cells, as well as macrophages, in both hu-mice and cell lines (Balazs et al., 2014; Denton et al., 2008; Jamieson et al., 1995; Schweighardt et al., 2004; Sun et al., 2007). The JR-CSF strain is an R5-tropic molecular clone that was first derived from a primary HIV-1 isolate and has been shown in previous literature to have a slightly reduced binding affinity to the CCR5-coreceptor compared to some other R5-tropic variants, resulting in mildly reduced infectivity and replication (Koyanagi et al., 1987; Pastore et al., 2004; Zhu et al., 1993). So far we have used both these strains in the huNRG model and did not see any significant differences in viral load or T cell depletion between the two. However, it's difficult to compare these experiments as different infectious doses and routes of inoculation were used and the variability in immune reconstitution between mice likely contributes to differences in viral replication. Infection with R5-tropic strains is generally associated with lower viral loads and less severe CD4+ T cell depletion compared to X4-tropic strains in primary CD4+ T cell cultures and hu-Scid mice reconstituted with liver and thymus (Berkowitz, Alexander, et al., 1998; Schweighardt et al., 2004; Uittenbogaart et al., 1996). Although the viral load in the plasma varied between mice, as well as over time, we measured a viral load of between 10^3 and 10^6 RNA copies/mL in successfully infected mice. Similar hu-mouse models of HIV-1 infection generally had comparable viral loads although variability was seen in the literature as well (Corleis et al., 2019; Gorantla et al., 2007; Nguyen et al., 2017; Wessels et al., 2021). X4-tropic strains of HIV-1 have long been considered to be more cytopathic towards a wider range of T cell subsets and conversion to X4- or dual-tropic

strains is associated with disease progression and worsening pathology (Penn et al., 1999; Scarlatti et al., 1997; Tersmette et al., 1989; Zhu et al., 1993).

Following intravaginal HIV-1 infection with NL4.3-Bal-Env, viral RNA was detectable in the vaginal wash and blood plasma of both huNRG and huDRAG-A2 mice starting at 2 weeks post-infection (Fig. 10a). Both models showed depleted targets cells in the blood and certain tissues indicating productive infection and viral dissemination. Human CD4+ T cell counts were slightly more reduced in the huDRAG-A2 mice indicating potentially increased susceptibility of these mice to HIV-1 (Fig. 10, 11 & 12). CD4+ T cell depletion was also measurable in the blood at around 8 weeks post-intravaginal infection when using R5-tropic strains of HIV-1 in similar non-transgenic hu-mouse models engrafted with CD34+ HSCs (Baenziger et al., 2006; Berges et al., 2008, 2010; Corleis et al., 2019; Sun et al., 2007). Considering the improved T cell reconstitution and function observed in similar HLA transgenic in the literature, it is likely that they possess a higher frequency of activated CCR5-expressing target human CD4+ T cells, which are known to be more permissible to infection (Danner et al., 2011; Majji et al., 2016; Meijerink et al., 2014; Veazey et al., 2000). In future experiments, we will add CCR5 to our flow cytometry panel in order to measure differences in T cell activation between these models and how these levels change following HIV infection.

The improved T cell reconstitution and function reported in the huDRAG-A2 mice is thought be a result of HLA-restricted T cell education in the thymus of these mice following engraftment with HLA-matched HSCs (Danner et al., 2011; Majji et al., 2016; Shultz et al.,

2010). Improved T cell functionality also indirectly results in improved B cell and antibody responses as T cell help (in the form of MHC class II binding, CD40 co-stimulation and cytokine secretion) is needed for B cell proliferation and Ig isotype class switching (Blum et al., 2013; Mayumi et al., 1983; Takatsu', 1997). Previous studies have indicated that humanized DR4/A2 mice are able to produce isotype-switched human IgG, IgE and IgA (Danner et al., 2011; Majji et al., 2016). This is consistent with our findings as we were able to detect HIV-specific IgG antibodies in the plasma of huDRAG-A2 mice at 8 weeks post-infection, but not the huNRG model (Fig.14). Not only are certain helper T cell-associated cytokines (such as IL-2, -4 and -5, TGF-β and IFN-γ) important in initiating the process of Ig isotype class switching but they are also required for the generation of Ag-specific antibodies (Fairfax et al., 2008; Pieper et al., 2013; Takatsu', 1997). Although helper T cell-dependent activation is thought to be important for generating Ag-specific isotype-switched antibody responses in this model, it remains unclear how HLA-restricted interactions with APCs affects early B cell development and maturation. Previous literature has found the levels of APCs like dendritic cells to be generally low in these models, although DR4-transgenic mice did have significantly higher levels compared to non-transgenic controls (Danner et al., 2011). As such, there may be some value to add HLA-DR to our flow cytometry panel in order to measure the frequency of APCs in the blood of these mice. To further elucidate the role of CD4+ T cells and APCs in the development of Ag-specific isotype-switched antibody responses in this model, we could deplete CD4+ T cells from successfully engrafted huDRAG-A2s and then vaccinate the mice. If they are still able to generate Ag-specific IgG in the absence of helper CD4+ T cells (although levels

would likely be low), this would indicate the involvement of other factors in early B cell development and maturation that may not occur without HLA-matching (Adler et al., 2017; Scholl & Geha, 1994). Although the level of anti-gp120 IgG antibodies detected by ELISA in the huDRAG-A2s at 8 weeks was impossible to accurately quantify as the signal was much lower than what would be expected in humans based on the controls that were provided by the manufacturer. As such, an alternative method for quantifying low signals outlined by the manufacturer was used, allowing us to determine which samples were measured above the detection threshold (see methods section 2.2.5). Previous literature has shown IgG levels are much lower in these mice compared to humans so this is not unexpected, however it still highlights the improved B function seen in these mice and may be useful for future experiments (Danner et al., 2011; Fouda et al., 2011). Our preliminary cytokine data also indicated that the huDRAG-A2 mice may trend towards higher levels of certain T cell-associated cytokines (Fig. 13), however only a few mice were analysed, variability within groups was high and samples were only collected at experimental endpoint, which may have not been the optimal time to measure peak cytokine responses. Although this preliminary data supports that T function is improved in these mice, it is by no means conclusive and will need to be repeated in future experiments. Overall cytokine levels were lower in both models at 8 weeks post-infection compared to uninfected controls, but T cell depletion was more severe in the huDRAG-A2 mice. This likely results in reduced cytokine production overall as T cells are thought to be the primary producers of these particular cytokines in similar hu-mouse models (Gendelman et al., 2021; Shultz et al., 2010, 2012; Skelton et al., 2018; Vudattu et al., 2014). Once the number of T cells

remaining is taken into account (see methods section 2.2.5), huDRAG-A2 mice trended towards increased cytokine levels, however levels were still low compared to humans and the physiological implications of these low levels are not yet clear (Danner et al., 2011; Majji et al., 2016). Since DR4-transgenic hu-mice have previously been shown to generate more robust Ag-specific T cell responses compared to non-transgenic controls, these mice may have higher frequencies of IFNγ, TNFα and IL-2 secreting T cells following stimulation with an HIV antigen such as gp120. In future experiments, we are interested in further exploring the differences in ability to generate HIV-specific T cell responses in these models (Danner et al., 2011; Majji et al., 2018).

huNRG mice have also been successfully infected with the JR-CSF strain of HIV-1 either systemically or intravaginally. Viral RNA was detectable in the plasma of most mice at 1 week post-systemic infection, compared to 2 weeks for intravaginal infection, indicating systemic infection results in more rapid viral dissemination and progression (Fig. 15a). Target CD4+ T cells also trended towards depletion by 4 weeks post-infection, regardless of route of infection (Fig. 15b & c). Two infectious doses were tested for the systemic route of infection (10^5 and 10^6 IU) and both were found to be sufficient for productive infection in successfully engrafted mice (>10% hCD45+ leukocytes), although there was significant variability between some mice that may be a result of differences in immune reconstitution. In fact, the only mouse that was not successfully infected was the mouse with the lowest CD4+ T cell reconstitution pre-infection, which highlights the importance of adequate target cells for productive infection in these mice that has also been described in the literature (Nguyen et al., 2017).

Preliminary TB infections have been successful in both the huNRG and huDRAG-A2 models using the mCherry-Erdman, YFP-H37Rv or non-tagged H37Rv strains of *Mtb*. Intranasal *Mtb* infection with H37Rv resulted in elevated bacterial load in the lungs and spleen of both huNRG and huDRAG-A2 mice, as well as the formation of significant granulomatous tissue in the lungs of both models. These granulomas were characterised by immune cell infiltration, classical granuloma organization and caseous necrotic cores in both huNRG mice with Erdman and huDRAG-A2 mice with H37Rv (Fig. 17 & 19). Using the mCherry-tagged Erdman, 79.1% of the human CD206+CD169+ alveolar macrophages in the lung tissue of huNRG mice were determined to be infected with *Mtb,* indicating productive infection of human target cells (Fig. 16b). A portion of the other human macrophages, including the CD206+CD14+CD169- interstitial macrophages population, as well as some of the CD3+ T cells in the lung were also found to be infected with the *Mtb*. The involvement of multiple immune cell populations is a known feature of TB in humans, NHP and normal mouse models (Hernández-Pando et al., 2000; Lerner et al., 2017; Mayito et al., 2019). Since *Mtb* is also able to infect murine cells, it is important to prove the involvement of the engrafted human immune cells in the pathogenesis of the infection. Although well-known alveolar macrophage markers were used in the previous experiment (Yu et al., 2016), these cells are more commonly collected from the airway lumen by BAL as this avoids contamination from other lung macrophage populations (Busch et al., 2019; Davies & Gordon, 2005).

Unfortunately, we were unable to accurately measure the frequency of *Mtb*-infected target alveolar macrophages in the BAL of the YFP-H37Rv infected mice as the lungs were

severely hemorrhaged and as a result, there was significant blood contamination and few macrophages collected. The YFP-H37Rv that was used for this experiment was obtained as a generous gift from Drs. Samuel Behar and Rocky Lai and had not yet been used in our hands. It is possible that this stock of H37Rv may have been more virulent compared to the non-fluorescent H37Rv stocks that are maintained at McMaster University and this may have caused increased damage to the airways and apoptosis of the alveolar macrophages (Grabiec & Hussell, 2016). CFU quantification of the lung and spleen of the mice indicated the bacterial burden was significant (mean of $10^{7.82}$ and $10^{5.79}$ CFU in the lung and spleen, respectively), similar to what was observed in the mice infected with a slightly lower dose of the highly virulent Erdman strain, which would support the theory that this particular stock is more virulent than expected. It is also possible that this is a result of GvHD as the T cells involved in mediating GvHD are known to cause tissue damage. However, these mice did not show any symptoms of GvHD (weight loss, skin issues) during this experiment. To our knowledge, BAL has never been examined in hu-mice infected with *Mtb* so we are unsure what immune cell populations to expect. Using a similar huNSG model of respiratory syncytial virus (RSV), Sharma et al. was able to show that the BAL collected from similar hu-mice contained approx. 10^5 macrophages per mouse (Sharma et al., 2016), indicating that we should be able to collect a decent macrophage population via BAL. In future studies, we may repeat this experiment with a lower infectious dose of the YFP-H37Rv or mCherry-Erdman and re-examine the BAL. We are also planning on collecting BAL from healthy uninfected mice to elucidate whether there is limited immune cell engraftment in the airways of these mice to begin with or if the pathogenesis of the *Mtb*

infection is causing cell death. Histopathology of the lungs of the YFP-H37Rv-infected mice is not yet available but may offer some further insights on the degree of tissue damage observed.

In a proof-of-concept experiment, huNRG and huDRAG-A2 mice were infected with non-tagged H37Rv and assessed for hallmarks of pulmonary TB and bacterial dissemination. There was no significant difference observed the bacterial burden measured in the lungs or spleen of the mice (Fig. 18a) and both models developed human-like granuloma pathology (Fig. 19 & 20). However, the huDRAG-A2 mice showed a more classical granuloma organization compared to the huNRGs, which was characterized by a ring of CD4+ T cells surrounding the granuloma with CD68+ macrophages located within the core of the granuloma (Fig. 19d &e). This indicates the involvement of the engrafted human immune system in the containment and control of the *Mtb* infection. H&E staining revealed more caseating necrosis within the cores of the huDRAG-A2 granulomas infected with H37Rv and huNRGs infected with the more virulent Erdman strain of *Mtb* (Fig. 17 & 19), which is a hallmark characteristic human granuloma pathology and the lack of caseating necrosis within the granuloma is major limitation of most normal mouse models of TB (Calderon et al., 2013; Singh & Gupta, 2018). Another hallmark feature of TB granulomas in humans in the formation of multinucleated giant cells, masses of fused monocytes and macrophages, that may occur following infection of the cells with *Mtb* (Brooks et al., 2019; Lösslein et al., 2021). In particular, multinucleated giant cells found in human TB granulomas are often known as Langhans giant cells, which are typically associated with inflammatory granulomatous conditions such as mycobacterial infections (Kumar et al., 2013). Since this

is also a key feature of TB pathology in humans, we are interested in further evaluating the histopathology from these experiments with the help of a pathologist to assess for the presence of multinucleated giant cells. The *Mtb* bacilli were also visualized using AFB staining and were found to be mostly localized within the core of the granulomas in both models following infection with H37Rv, while the bacilli were spread more diffusely throughout the lung tissue with the more virulent Erdman (Fig. 17, 19 & 20). Although AFB staining is difficult to quantify, the huDRAG-A2 mice appeared to have less *Mtb* within the granuloma core compared to the huNRGs, which may indicate improved anti-mycobacterial responses and enhanced containment of the infection.

The huDRAG-A2 mice were also found to have a trend towards reduced human CD3+ T cell frequency and CD4+:CD8+ T cell ratio compared to huNRG mice (not significant) (Fig. 18b, d & e). Although this mechanism is not well understood, it has been observed in clinical manifestations of pulmonary TB in humans and may be a result of apoptosis or activation-induced cell death (Uppal et al., 2004; Venturini et al., 2019; Yin et al., 2015). It is also possible that the bias towards CD8+ T cells seen in the huDRAG-A2 mice may be a results of the enhanced cytotoxic CD8+ T cell responses seen in A2-transgenic hu-mice (Majji et al., 2016). CD8+ T cells are known to have an important role in anti-TB responses and may be expanding in response to the *Mtb* infection (Lin & Flynn, 2015). Flow data from the huDRAG-A2 mice indicated that the frequency of certain monocyte (CD14+) and macrophage (CD11b+, CD206+) populations were slightly elevated (not significant) in the lungs of huDRAG-A2 mice compared to huNRGs, however this is expected due to the higher monocyte engraftment reported in these mice before infection.

Although inconclusive, an increased number of monocytes/macrophages may potentially result in enhanced clearance of *Mtb* by phagocytosis and improved containment of the infection (D'Agostino et al., 2020; Verrall et al., 2014). Due to the improved immune cell function seen in the huDRAG-A2 mice in previous literature (Danner et al., 2011; Majji et al., 2016), the presence of *Mtb*-specific human IgG and certain pro-inflammatory cytokines were measured in the blood plasma and lung homogenates respectively. Unfortunately we were not able to detect any IgG signal in the huDRAG-A2 mice in this experiment, but this is not entirely unexpected considering the 4 week timeline of this infection and *Mtb*'s ability to supress and delay the activation of the adaptive immune system (Wolf et al., 2008). We will likely need to repeat this experiment with a longer timeline in order to capture antibody responses against *Mtb*. Antibodies specific to the antigens used in this ELISA kit (18, 36 and 40 kDa antigens) have been detected in patients with both active and latent TB and are sometimes used to help diagnose TB, although the relevance of their role in protective responses is not well understood (Anderson et al., 2008; Wang et al., 2018; WHO, 2010). Certain pro-inflammatory cytokines (IFNγ and TNFα) were also detected in the lung homogenates of both huNRG and huDRAG-A2 mice, with the huDRAG-A2 mice trending towards a slightly higher mean level of these cytokines that is not significant due to considerable variability between mice in the huDRAG-A2 group (Fig. 21). These cytokines are known to be important in mediating anti-mycobacterial responses and granuloma formation so this is likely important for our model, however the levels detected were much lower compared to what is normally seen in humans (Danner et al., 2011; Majji et al., 2016).

5. CONCLUSION & FUTURE DIRECTIONS:

Now that we have optimized our protocols and successfully established models of HIV-1 and TB in both huNRG and huDRAG-A2 mice, our next steps are to conduct a pilot co-infection experiment in a group of huNRG mice (Fig. 22 - this experiment in currently ongoing). More extensive co-infection experiments will be conducted in both hu-mouse models as soon as more successful huDRAG-A2 mice are available. Once these models of HIV-1, TB and co-infection have been validated, they will be used to investigate several research questions within those fields. Firstly, the huDRAG-A2 mouse model will be especially helpful to investigate novel vaccine formulations for both HIV-1 and TB as these mice are able to develop a diverse T cell repertoire and consequently, are able to produce a wide variety of antigen-specific human IgG and IgA antibody responses, both of which are critical for measuring vaccine-induced systemic and mucosal immunity. The hu-mouse models of HIV-1 will be useful to investigate various PrEP and PEP drug formulations and schedules (including novel mucosal prophylactic treatments such as nano-curcumin). Both the HIV-1 and TB models alone, as well as the co-infection models, will be helpful for investigating the effectiveness and tolerability of ART, anti-TB drugs and vaccines when taken separately or in conjunction.

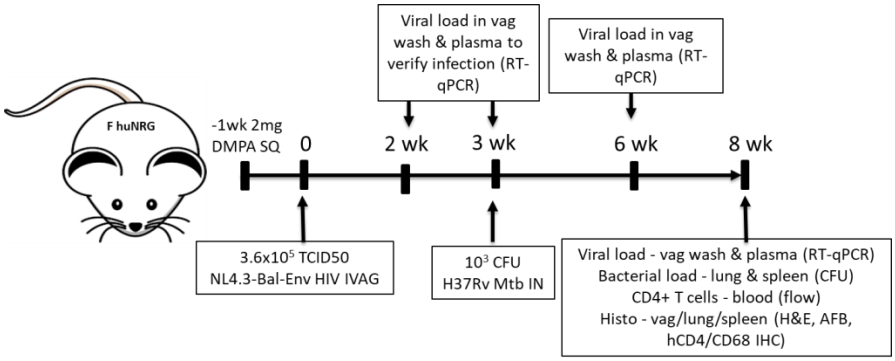

Fig. 22. *Experimental timeline for preliminary Mtb infections in HIV-1 co-infected huNRG mice (currently ongoing).*

6. REFERENCES

Abad-Fernández, M., Vallejo, A., Hernández-Novoa, B., Díaz, L., Gutiérrez, C., Madrid, N., Muñoz, M. Á., & Moreno, S. (2013). Correlation between different methods to measure microbial translocation and its association with immune activation in long-term suppressed HIV-1-infected individuals. *Journal of Acquired Immune Deficiency Syndromes (1999)*, *64*(2), 149–153. https://doi.org/10.1097/QAI.0B013E31829A2F12

Aderem, A., & Underhill, D. M. (1999). MECHANISMS OF PHAGOCYTOSIS IN MACROPHAGES. *Annual Review of Immunology*, *17*(1), 593–623. https://doi.org/10.1146/annurev.immunol.17.1.593

Adler, L. N., Jiang, W., Bhamidipati, K., Millican, M., Macaubas, C., Hung, S. chen, & Mellins, E. D. (2017). The other function: Class II-restricted antigen presentation by B cells. *Frontiers in Immunology*, *8*(MAR), 319. https://doi.org/10.3389/fimmu.2017.00319

Agostini, C., Trentin, L., Zambello, R., & Semenzato, G. (1993). HIV-1 and the lung : infectivity, pathogenic mechanisms, and cellular immune responses taking place in the lower respiratory tract. *The American Review of Respiratory Disease*, *147*(4).

Akanbi, M. O., Scarci, K., Taiwo, B., & Murphy, R. L. (2012). Combination Nucleoside/ Nucleotide Reverse Transcriptase Inhibitors. *Expert Opinion on Pharmacotherapy*, *13*(1), 65. https://doi.org/10.1517/14656566.2012.642865

Alkhatib, G., Broder, C. C., & Berger, E. A. (1996). Cell Type-Specific Fusion Cofactors Determine Human Immunodeficiency Virus Type 1 Tropism for T-Cell Lines versus Primary Macrophages. *JOURNAL OF VIROLOGY*, *70*(8), 5487–5494.

Allam, A., Majji, S., Peachman, K., Jagodzinski, L., Kim, J., Ratto-Kim, S., Wijayalath, W., Merbah, M., Kim, J. H., Michael, N. L., Alving, C. R., Casares, S., & Rao, M. (2015). TFH cells accumulate in mucosal tissues of humanized-DRAG mice and are highly permissive to HIV-1. *Scientific Reports 2015 5:1*, *5*(1), 1–16. https://doi.org/10.1038/srep10443

Anderson, B. L., Welch, R. J., & Litwin, C. M. (2008). Assessment of Three Commercially Available Serologic Assays for Detection of Antibodies to Mycobacterium tuberculosis and Identification of Active Tuberculosis. *Clinical and Vaccine Immunology : CVI*, *15*(11), 1644. https://doi.org/10.1128/CVI.00271-08

Andersson, S., Norrgren, H., Da Silva, Z., Biague, A., Bamba, S., Kwok, S., Christopherson, C., Biberfeld, G., & Albert, J. (2000). Plasma viral load in HIV-1 and HIV-2 singly and dually infected individuals in Guinea-Bissau, West Afica. Significantly lower plasma virus set point in HIV-2 infection than in HIV-1 infection. *Archives of Internal Medicine*, *160*(21), 3286–3293. https://doi.org/10.1001/archinte.160.21.3286

Antonucci, G. (1995). Risk Factors for Tuberculosis in HIV-lnfected Persons. *Jama*, *274*(2), 143. https://doi.org/10.1001/jama.1995.03530020061033

Apt, A., & Kramnik, I. (2009). Man and mouse TB: contradictions and solutions. *Tuberculosis (Edinburgh, Scotland)*, *89*(3), 195. https://doi.org/10.1016/J.TUBE.2009.02.002

Arrey, F., Löwe, D., Kuhlmann, S., Kaiser, P., Moura-Alves, P., Krishnamoorthy, G., Lozza, L., Maertzdorf, J., Skrahina, T., Skrahina, A., Gengenbacher, M., Nouailles, G., & Kaufmann, S. H. E. (2019). Humanized Mouse Model Mimicking Pathology of Human Tuberculosis for in vivo Evaluation of Drug Regimens. *Frontiers in Immunology*, *0*(JAN), 89. https://doi.org/10.3389/FIMMU.2019.00089

Baenziger, S., Tussiwand, R., Schlaepfer, E., Mazzucchelli, L., Heikenwalder, M., Kurrer, M. O., Behnke, S., Frey, J., Oxenius, A., Joller, H., Aguzzi, A., Manz, M. G., & Speck, R. F. (2006). *Disseminated and sustained HIV infection in CD34 cord blood cell-transplanted Rag2 / c / mice*. www.pnas.orgcgidoi10.1073pnas.0604493103

Balazs, A. B., Ouyang, Y., Hong, C. M., Chen, J., Nguyen, S. M., Rao, D. S., An, D. S., & Baltimore, D. (2014). Vectored immunoprophylaxis protects humanized mice from mucosal HIV transmission. *Nature Medicine*, *20*(3), 296–300. https://doi.org/10.1038/nm.3471

Bar, K. J., Coronado, E., Hensley-McBain, T., O'Connor, M. A., Osborn, J. M., Miller, C., Gott, T. M., Wangari, S., Iwayama, N., Ahrens, C. Y., Smedley, J., Moats, C., Lynch, R. M., Haddad, E. K., Haigwood, N. L., Fuller, D. H., Shaw, G. M., Klatt, N. R., & Manuzak, J. A. (2019). Simian-Human Immunodeficiency Virus SHIV.CH505

Infection of Rhesus Macaques Results in Persistent Viral Replication and Induces Intestinal Immunopathology. *Journal of Virology*, *93*(18). https://doi.org/10.1128/JVI.00372-19/ASSET/16BE66BD-22CC-4E6E-93B5-3650EBB3E1F1/ASSETS/GRAPHIC/JVI.00372-19-F0013.JPEG

Barber, S. A., Gama, L., Li, M., Voelker, T., Anderson, J. E., Zink, M. C., Tarwater, P. M., Carruth, L. M., & Clements, J. E. (2006). Longitudinal Analysis of Simian Immunodeficiency Virus (SIV) Replication in the Lungs: Compartmentalized Regulation of SIV. *The Journal of Infectious Diseases*, *194*(7), 931–938. https://doi.org/10.1086/507429

Barré-Sinoussi, F., Chermann, J. C., Rey, F., Nugeyre, M. T., Chamaret, S., Gruest, J., Dauguet, C., Axler-Blin, C., Vézinet-Brun, F., Rouzioux, C., Rozenbaum, W., & Montagnier, L. (1983). Isolation of a T-Lymphotropic Retrovirus from a Patient at Risk for Acquired Immune Deficiency Syndrome (AIDS). *Science*, *220*(4599), 868–871. https://doi.org/10.1126/SCIENCE.6189183

Baxter, A. E., Russell, R. A., Duncan, C. J. A., Moore, M. D., Willberg, C. B., Pablos, J. L., Finzi, A., Kaufmann, D. E., Ochsenbauer, C., Kappes, J. C., Groot, F., & Sattentau, Q. J. (2014). Macrophage infection via selective capture of HIV-1-infected CD4+ T cells. *Cell Host and Microbe*, *16*(6), 711–721. https://doi.org/10.1016/j.chom.2014.10.010

Behrens, M., Trejo, T., Luthra, H., Griffiths, M., David, C. S., & Taneja, V. (2010). Mechanism by which HLA-DR4 Regulates Sex-bias of Arthritis in humanized mice.

Journal of Autoimmunity, *35*(1), 1. https://doi.org/10.1016/J.JAUT.2009.12.007

Beigier-Bompadre, M., Montagna, G. N., Kühl, A. A., Lozza, L., Weiner, J., Kupz, A., Vogelzang, A., Mollenkopf, H. J., Löwe, D., Bandermann, S., Dorhoi, A., Brinkmann, V., Matuschewski, K., & Kaufmann, S. H. E. (2017). Mycobacterium tuberculosis infection modulates adipose tissue biology. *PLoS Pathogens*, *13*(10), e1006676. https://doi.org/10.1371/journal.ppat.1006676

Beliakova-Bethell, N., Massanella, M., White, C., Lada, S. M., Du, P., Vaida, F., Blanco, J., Spina, C. A., & Woelk, C. H. (2014). The effect of cell subset isolation method on gene expression in leukocytes. *Cytometry Part A*, *85*(1), 94–104. https://doi.org/10.1002/cyto.a.22352

Bell, L. C. K., & Noursadeghi, M. (2018). Pathogenesis of HIV-1 and mycobacterium tuberculosis co-infection. In *Nature Reviews Microbiology* (Vol. 16, Issue 2, pp. 80–90). Nature Publishing Group. https://doi.org/10.1038/nrmicro.2017.128

Berges, B. K., Akkina, S. R., Folkvord, J. M., Connick, E., & Akkina, R. (2008a). Mucosal transmission of R5 and X4 tropic HIV-1 via vaginal and rectal routes in humanized Rag2-/-γc-/- (RAG-hu) mice. *Virology*, *373*(2), 342–351. https://doi.org/10.1016/j.virol.2007.11.020

Berges, B. K., Akkina, S. R., Folkvord, J. M., Connick, E., & Akkina, R. (2008b). Mucosal transmission of R5 and X4 tropic HIV-1 via vaginal and rectal routes in humanized Rag2-/-γc-/- (RAG-hu) mice. *Virology*, *373*(2), 342–351.

https://doi.org/10.1016/j.virol.2007.11.020

Berges, B. K., Akkina, S. R., Remling, L., & Akkina, R. (2010). Humanized Rag2-/-γc-/- (RAG-hu) mice can sustain long-term chronic HIV-1 infection lasting more than a year. *Virology*, *397*(1), 100–103. https://doi.org/10.1016/j.virol.2009.10.034

Berkman, N., John, M., Roesems, G., Jose, P. J., Barnes, P. J., & Chung, K. F. (1995). Inhibition of macrophage inflammatory protein-1 alpha expression by IL-10. Differential sensitivities in human blood monocytes and alveolar macrophages. *The Journal of Immunology*, *155*(9).

Berkowitz, R. D., Alexander, S., Bare, C., Linquist-Stepps, V., Bogan, M., Moreno, M. E., Gibson, L., Wieder, E. D., Kosek, J., Stoddart, C. A., & McCune, J. M. (1998). CCR5- and CXCR4-Utilizing Strains of Human Immunodeficiency Virus Type 1 Exhibit Differential Tropism and Pathogenesis In Vivo. *Journal of Virology*, *72*(12), 10108. https://doi.org/10.1128/jvi.72.12.10108-10117.1998

Berkowitz, R. D., Beckerman, K. P., Schall, T. J., & McCune, J. M. (1998). CXCR4 and CCR5 expression delineates targets for HIV-1 disruption of T cell differentiation. *Journal of Immunology (Baltimore, Md. : 1950)*, *161*(7), 3702–37010. http://www.jimmunol.org/content/161/7/3702

Bernard, D., Peakman, M., & Hayday, A. C. (2008). *Establishing humanized mice using stem cells: maximizing the potential The need for humanized mice*. https://doi.org/10.1111/j.1365-2249.2008.03659.x

Berón, W., Alvarez-Dominguez, C., Mayorga, L., & Stahl, P. D. (1995). Membrane trafficking along the phagocytic pathway. In *Trends in Cell Biology* (Vol. 5, Issue 3, pp. 100–104). https://doi.org/10.1016/S0962-8924(00)88958-8

Bevan, M. J. (1981). Thymic education. *Immunology Today*, *2*(11), 216–219. https://doi.org/10.1016/0167-5699(81)90050-5

Bezuidenhout, J., Roberts, T., Muller, L., van Helden, P., & Walzl, G. (2009). Pleural tuberculosis in patients with early HIV infection is associated with increased TNF-alpha expression and necrosis in granulomas. *PloS One*, *4*(1). https://doi.org/10.1371/JOURNAL.PONE.0004228

Bhatt, K., Verma, S., Ellner, J. J., & Salgame, P. (2015). *Quest for Correlates of Protection against Tuberculosis*. https://doi.org/10.1128/CVI.00721-14

Billerbeck, E., Horwitz, J. A., Labitt, R. N., Donovan, B. M., Vega, K., Budell, W. C., Koo, G. C., Rice, C. M., & Ploss, A. (2013). Characterization of Human Antiviral Adaptive Immune Responses during Hepatotropic Virus Infection in HLA-Transgenic Human Immune System Mice. *The Journal of Immunology*, *191*(4), 1753–1764. https://doi.org/10.4049/jimmunol.1201518

Bleul, C. C., Wu, L., Hoxie, J. A., Springer, T. A., & Mackay, C. R. (1997). The HIV coreceptors CXCR4 and CCR5 are differentially expressed and regulated on human T lymphocytes. *Proceedings of the National Academy of Sciences*, *94*(5), 1925–1930. https://doi.org/10.1073/PNAS.94.5.1925

Blum, J. S., Wearsch, P. A., & Cresswell, P. (2013). Pathways of Antigen Processing. *Annual Review of Immunology*, *31*, 443. https://doi.org/10.1146/ANNUREV-IMMUNOL-032712-095910

Bonora, S., Nicastri, E., Calcagno, A., De Requena, D. G., D'Ettorre, G., Sarmati, L., Palmisano, L., Vullo, V., Di Perri, G., & Andreoni, M. (2009). Ultrasensitive assessment of residual HIV viraemia in HAART-treated patients with persistently undetectable plasma HIV-RNA: A cross-sectional evaluation. *Journal of Medical Virology*, *81*(3), 400–405. https://doi.org/10.1002/jmv.21405

Booiman, T., Wit, F. W., Maurer, I., De Francesco, D., Sabin, C. A., Harskamp, A. M., Prins, M., Garagnani, P., Pirazzini, C., Franceschi, C., Fuchs, D., Gisslén, M., Winston, A., Reiss, P., Kootstra, N. A., Schouten, J., Kooij, K. W., van Zoest, R. A., Elsenga, B. C., … Dewaele, S. (2017). High Cellular Monocyte Activation in People Living With Human Immunodeficiency Virus on Combination Antiretroviral Therapy and Lifestyle-Matched Controls Is Associated With Greater Inflammation in Cerebrospinal Fluid. *Open Forum Infectious Diseases*, *4*(3), 1–11. https://doi.org/10.1093/OFID/OFX108

Borisov, S. E., Dheda, K., Enwerem, M., Leyet, R. R., D'Ambrosio, L., Centis, R., Sotgiu, G., Tiberi, S., Alffenaar, J. W., Maryandyshev, A., Belilovski, E., Ganatra, S., Skrahina, A., Akkerman, O., Aleksa, A., Amale, R., Artsukevich, J., Bruchfeld, J., Caminero, J. A., … Migliori, G. B. (2017). Effectiveness and safety of bedaquilinecontaining regimens in the treatment of MDR- and XDR-TB: A

multicentre study. *European Respiratory Journal*, *49*(5). https://doi.org/10.1183/13993003.00387-2017

Bosco, S. C., Pawson, M., Parsons, J. T., & Starks, T. J. (2019). Biomedical HIV Prevention among Gay Male Couples: A Qualitative Study of Motivations and Concerns. *Https://Doi.Org/10.1080/00918369.2019.1696105*, *68*(8), 1353–1370. https://doi.org/10.1080/00918369.2019.1696105

Bosho, D. D., Dube, L., Mega, T. A., Adare, D. A., Tesfaye, M. G., & Eshetie, T. C. (2018). Prevalence and predictors of metabolic syndrome among people living with human immunodeficiency virus (PLWHIV). *Diabetology & Metabolic Syndrome*, *10*(1). https://doi.org/10.1186/S13098-018-0312-Y

Bosma, G. C., Custer, R. P., & Bosma, M. J. (1983). A severe combined immunodeficiency mutation in the mouse. *Nature*, *301*(5900), 527–530. https://doi.org/10.1038/301527a0

Bozzano, F., Marras, F., & De Maria, A. (2014). Immunology of tuberculosis. In *Mediterranean Journal of Hematology and Infectious Diseases* (Vol. 6, Issue 1). Universita Cattolica del Sacro Cuore. https://doi.org/10.4084/MJHID.2014.027

Brechtl, J. R., Breitbart, W., Galietta, M., Krivo, S., & Rosenfeld, B. (2001). The Use of Highly Active Antiretroviral Therapy (HAART) in Patients With Advanced HIV Infection: Impact on Medical, Palliative Care, and Quality of Life Outcomes. *Journal of Pain and Symptom Management*, *21*(1), 41–51.

https://doi.org/10.1016/S0885-3924(00)00245-1

Brett, K., & Severn, M. (2020). *Bacille Calmette-Guérin Vaccination: A Review of Clinical Effectiveness and Guidelines SUMMARY WITH CRITICAL APPRAISAL Bacille Calmette-Guérin Vaccination*.

Briz, V., Poveda, E., & Soriano, V. (2006). HIV entry inhibitors: mechanisms of action and resistance pathways. *Journal of Antimicrobial Chemotherapy*, *57*(4), 619–627. https://doi.org/10.1093/JAC/DKL027

Brooks, P. J., Glogauer, M., & McCulloch, C. A. (2019). An Overview of the Derivation and Function of Multinucleated Giant Cells and Their Role in Pathologic Processes. *American Journal of Pathology*, *189*(6), 1145–1158. https://doi.org/10.1016/j.ajpath.2019.02.006

Brumeanu, T.-D., Vir, P., Karim, A. F., Kar, S., Benetiene, D., Lok, M., Greenhouse, J., Putmon-Taylor, T., Kitajewski, C., Chung, K. K., Pratt, K. P., & Casares, S. A. (2020). A Human-Immune-System (HIS) humanized mouse model (DRAGA: HLA-A2. HLA-DR4. Rag1 KO.IL-2Rγc KO. NOD) for COVID-19. *BioRxiv*. https://doi.org/10.1101/2020.08.19.251249

Bucşan, A. N., Chatterjee, A., Singh, D. K., Foreman, T. W., Lee, T. H., Threeton, B., Kirkpatrick, M. G., Ahmed, M., Golden, N., Alvarez, X., Hoxie, J. A., Mehra, S., Rengarajan, J., Khader, S. A., & Kaushal, D. (2019). Mechanisms of reactivation of latent tuberculosis infection due to SIV coinfection. *The Journal of Clinical*

Investigation, *129*(12), 5254–5260. https://doi.org/10.1172/JCI125810

Bunjun, R., Riou, C., Soares, A. P., Thawer, N., Müller, T. L., Kiravu, A., Ginbot, Z., Oni, T., Goliath, R., Kalsdorf, B., Von Groote-Bidlingmaier, F., Hanekom, W., Walzl, G., Wilkinson, R. J., & Burgers, W. A. (2017). Effect of HIV on the Frequency and Number of Mycobacterium tuberculosis-Specific CD4 + T Cells in Blood and Airways during Latent M. tuberculosis Infection. *Journal of Infectious Diseases*, *216*(12), 1550–1560. https://doi.org/10.1093/infdis/jix529

Busch, C. J.-L., Favret, J., Geirsdóttir, L., Molawi, K., & Sieweke, M. H. (2019). Isolation and Long-term Cultivation of Mouse Alveolar Macrophages. *Bio-Protocol*, *9*(14). https://doi.org/10.21769/BIOPROTOC.3302

Calderon, V. E., Valbuena, G., Goez, Y., Judy, B. M., Huante, M. B., Sutjita, P., Johnston, R. K., Estes, D. M., Hunter, R. L., Actor, J. K., Cirillo, J. D., & Endsley, J. J. (2013). *A Humanized Mouse Model of Tuberculosis*. *8*(5). https://journals.plos.org/plosone/article?id=10.1371/journal.pone.0063331

Call, S. A., Klapow, J. C., Stewart, K. E., Westfall, A. O., Mallinger, A. P., DeMasi, R. A., Centor, R., & Saag, M. S. (2000). Health-related quality of life and virologic outcomes in an HIV clinic. *Quality of Life Research*, *9*(9), 977–985. https://doi.org/10.1023/A:1016668802328

Carter, C. A., & Ehrlich, L. S. (2008). Cell Biology of HIV-1 Infection of Macrophages. *Annual Review of Microbiology*, *62*(1), 425–443.

https://doi.org/10.1146/annurev.micro.62.081307.162758

Caruso, A. M., Serbina, N., Klein, E., Triebold, K., Bloom, B. R., & Flynn, J. L. (1999). Mice deficient in CD4 T cells have only transiently diminished levels of IFN-gamma, yet succumb to tuberculosis. *Journal of Immunology (Baltimore, Md. : 1950)*, *162*(9), 5407–5416. http://www.ncbi.nlm.nih.gov/pubmed/10228018

Cary, D. C., Fujinaga, K., & Peterlin, B. M. (2016). Molecular mechanisms of HIV latency. *The Journal of Clinical Investigation*, *126*(2), 448–454. https://doi.org/10.1172/JCI80565

Cassol, E., Cassetta, L., Alfano, M., & Poli, G. (2010). Macrophage polarization and HIV-1 infection. *Journal of Leukocyte Biology*, *87*(4), 599–608. https://doi.org/10.1189/jlb.1009673

Castellano, P., Prevedel, L., Valdebenito, S., & Eugenin, E. A. (2019). HIV infection and latency induce a unique metabolic signature in human macrophages. *Scientific Reports 2019 9:1*, *9*(1), 1–14. https://doi.org/10.1038/s41598-019-39898-5

Celum, C. L., Delany-Moretlwe, S., Baeten, J. M., van der Straten, A., Hosek, S., Bukusi, E. A., McConnell, M., Barnabas, R. V., & Bekker, L. G. (2019). HIV pre-exposure prophylaxis for adolescent girls and young women in Africa: from efficacy trials to delivery. *Journal of the International AIDS Society*, *22*(S4), e25298. https://doi.org/10.1002/JIA2.25298

Chackerian, A. A., Perera, T. V., & Behar, S. M. (2001). Gamma interferon-producing

CD4+ T lymphocytes in the lung correlate with resistance to infection with Mycobacterium tuberculosis. *Infection and Immunity*, *69*(4), 2666–2674. https://doi.org/10.1128/IAI.69.4.2666-2674.2001

Chackerian, Alissa A., Alt, J. M., Perera, T. V., Dascher, C. C., & Behar, S. M. (2002). Dissemination of Mycobacterium tuberculosis is influenced by host factors and precedes the initiation of T-cell immunity. *Infection and Immunity*, *70*(8), 4501–4509. https://doi.org/10.1128/IAI.70.8.4501-4509.2002

Chan, J., Mehta, S., Bharrhan, S., Chen, Y., Achkar, J. M., Casadevall, A., & Flynn, J. A. (2014). The role of B cells and humoral immunity in Mycobacterium tuberculosis infection. *Seminars in Immunology*, *26*(6), 588–600. https://doi.org/10.1016/J.SMIM.2014.10.005

Charles A Janeway, J., Travers, P., Walport, M., & Shlomchik, M. J. (2001). *Principles of innate and adaptive immunity*. https://www.ncbi.nlm.nih.gov/books/NBK27090/

Charles, T. P., & Shellito, J. E. (2016). Human Immunodeficiency Virus Infection and Host Defense in the Lungs. *Seminars in Respiratory and Critical Care Medicine*, *37*(2), 147–156. https://doi.org/10.1055/s-0036-1572553

Chelkeba, L., Fekadu, G., Tesfaye, G., Belayneh, F., Melaku, T., & Mekonnen, Z. (2020). Effects of time of initiation of antiretroviral therapy in the treatment of patients with HIV/TB co-infection: A systemic review and meta-analysis. *Annals of Medicine and Surgery*, *55*, 148–158. https://doi.org/10.1016/J.AMSU.2020.05.004

Chen, D. S., Tang, T. F., Pulyaeva, H., Slack, R., Tu, B., Wagage, D., Li, L., Perlee, L., Ng, J., Hartzman, R. J., & Katovich Hurley, C. (2002). Relative HLA-DRB1*04 allele frequencies in five United States populations found in a hematopoietic stem cell volunteer donor registry and seven new DRB1*04 alleles. *Human Immunology*, *63*(8), 665–672. https://doi.org/10.1016/S0198-8859(02)00418-4

Cheng, L., Ma, J., Li, G., & Su, L. (2018). Humanized mice engrafted with human HSC only or HSC and thymus support comparable HIV-1 replication, immunopathology, and responses to ART and immune therapy. *Frontiers in Immunology*, *9*(APR). https://doi.org/10.3389/fimmu.2018.00817

Cheng, L., Yu, H., Li, G., Li, F., Ma, J., Li, J., Chi, L., Zhang, L., & Su, L. (2017). Type I interferons suppress viral replication but contribute to T cell depletion and dysfunction during chronic HIV-1 infection. *Journal of Clinical Investigation*, *2*(12). https://doi.org/10.1172/jci.insight.94366

Cheng, L., Zhang, Z., Li, G., Li, F., Wang, L., Zhang, L., Zurawski, S. M., Zurawski, G., Levy, Y., & Su, L. (2017). Human innate responses and adjuvant activity of TLR ligands in vivo in mice reconstituted with a human immune system. *Vaccine*, *35*(45), 6143. https://doi.org/10.1016/J.VACCINE.2017.09.052

Chetty, S., Govender, P., Zupkosky, J., Pillay, M., Ghebremichael, M., Moosa, M. Y. S., Ndung'U, T., Porichis, F., & Kasprowicz, V. O. (2015). Co-Infection with Mycobacterium tuberculosis Impairs HIV-Specific CD8+ and CD4+ T Cell Functionality. *PLOS ONE*, *10*(3), e0118654.

https://doi.org/10.1371/JOURNAL.PONE.0118654

Cheynier, R., Gratton, S., Halloran, M., Stahmer, I., Letvin, N. L., & Wain-Hobson, S. (1998). Antigenic stimulation by BCG vaccine as an in vivo driving force for SIV replication and dissemination. *Nature Medicine*, *4*(4), 421–427. https://doi.org/10.1038/nm0498-421

Chihara, T., Hashimoto, M., Osman, A., Hiyoshi-Yoshidomi, Y., Suzu, I., Chutiwitoonchai, N., Hiyoshi, M., Okada, S., & Suzu, S. (2012). HIV-1 Proteins Preferentially Activate Anti-Inflammatory M2-Type Macrophages. *The Journal of Immunology*, *188*(8), 3620–3627. https://doi.org/10.4049/jimmunol.1101593

Choi, B., Chun, E., Kim, M., Kim, S. Y., Kim, S. T., Yoon, K., Lee, K. Y., & Kim, S. J. (2011). Human T cell development in the liver of humanized NOD/SCID/IL-2Rγnull(NSG) mice generated by intrahepatic injection of CD34+ human (h) cord blood (CB) cells. *Clinical Immunology*, *139*(3), 321–335. https://doi.org/10.1016/J.CLIM.2011.02.019

Choopanya, K., Martin, M., Suntharasamai, P., Sangkum, U., Mock, P. A., Leethochawalit, M., Chiamwongpaet, S., Kitisin, P., Natrujirote, P., Kittimunkong, S., Chuachoowong, R., Gvetadze, R. J., McNicholl, J. M., Paxton, L. A., Curlin, M. E., Hendrix, C. W., & Vanichseni, S. (2013). Antiretroviral prophylaxis for HIV infection in injecting drug users in Bangkok, Thailand (the Bangkok Tenofovir Study): a randomised, double-blind, placebo-controlled phase 3 trial. *Lancet (London, England)*, *381*(9883), 2083–2090. https://doi.org/10.1016/S0140-

6736(13)61127-7

Chua, B. Y., Wong, C. Y., Mifsud, E. J., Edenborough, K. M., Sekiya, T., Tan, A. C. L., Mercuri, F., Rockman, S., Chen, W., Turner, S. J., Doherty, P. C., Kelso, A., Brown, L. E., & Jackson, D. C. (2015). Inactivated influenza vaccine that provides rapid, innate-immune- system-mediated protection and subsequent long-term adaptive immunity. *MBio*, *6*(6). https://doi.org/10.1128/mBio.01024-15

Chua, J., Vergne, I., Master, S., & Deretic, V. (2004). A tale of two lipids: Mycobacterium tuberculosis phagosome maturation arrest. *Current Opinion in Microbiology*, *7*(1), 71–77. https://doi.org/10.1016/j.mib.2003.12.011

Cígler, P., Koz, M., ˇová, ezá, Brynda, J., Otwinowski, Z., Pokorná, J., Plešek, J., Grü ner, B., Dolečková -Marešová, L., Má ˇa, M., Sedlá ˇek, J., Bodem, J., Krä usslich, H.-G., Krá, V., & Konvalinka, J. (2005). *From nonpeptide toward noncarbon protease inhibitors: Metallacarboranes as specific and potent inhibitors of HIV protease*. www.rcsb.orgpdb

Clapp, D. W., Freie, B., Lee, W. H., & Zhang, Y. Y. (1995). Molecular Evidence That In Situ-Transduced Fetal Liver Hematopoietic Stem/Progenitor Cells Give Rise to Medullary Hematopoiesis in Adult Rats. *Blood*, *86*(6), 2113–2122. https://doi.org/10.1182/BLOOD.V86.6.2113.BLOODJOURNAL8662113

Colditz, G. A., Brewer, T. F., Berkey, C. S., Wilson, M. E., Burdick, E., Fineberg, H. V., & Mosteller, F. (1994). Efficacy of BCG Vaccine in the Prevention of Tuberculosis:

Meta-analysis of the Published Literature. *JAMA: The Journal of the American Medical Association*, *271*(9), 698–702. https://doi.org/10.1001/jama.1994.03510330076038

Coope, C., Gruber, J., Medina Lara, A., & Theobald, S. (2004). *Vulnerability to malaria, tuberculosis, and HIV/AIDS infection and disease. Part 1: Determinants operating at individual and household level*. https://doi.org/10.1016/S1473-3099(04)01002-3

Corbett, E. L., Watt, C. J., Walker, N., Maher, D., Williams, B. G., Raviglione, M. C., & Dye, C. (2003). The Growing Burden of Tuberculosis: Global Trends and Interactions With the HIV Epidemic. *Archives of Internal Medicine*, *163*(9), 1009–1021. https://doi.org/10.1001/ARCHINTE.163.9.1009

Corleis, B., Bucsan, A. N., Deruaz, M., Vrbanac, V. D., Lisanti-Park, A. C., Gates, S. J., Linder, A. H., Paer, J. M., Olson, G. S., Bowman, B. A., Schiff, A. E., Medoff, B. D., Tager, A. M., Luster, A. D., Khader, S. A., Kaushal, D., & Kwon, D. S. (2019). HIV-1 and SIV Infection Are Associated with Early Loss of Lung Interstitial CD4+ T Cells and Dissemination of Pulmonary Tuberculosis. *Cell Reports*, *26*(6), 1409-1418.e5. https://doi.org/10.1016/j.celrep.2019.01.021

Coughlan, A. M., Harmon, C., Whelan, S., O'Brien, E. C., O'Reilly, V. P., Crotty, P., Kelly, P., Ryan, M., Hickey, F. B., O'Farrelly, C., & Little, M. A. (2016). Myeloid engraftment in humanized mice: Impact of granulocyte-colony stimulating factor treatment and transgenic mouse strain. *Stem Cells and Development*, *25*(7), 530–541. https://doi.org/10.1089/scd.2015.0289

Cozmei, C., Constantinescu, D., Carasevici, E., Anisie, E., Ungureanu, D., Sorete-Arbore, A., Gramadă, D., Mihăescu, T., Croitoru, C., & Popa, D. (2007). Th1 and Th2 cytokine response in patients with pulmonary tuberculosis and health care workers occupationally exposed to M. tuberculosis. *Revista Medico-Chirurgicala a Societatii de Medici Si Naturalisti Din Iasi*, *111*(3), 702–709. https://europepmc.org/article/med/18293704

Cribbs, S. K., Lennox, J., Caliendo, A. M., Brown, L. A., & Guidot, D. M. (2015). Healthy HIV-1-infected individuals on highly active antiretroviral therapy harbor HIV-1 in their alveolar macrophages. *AIDS Research and Human Retroviruses*, *31*(1), 64–70. https://doi.org/10.1089/aid.2014.0133

Cunningham, A. L., Harman, A., & Nasr, N. (2013). Initial HIV mucosal infection and dendritic cells. *EMBO Molecular Medicine*, *5*(5), 658–660. https://doi.org/10.1002/EMMM.201202763

Currie, S., Rogstad, K. E., Piyadigamage, A., & Herman, S. (2009). Time taken to undetectable viral load, following the initiation of HAART. *International Journal of STD and AIDS*, *20*(4), 265–266. https://doi.org/10.1258/ijsa.2008.008268

D'Agostino, M. R., Lai, R., Afkhami, S., Khera, A., Yao, Y., Vaseghi-Shanjani, M., Zganiacz, A., Jeyanathan, M., & Xing, Z. (2020). Airway Macrophages Mediate Mucosal Vaccine–Induced Trained Innate Immunity against Mycobacterium tuberculosis in Early Stages of Infection . *The Journal of Immunology*, *205*(10), 2750–2762. https://doi.org/10.4049/jimmunol.2000532

da Glória Bonecini-Almeida, M., Werneck-Barroso, E., Baptista Carvalho, P., Pereira de Moura, C., Ferreira Andrade, E., Hafner, A., Eduardo Carvalho, C., Ho, J. L., nio Lineu Kritski, A., & Gonçalves Morgado, M. (1998). *Functional Activity of Alveolar and Peripheral Cells in Patients with Human Acquired Immunodeficiency Syndrome and Pulmonary Tuberculosis*.

Da Glória Bonecini-Almeida, M., Werneck-Barroso, E., Carvalho, P. B., De Moura, C. P., Andrade, E. F., Hafner, A., Carvalho, C. E., Ho, J. L., Kritski, A. L., & Morgado, M. G. (1998). Functional Activity of Alveolar and Peripheral Cells in Patients with Human Acquired Immunodeficiency Syndrome and Pulmonary Tuberculosis. *Cellular Immunology*, *190*(2), 112–120. https://doi.org/10.1006/CIMM.1998.1399

Dalgleish, A. G., Beverley, P. C. L., Clapham, P. R., Crawford, D. H., Greaves, M. F., & Weiss, R. A. (1984). The CD4 (T4) antigen is an essential component of the receptor for the AIDS retrovirus. *Nature*, *312*(5996), 763–767. https://doi.org/10.1038/312763a0

Danner, R., Chaudhari, S. N., Rosenberger, J., Surls, J., Richie, T. L., Brumeanu, T. D., & Casares, S. (2011). Expression of HLA class II molecules in humanized NOD.Rag1KO.IL2RgcKO mice is critical for development and function of human T and B cells. *PLoS ONE*, *6*(5). https://doi.org/10.1371/journal.pone.0019826

Darrah, P. A., Zeppa, J. J., Maiello, P., Hackney, J. A., Wadsworth, M. H., Hughes, T. K., Pokkali, S., Swanson, P. A., Grant, N. L., Rodgers, M. A., Kamath, M., Causgrove, C. M., Laddy, D. J., Bonavia, A., Casimiro, D., Lin, P. L., Klein, E., White, A. G.,

Scanga, C. A., … Seder, R. A. (2020). Prevention of tuberculosis in macaques after intravenous BCG immunization. *Nature*, *577*(7788), 95–102. https://doi.org/10.1038/s41586-019-1817-8

Davies, J. Q., & Gordon, S. (2005). Isolation and Culture of Human Macrophages. *Basic Cell Culture Protocols*, 105–116.

Dawson, R., Harris, K., Conradie, A., Burger, D., Murray, S., & Mendel, C. and Spigelman, M. (2017). Efficacy of bedaquiline, pretomanid, moxifloxacin & PZA (BPaMZ) against DS-& MDR-TB. *Conference on Retroviruses and Opportunistic Infections (CROI), CROI Foundation in Partnership with the International Antiviral Society-USA, Seattle, WA.* https://www.croiconference.org/wp-content/uploads/sites/2/posters/2017/724LB_Harris.pdf

Dawson, Rodney, Diacon, A. H., Everitt, D., Van Niekerk, C., Donald, P. R., Burger, D. A., Schall, R., Spigelman, M., Conradie, A., Eisenach, K., Venter, A., Ive, P., Page-Shipp, L., Variava, E., Reither, K., Ntinginya, N. E., Pym, A., Von Groote-Bidlingmaier, F., & Mendel, C. M. (2015). Efficiency and safety of the combination of moxifloxacin, pretomanid (PA-824), and pyrazinamide during the first 8 weeks of antituberculosis treatment: a phase 2b, open-label, partly randomised trial in patients with drug-susceptible or drug-resistant pulmonary tuberculosis. *The Lancet*, *385*(9979), 1738–1747. https://doi.org/10.1016/S0140-6736(14)62002-X

Day, C. L., Abrahams, D. A., Lerumo, L., Janse van Rensburg, E., Stone, L., O'rie, T., Pienaar, B., de Kock, M., Kaplan, G., Mahomed, H., Dheda, K., & Hanekom, W. A.

(2011). Functional Capacity of Mycobacterium tuberculosis -Specific T Cell Responses in Humans Is Associated with Mycobacterial Load . *The Journal of Immunology*, *187*(5), 2222–2232. https://doi.org/10.4049/jimmunol.1101122

Day, C. L., Tameris, M., Mansoor, N., Van Rooyen, M., De Kock, M., Geldenhuys, H., Erasmus, M., Makhethe, L., Hughes, E. J., Gelderbloem, S., Bollaerts, A., Bourguignon, P., Cohen., J., Demoitie, M. A., Mettens, P., Moris, P., Sadoff, J. C., Hawkridge, A., D. Hussey, G., … Hanekom, W. A. (2013). Induction and regulation of T-cell immunity by the novel tuberculosis vaccine M72/AS01 in South African adults. *American Journal of Respiratory and Critical Care Medicine*, *188*(4), 492–502. https://doi.org/10.1164/rccm.201208-1385OC

De Clercq, E. (2006). From adefovir to Atripla™ via tenofovir, Viread™ and Truvada™. *Future Virology*, *1*(6), 709–715. https://doi.org/10.2217/17460794.1.6.709

de Mendoza, C., Rodriguez, C., García, F., Eiros, J. M., Ruíz, L., Caballero, E., Aguilera, A., Leiva, P., Colomina, J., Gutierrez, F., del Romero, J., Aguero, J., & Soriano, V. (2007). Prevalence of X4 tropic viruses in patients recently infected with HIV-1 and lack of association with transmission of drug resistance. *Journal of Antimicrobial Chemotherapy*, *59*(4), 698–704. https://doi.org/10.1093/JAC/DKM012

de Noronha, A. L. L., Báfica, A., Nogueira, L., Barral, A., & Barral-Netto, M. (2008). Lung granulomas from Mycobacterium tuberculosis/HIV-1 co-infected patients display decreased in situ TNF production. *Pathology Research and Practice*, *204*(3), 155–161. https://doi.org/10.1016/j.prp.2007.10.008

Deeks, E. D., & Perry, C. M. (2010). Efavirenz/emtricitabine/tenofovir disoproxil fumarate single-tablet regimen (atripla®): A review of its use in the management of HIV infection. *Drugs*, *70*(17), 2315–2338. https://doi.org/10.2165/11203800-000000000-00000

Deng, H. K., Liu, R., Ellmeier, W., Choe, S., Unutmaz, D., Burkhart, M., Di Marzio, P., Marmon, S., Sutton, R. E., Mark Hill, C., Davis, C. B., Peiper, S. C., Schall, T. J., Littman, D. R., & Landau, N. R. (1996). Identification of a major co-receptor for primary isolates of HIV-1. *Nature 1996 381:6584*, *381*(6584), 661–666. https://doi.org/10.1038/381661a0

Denton, P. W., Estes, J. D., Sun, Z., Othieno, F. A., Wei, B. L., Wege, A. K., Powell, D. A., Payne, D., Haase, A. T., & Garcia, J. V. (2008). *Antiretroviral Pre-exposure Prophylaxis Prevents Vaginal Transmission of HIV-1 in Humanized BLT Mice*. *5*(1), e16. https://journals.plos.org/plosmedicine/article?id=10.1371/journal.pmed.0050016

Denton, P. W., Olesen, R., Choudhary, S. K., Archin, N. M., Wahl, A., Swanson, M. D., Chateau, M., Nochi, T., Krisko, J. F., Spagnuolo, R. A., Margolis, D. M., & Garcia, J. V. (2012). Generation of HIV Latency in Humanized BLT Mice. *Journal of Virology*, *86*(1), 630. https://doi.org/10.1128/JVI.06120-11

Dharmaraja, A. T., Alvala, M., Sriram, D., Yogeeswari, P., & Chakrapani, H. (2012). Design, synthesis and evaluation of small molecule reactive oxygen species generators as selective Mycobacterium tuberculosis inhibitors. *Chemical*

Communications, *48*(83), 10325–10327. https://doi.org/10.1039/C2CC35343A

Diedrich, C. R., Mattila, J. T., Klein, E., Janssen, C., Phuah, J., Sturgeon, T. J., Montelaro, R. C., Lin, P. L., & Flynn, J. A. L. (2010). Reactivation of Latent Tuberculosis in Cynomolgus Macaques Infected with SIV Is Associated with Early Peripheral T Cell Depletion and Not Virus Load. *PLOS ONE*, *5*(3), e9611. https://doi.org/10.1371/JOURNAL.PONE.0009611

Diedrich, C., Rutledge, T., Maiello, P., Baranowski, T., White, A., Borish, H. J., Karell, P., Hopkins, F., Brown, J., Fortune, S., Flynn, J., Ambrose, Z., & Lin, P. L. (2020). *SIV and Mycobacterium tuberculosis synergy within the granuloma accelerates the reactivation pattern of latent tuberculosis*. https://doi.org/10.1101/2020.02.21.959353

Dillon, S. M., Kibbie, J., Lee, E. J., Guo, K., Santiago, M. L., Austin, G. L., Gianella, S., Landay, A. L., Donovan, A. M., Frank, D. N., McCarter, M. D., & Wilson, C. C. (2017). Low abundance of colonic butyrate-producing bacteria in HIV infection is associated with microbial translocation and immune activation. *AIDS (London, England)*, *31*(4), 511–521. https://doi.org/10.1097/QAD.0000000000001366

Dragic, T., Litwin, V., Allaway, G. P., Martin, S. R., Huang, Y., Nagashima, K. A., Cayanan, C., Maddon, P. J., Koup, R. A., Moore, J. P., & Paxton, W. A. (1996). HIV-1 entry into CD4+ cells is mediated by the chemokine receptor CC-CKR-5. *Nature*, *381*(6584), 667–673. https://doi.org/10.1038/381667a0

Drake, A. C., Chen, Q., & Chen, J. (2012). Engineering humanized mice for improved hematopoietic reconstitution. In *Cellular and Molecular Immunology* (Vol. 9, Issue 3, pp. 215–224). Nature Publishing Group. https://doi.org/10.1038/cmi.2012.6

Dykstra, C., Lee, A. J., Lusty, E. J., Shenouda, M. M., Shafai, M., Vahedi, F., Chew, M. V., Collins, S., & Ashkar, A. A. (2016). Reconstitution of immune cell in liver and lymph node of adult- and newborn-engrafted humanized mice. *BMC Immunology*, *17*(1), 18. https://doi.org/10.1186/s12865-016-0157-9

eART-linc collaboration, S, W., M, E., R, R., KE, N., C, C., C, L., T, L., A, N., J, T., L, V. der P., A, M., & M, Z. (2008). Duration from seroconversion to eligibility for antiretroviral therapy and from ART eligibility to death in adult HIV-infected patients from low and middle-income countries: collaborative analysis of prospective studies. *Sexually Transmitted Infections*, *84 Suppl 1*(SUPPL. 1), i31–i36. https://doi.org/10.1136/STI.2008.029793

Ellis, J. M., Henson, V., Tidwell, R. S. S., Ng, J., Hartzman, R., & Hurley, C. K. (2000). Frequencies of HLA-A2 alleles in five U.S. population groups. Predominance Of A*02011 and identification of HLA-A*0231 | Request PDF. *Human Immunology*, *61*(3), 334–340. https://www.researchgate.net/publication/12626681_Frequencies_of_HLA-A2_alleles_in_five_US_population_groups_Predominance_Of_A02011_and_identification_of_HLA-A0231

Esmail, H., Riou, C., du Bruyn, E., Lai, R. P.-J., Harley, Y. X. R., Meintjes, G.,

Wilkinson, K. A., & Wilkinson, R. J. (2018). The Immune Response to Mycobacterium tuberculosis in HIV-1-Coinfected Persons . *Annual Review of Immunology*, *36*(1). https://doi.org/10.1146/annurev-immunol-042617-053420

Essien, S. K., Epp, T., Waldner, C., Wobeser, W., & Hoeppner, V. (2019). Tuberculosis in Canada and the United States: a review of trends from 1953 to 2015. *Canadian Journal of Public Health*, *110*(6), 697–704. https://doi.org/10.17269/s41997-019-00236-x

Fahey, J. L., Taylor, J. M. G., Manna, B., Nishanian, P., Aziz, N., Giorgi, J. V., & Detels, R. (1998). Prognostic significance of plasma markers of immune activation, HIV viral load and CD4 T-cell measurements. *Aids*, *12*(13), 1581–1590. https://doi.org/10.1097/00002030-199813000-00004

Fairfax, K. A., Kallies, A., Nutt, S. L., & Tarlinton, D. M. (2008). Plasma cell development: From B-cell subsets to long-term survival niches. *Seminars in Immunology*, *20*(1), 49–58. https://doi.org/10.1016/J.SMIM.2007.12.002

Fang, F. C. (2004). *ANTIMICROBIAL REACTIVE OXYGEN AND NITROGEN SPECIES: CONCEPTS AND CONTROVERSIES*. *2*. https://doi.org/10.1038/nrmicro1004

Faust, L., Schreiber, Y., & Bocking, N. (2019). A systematic review of BCG vaccination policies among high-risk groups in low TB-burden countries: implications for vaccination strategy in Canadian indigenous communities. *BMC Public Health*,

19(1). https://doi.org/10.1186/S12889-019-7868-9

Feng, J. Y., Ly, J. K., Myrick, F., Goodman, D., White, K. L., Svarovskaia, E. S., Borroto-Esoda, K., & Miller, M. D. (2009). The triple combination of tenofovir, emtricitabine and efavirenz shows synergistic anti-HIV-1 activity in vitro: A mechanism of action study. *Retrovirology*, *6*(1), 1–16. https://doi.org/10.1186/1742-4690-6-44/FIGURES/5

Feng, Y., Broder, C. C., Kennedy, P. E., & Berger, E. A. (1996). HIV-1 Entry Cofactor: Functional cDNA Cloning of a Seven-Transmembrane, G Protein-Coupled Receptor. *Science*, *272*(5263), 872–877. https://doi.org/10.1126/SCIENCE.272.5263.872

Feng, Y., Broder, C. C., Kennedy, P. E., & Berger, E. A. (2011). Pillars article: HIV-1 entry cofactor: functional cDNA cloning of a seven-transmembrane, G protein-coupled receptor. Science. 1996. 272: 872-877. *Journal of Immunology (Baltimore, Md. : 1950)*, *186*(11), 6076–6081. http://www.ncbi.nlm.nih.gov/pubmed/21597040%0Ahttp://www.pubmedcentral.nih.gov/articlerender.fcgi?artid=PMC3412311

Ferguson, M. R., Rojo, D. R., Von Lindern, J. J., & O'Brien, W. A. (2002). HIV-1 replication cycle. *Clinics in Laboratory Medicine*, *22*(3), 611–635. https://doi.org/10.1016/S0272-2712(02)00015-X

Ferrer, P., Tello, M., Montecinos, L., Tordecilla, R., Rodríguez, C., Beltrán, C., Guzmán, M. A., Ferrés, M., Pérez, C. M., & Afani, A. (2014). Prevalence of R5 and X4 HIV

variants in antiretroviral treatment experienced patients with virologic failure. *Journal of Clinical Virology : The Official Publication of the Pan American Society for Clinical Virology*, *60*(3), 290–294. https://doi.org/10.1016/J.JCV.2014.04.004

Fine, P. E. M. (1989). The BCG Story: Lessons from the Past and Implications for the Future. *Reviews of Infectious Diseases*, *11*(Supplement_2), S353–S359. https://doi.org/10.1093/clinids/11.Supplement_2.S353

Fong, Y., Shen, X., Ashley, V. C., Deal, A., Seaton, K. E., Yu, C., Grant, S. P., Ferrari, G., Decamp, A. C., Bailer, R. T., Koup, R. A., Montefiori, D., Haynes, B. F., Sarzotti-Kelsoe, M., Graham, B. S., Carpp, L. N., Hammer, S. M., Sobieszczyk, M., Karuna, S., … Tomaras, G. D. (2018). Modification of the Association Between T-Cell Immune Responses and Human Immunodeficiency Virus Type 1 Infection Risk by Vaccine-Induced Antibody Responses in the HVTN 505 Trial. *The Journal of Infectious Diseases*, *217*(8), 1280–1288. https://doi.org/10.1093/INFDIS/JIY008

Fonner, V. A., Dalglish, S. L., Kennedy, C. E., Baggaley, R., O'Reilly, K. R., Koechlin, F. M., Rodolph, M., Hodges-Mameletzis, I., & Grant, R. M. (2016). Effectiveness and safety of oral HIV preexposure prophylaxis for all populations. *AIDS (London, England)*, *30*(12), 1973. https://doi.org/10.1097/QAD.0000000000001145

Fouda, G. G., Yates, N. L., Pollara, J., Shen, X., Overman, G. R., Mahlokozera, T., Wilks, A. B., Kang, H. H., Salazar-Gonzalez, J. F., Salazar, M. G., Kalilani, L., Meshnick, S. R., Hahn, B. H., Shaw, G. M., Lovingood, R. V., Denny, T. N., Haynes, B., Letvin, N. L., Ferrari, G., … Immunology, the C. for H. V. (2011).

HIV-Specific Functional Antibody Responses in Breast Milk Mirror Those in Plasma and Are Primarily Mediated by IgG Antibodies. *Journal of Virology*, *85*(18), 9555. https://doi.org/10.1128/JVI.05174-11

Fourcade, L., Poudrier, J., & Roger, M. (2018). Natural Immunity to HIV: A Template for Vaccine Strategies. *Viruses 2018, Vol. 10, Page 215*, *10*(4), 215. https://doi.org/10.3390/V10040215

Franco, N. H., Correia-Neves, M., & Olsson, I. A. S. (2012). How "Humane" Is Your Endpoint?—Refining the Science-Driven Approach for Termination of Animal Studies of Chronic Infection. *PLOS Pathogens*, *8*(1), e1002399. https://doi.org/10.1371/JOURNAL.PPAT.1002399

Freed, E. 0, Myers, D. J., & Risser, R. (1990). Characterization of the fusion domain of the human immunodeficiency virus type 1 envelope glycoprotein gp4l (retrovirus/transmembrane/AIDS/syncytium). *Proc. Natl. Acad. Sci. USA*, *87*, 4650–4654.

Gallant, J. E., DeJesus, E., Arribas, J. R., Pozniak, A. L., Gazzard, B., Campo, R. E., Lu, B., McColl, D., Chuck, S., Enejosa, J., Toole, J. J., & Cheng, A. K. (2006). Tenofovir DF, Emtricitabine, and Efavirenz vs. Zidovudine, Lamivudine, and Efavirenz for HIV. *New England Journal of Medicine*, *354*(3), 251–260. https://doi.org/10.1056/nejmoa051871

Gallant, J., Lazzarin, A., Mills, A., Orkin, C., Podzamczer, D., Tebas, P., Girard, P. M.,

Brar, I., Daar, E. S., Wohl, D., Rockstroh, J., Wei, X., Custodio, J., White, K., Martin, H., Cheng, A., & Quirk, E. (2017). Bictegravir, emtricitabine, and tenofovir alafenamide versus dolutegravir, abacavir, and lamivudine for initial treatment of HIV-1 infection (GS-US-380-1489): a double-blind, multicentre, phase 3, randomised controlled non-inferiority trial. *The Lancet*, *390*(10107), 2063–2072. https://doi.org/10.1016/S0140-6736(17)32299-7

Gallo, R. C., Sarin, P. S., Gelmann, E. P., Robert-Guroff, M., Richardson, E., Kalyanaraman, V. S., Mann, D., Sidhu, G. D., Stahl, R. E., Zolla-Pazner, S., Leibowitch, J., & Popovic, M. (1983). Isolation of Human T-Cell Leukemia Virus in Acquired Immune Deficiency Syndrome (AIDS). *Science*, *220*(4599), 865–867. https://doi.org/10.1126/SCIENCE.6601823

García, F., De Lazzari, E., Plana, M., Castro, P., Mestre, G., Nomdedeu, M., Fumero, E., Martínez, E., Mallolas, J., Blanco, J. L., Miró, J. M., Pumarola, T., Gallart, T., & Gatell, J. M. (2004). Long-term CD4+ T-cell response to highly active antiretroviral therapy according to baseline CD4+ T-cell count. *Journal of Acquired Immune Deficiency Syndromes*, *36*(2), 702–713. https://doi.org/10.1097/00126334-200406010-00007

Gaschen, B., Taylor, J., Yusim, K., Foley, B., Gao, F., Lang, D., Novitsky, V., Haynes, B., Hahn, B. H., Bhattacharya, T., & Korber, B. (2002). Diversity considerations in HIV-1 vaccine selection. *Science*, *296*(5577), 2354–2360. https://doi.org/10.1126/science.1070441

Gelaw, Y. A., Williams, G., Soares Magalhães, R. J., Gilks, C. F., & Assefa, Y. (2019). HIV Prevalence Among Tuberculosis Patients in Sub-Saharan Africa: A Systematic Review and Meta-analysis. *AIDS and Behavior*, *23*(6), 1561–1575. https://doi.org/10.1007/S10461-018-02386-4/FIGURES/6

Geldmacher, C., Ngwenyama, N., Schuetz, A., Petrovas, C., Reither, K., Heeregrave, E. J., Casazza, J. P., Ambrozak, D. R., Louder, M., Ampofo, W., Pollakis, G., Hill, B., Sanga, E., Saathoff, E., Maboko, L., Roederer, M., Paxton, W. A., Hoelscher, M., & Koup, R. A. (2010). Preferential infection and depletion of Mycobacterium tuberculosis–specific CD4 T cells after HIV-1 infection. *Journal of Experimental Medicine*, *207*(13), 2869–2881. https://doi.org/10.1084/JEM.20100090

Gendelman, H. E., Poluektova, L. Y., Gebhart, C. L., Domm, W., Dewhurst, S., Gorantla, S., Makarov, E., & Finke-Dwyer, J. (2021). Immunopathology in Humanized Mice Cell Depletion Accelerates HIV-1 + CD8. *J Immunol*, *184*, 7082–7091. https://doi.org/10.4049/jimmunol.1000438

Gilbert, P. B., McKeague, I. W., Eisen, G., Mullins, C., Guéye-NDiaye, A., Mboup, S., & Kanki, P. J. (2003). Comparison of HIV-1 and HIV-2 infectivity from a prospective cohort study in Senegal. *Statistics in Medicine*, *22*(4), 573–593. https://doi.org/10.1002/SIM.1342

Gillespie, S. H. (2016). The role of moxifloxacin in tuberculosis therapy. In *European respiratory review : an official journal of the European Respiratory Society* (Vol. 25, Issue 139, pp. 19–28). https://doi.org/10.1183/16000617.0085-2015

Giorgi, J. V., Hultin, L. E., McKeating, J. A., Johnson, T. D., Owens, B., Jacobson, L. P., Shih, R., Lewis, J., Wiley, D. J., Phair, J. P., Wolinsky, S. M., & Detels, R. (1999). Shorter survival in advanced human immunodeficiency virus type 1 infection is more closely associated with T lymphocyte activation than with plasma virus burden or virus chemokine coreceptor usage. *Journal of Infectious Diseases*, *179*(4), 859–870. https://doi.org/10.1086/314660

Giorgi, J. V., Lyles, R. H., Matud, J. L., Yamashita, T. E., Mellors, J. W., Hultin, L. E., Jamieson, B. D., Margolick, J. B., Rinaldo, C. R., Phair, J. P., & Detels, R. (2002). Predictive value of immunologic and virologic markers after long or short duration of HIV-1 infection. *Journal of Acquired Immune Deficiency Syndromes*, *29*(4), 346–355. https://doi.org/10.1097/00126334-200204010-00004

Gluckman, E., Broxmeyer, H. E., Auerbach, A. D., Friedman, H. S., Douglas, G. W., Devergie, A., Esperou, H., Thierry, D., Socie, G., Lehn, P., Cooper, S., English, D., Kurtzberg, J., Bard, J., & Boyse, E. A. (1989). Hematopoietic Reconstitution in a Patient with Fanconi's Anemia by Means of Umbilical-Cord Blood from an HLA-Identical Sibling. *New England Journal of Medicine*, *321*(17), 1174–1178. https://doi.org/10.1056/nejm198910263211707

Golden, M. P., & Vikram, H. R. (2005). Extrapulmonary Tuberculosis: An Overview. *American Family Physician*, *72*(9), 1761–1768. www.aafp.org/afpAmericanFamilyPhysician1761

Gomez, C., & Hope, T. J. (2005). The ins and outs of HIV replication. *Cellular*

Microbiology, *7*(5), 621–626. https://doi.org/10.1111/j.1462-5822.2005.00516.x

Gootenberg, D. B., Paer, J. M., Luevano, J. M., & Kwon, D. S. (2017). HIV-associated changes in the enteric microbial community: potential role in loss of homeostasis and development of systemic inflammation. *Current Opinion in Infectious Diseases*, *30*(1), 31–43. https://doi.org/10.1097/QCO.0000000000000341

Gorantla, S., Sneller, H., Walters, L., Sharp, J. G., Pirruccello, S. J., West, J. T., Wood, C., Dewhurst, S., Gendelman, H. E., & Poluektova, L. (2007). Human Immunodeficiency Virus Type 1 Pathobiology Studied in Humanized BALB/c-Rag2 / c / Mice. *JOURNAL OF VIROLOGY*, *81*(6), 2700–2712. https://doi.org/10.1128/JVI.02010-06

Gottlieb, M. S., Schroff, R., Schanker, H. M., Weisman, J. D., Fan, P. T., Wolf, R. A., & Saxon, A. (1981). Pneumocystis carinii Pneumonia and Mucosal Candidiasis in Previously Healthy Homosexual Men . *New England Journal of Medicine*, *305*(24), 1425–1431. https://doi.org/10.1056/nejm198112103052401

Grabiec, A. M., & Hussell, T. (2016). The role of airway macrophages in apoptotic cell clearance following acute and chronic lung inflammation. *Seminars in Immunopathology*, *38*(4), 409. https://doi.org/10.1007/S00281-016-0555-3

Grant, R. M., Lama, J. R., Anderson, P. L., McMahan, V., Liu, A. Y., Vargas, L., Goicochea, P., Casapía, M., Guanira-Carranza, J. V., Ramirez-Cardich, M. E., Montoya-Herrera, O., Fernández, T., Veloso, V. G., Buchbinder, S. P.,

Chariyalertsak, S., Schechter, M., Bekker, L.-G., Mayer, K. H., Kallás, E. G., … Glidden, D. V. (2010). Preexposure Chemoprophylaxis for HIV Prevention in Men Who Have Sex with Men. *New England Journal of Medicine*, *363*(27), 2587–2599. https://doi.org/10.1056/NEJMOA1011205/SUPPL_FILE/NEJMOA1011205_DISCLOSURES.PDF

Green, A. M., DiFazio, R., & Flynn, J. L. (2013). IFN-γ from CD4 T Cells Is Essential for Host Survival and Enhances CD8 T Cell Function during Mycobacterium tuberculosis Infection . *The Journal of Immunology*, *190*(1), 270–277. https://doi.org/10.4049/jimmunol.1200061

Greenblatt, M. B., Vbranac, V., Tivey, T., Tsang, K., Tager, A. M., & Aliprantis, A. O. (2012). Graft versus Host Disease in the Bone Marrow, Liver and Thymus Humanized Mouse Model. *PLOS ONE*, *7*(9), e44664. https://doi.org/10.1371/JOURNAL.PONE.0044664

Grivel, J. C., & Margolis, L. B. (1999). CCR5-and CXCR4-tropic HIV-1 are equally cytopathic for their T-cell targets in human lymphoid tissue. *Nature Medicine*, *5*(3), 344–346. https://doi.org/10.1038/6565

Grobler, J. A., Dornadula, G., Rice, M. R., Simcoe, A. L., Hazuda, D. J., & Miller, M. D. (2007). HIV-1 Reverse Transcriptase Plus-strand Initiation Exhibits Preferential Sensitivity to Non-nucleoside Reverse Transcriptase Inhibitors in Vitro*. *Journal of Biological Chemistry*, *282*(11), 8005–8010. https://doi.org/10.1074/JBC.M608274200

Gulick, R. M., Mellors, J. W., Havlir, D., Eron, J. J., Gonzalez, C., McMahon, D., Richman, D. D., Valentine, F. T., Jonas, L., Meibohm, A., Emini, E. A., Chodakewitz, J. A., Deutsch, P., Holder, D., Schleif, W. A., & Condra, J. H. (1997). Treatment with Indinavir, Zidovudine, and Lamivudine in Adults with Human Immunodeficiency Virus Infection and Prior Antiretroviral Therapy. *New England Journal of Medicine*, *337*(11), 734–739. https://doi.org/10.1056/nejm199709113371102

Hammer, S. M., Squires, K. E., Hughes, M. D., Grimes, J. M., Demeter, L. M., Currier, J. S., Eron, J. J., Feinberg, J. E., Balfour, H. H., Deyton, L. R., Chodakewitz, J. A., Fischl, M. A., Phair, J. P., Pedneault, L., Nguyen, B.-Y., & Cook, J. C. (1997). A Controlled Trial of Two Nucleoside Analogues plus Indinavir in Persons with Human Immunodeficiency Virus Infection and CD4 Cell Counts of 200 per Cubic Millimeter or Less. *New England Journal of Medicine*, *337*(11), 725–733. https://doi.org/10.1056/nejm199709113371101

Harris, D. T., Badowski, M., Balamurugan, A., & Yang, O. O. (2013). Long-term human immune system reconstitution in non-obese diabetic (NOD)-Rag (–)-γ chain (–) (NRG) mice is similar but not identical to the original stem cell donor. *Clinical & Experimental Immunology*, *174*(3), 402–413. https://doi.org/10.1111/CEI.12192

Harris, T., Panaro, L., Phypers, M., Choudhri, Y., & Archibald, C. P. (2006). HIV testing among Canadian tuberculosis cases from 1997 to 1998. *Canadian Journal of Infectious Diseases and Medical Microbiology*, *17*(3), 165–168.

https://doi.org/10.1155/2006/321765

Hart, P. D. arc. (1967). Efficacy and Applicability of Mass B.C.G. Vaccination in Tuberculosis Control. *British Medical Journal*, *1*(5540), 587–592. https://doi.org/10.1136/bmj.1.5540.587

Hays, R. D., Cunningham, W. E., Sherbourne, C. D., Wilson, I. B., Wu, A. W., Cleary, P. D., McCaffrey, D. F., Fleishman, J. A., Crystal, S., Collins, R., Eggan, F., Shapiro, M. F., & Bozzette, S. A. (2000). Health-related quality of life in patients with human immunodeficiency virus infection in the United States: Results from the HIV cost and services utilization study. *American Journal of Medicine*, *108*(9), 714–722. https://doi.org/10.1016/S0002-9343(00)00387-9

Heather, J. M., Best, K., Oakes, T., Gray, E. R., Roe, J. K., Thomas, N., Friedman, N., Noursadeghi, M., & Chain, B. (2016). Dynamic perturbations of the T-Cell receptor repertoire in chronic HIV infection and following antiretroviral therapy. *Frontiers in Immunology*, *6*(JAN), 644. https://doi.org/10.3389/fimmu.2015.00644

Hernández-Pando, R., Jeyanathan, M., Mengistu, G., Aguilar, D., Orozco, H., Harboe, M., Rook, G. A. W., & Bjune, G. (2000). Persistence of DNA from Mycobacterium tuberculosis in superficially normal lung tissue during latent infection. *The Lancet*, *356*(9248), 2133–2138. https://doi.org/10.1016/S0140-6736(00)03493-0

Hirsch, C. S., Yoneda, T., Averill, L., Ellner, J. J., & Toossi, Z. (1994). Enhancement of intracellular growth of mycobacterium tuberculosis in human monocytes by

transforming growth factor-βl. *Journal of Infectious Diseases*, *170*(5), 1229–1237. https://doi.org/10.1093/infdis/170.5.1229

Hladik, F., & McElrath, M. J. (2008). Setting the stage: host invasion by HIV. *Nature Reviews Immunology 2008 8:6*, *8*(6), 447–457. https://doi.org/10.1038/nri2302

Hladik, F., Sakchalathorn, P., Ballweber, L., Lentz, G., Fialkow, M., Eschenbach, D., & McElrath, M. J. (2007). Initial Events in Establishing Vaginal Entry and Infection by Human Immunodeficiency Virus Type-1. *Immunity*, *26*(2), 257–270. https://doi.org/10.1016/j.immuni.2007.01.007

Honeycutt, J. B., Thayer, W. O., Baker, C. E., Ribeiro, R. M., Lada, S. M., Cao, Y., Cleary, R. A., Hudgens, M. G., Richman, D. D., & Victor Garcia, J. (2017). HIV persistence in tissue macrophages of humanized myeloid-only mice during antiretroviral therapy. *Nature Medicine*, *23*(5), 638–643. https://doi.org/10.1038/nm.4319

Honeycutt, J. B., Wahl, A., Baker, C., Spagnuolo, R. A., Foster, J., Zakharova, O., Wietgrefe, S., Caro-Vegas, C., Madden, V., Sharpe, G., Haase, A. T., Eron, J. J., & Garcia, J. V. (2016). Macrophages sustain HIV replication in vivo independently of T cells. *Journal of Clinical Investigation*, *126*(4), 1353–1366. https://doi.org/10.1172/JCI84456

Hsu, D. C., & O'Connell, R. J. (2017). Progress in HIV vaccine development. *Https://Doi.Org/10.1080/21645515.2016.1276138*, *13*(5), 1018–1030.

https://doi.org/10.1080/21645515.2016.1276138

Hu, Jianming, & Seeger, C. (1996). Expression and characterization of hepadnavirus reverse transcriptases. *Methods in Enzymology*, *275*, 195–208. https://doi.org/10.1016/S0076-6879(96)75013-9

Hu, Jinjie, Gardner, M. B., & Miller, C. J. (2000). Simian Immunodeficiency Virus Rapidly Penetrates the Cervicovaginal Mucosa after Intravaginal Inoculation and Infects Intraepithelial Dendritic Cells. In *JOURNAL OF VIROLOGY* (Vol. 74, Issue 13). http://jvi.asm.org/

Huang, Z., Luo, Q., Guo, Y., Chen, J., Xiong, G., Peng, Y., Ye, J., & Li, J. (2015). Mycobacterium tuberculosis-Induced Polarization of Human Macrophage Orchestrates the Formation and Development of Tuberculous Granulomas In Vitro. *PLOS ONE*, *10*(6), e0129744. https://doi.org/10.1371/JOURNAL.PONE.0129744

Huante, M. B., Saito, T. B., Nusbaum, R. J., Naqvi, K. F., Chauhan, S., Hunter, R. L., Actor, J. K., Rudra, J. S., Endsley, M. A., Lisinicchia, J. G., Gelman, B. B., & Endsley, J. J. (2020). Small Animal Model of Post-chemotherapy Tuberculosis Relapse in the Setting of HIV Co-infection. *Frontiers in Cellular and Infection Microbiology*, *10*, 150. https://doi.org/10.3389/FCIMB.2020.00150/BIBTEX

Hudig, D., Ewoldt, G. R., & Woodard, S. L. (1993). Proteases and lymphocyte cytotoxic killing mechanisms. *Current Opinion in Immunology*, *5*(1), 90–96. https://doi.org/10.1016/0952-7915(93)90086-8

Ingole, N. A., Sarkate, P. P., Paranjpe, S. M., Shinde, S. D., Lall, S. S., & Mehta, P. R. (2013). HIV-2 infection: Where are we today? *Journal of Global Infectious Diseases*, *5*(3), 110–113. https://doi.org/10.4103/0974-777X.116872

Ito, M., Hiramatsu, H., Kobayashi, K., Suzue, K., Kawahata, M., Hioki, K., Ueyama, Y., Koyanagi, Y., Sugamura, K., Tsuji, K., Heike, T., & Nakahata, T. (2002). NOD/SCID/γcnull mouse: An excellent recipient mouse model for engraftment of human cells. *Blood*, *100*(9), 3175–3182. https://doi.org/10.1182/blood-2001-12-0207

Jaiswal, S., Pazoles, P., Woda, M., Shultz, L. D., Greiner, D. L., Brehm, M. A., & Mathew, A. (2012). Enhanced humoral and HLA-A2-restricted dengue virus-specific T-cell responses in humanized BLT NSG mice. *Immunology*, *136*(3), 334–343. https://doi.org/10.1111/J.1365-2567.2012.03585.X

Jambo, K. C., Banda, D. H., Kankwatira, A. M., Sukumar, N., Allain, T. J., Heyderman, R. S., Russell, D. G., & Mwandumba, H. C. (2014). Small alveolar macrophages are infected preferentially by HIV and exhibit impaired phagocytic function. *Mucosal Immunology*, *7*(5), 1116–1126. https://doi.org/10.1038/mi.2013.127

Jambo, Kondwani C., Sepako, E., Fullerton, D. G., Mzinza, D., Glennie, S., Wright, A. K., Heyderman, R. S., & Gordon, S. B. (2011). Bronchoalveolar CD4+ T cell responses to respiratory antigens are impaired in HIV-infected adults. *Thorax*, *66*(5), 375–382. https://doi.org/10.1136/thx.2010.153825

Jamieson, B. D., Pang, S., Aldrovandi, G. M., Zha, J., & Zack, J. A. (1995). In vivo

pathogenic properties of two clonal human immunodeficiency virus type 1 isolates. *Journal of Virology*, *69*(10), 6259–6264. https://doi.org/10.1128/jvi.69.10.6259-6264.1995

Janes, H., Corey, L., Ramjee, G., Carpp, L. N., Lombard, C., Cohen, M. S., Gilbert, P. B., & Gray, G. E. (2018). Weighing the Evidence of Efficacy of Oral PrEP for HIV Prevention in Women in Southern Africa. *AIDS Research and Human Retroviruses*, *34*(8), 645. https://doi.org/10.1089/AID.2018.0031

Joag, Sanjay V., Li, Z., Foresman, L., Pinson, D. M., Raghavan, R., Zhuge, W., Adany, I., Wang, C., Jia, F., Sheffer, D., Ranchalis, J., Watson, A., & Narayan, O. (1997). Characterization of the pathogenic KU-SHIV model of acquired immunodeficiency syndrome in macaques. *AIDS Research and Human Retroviruses*, *13*(8), 635–645. https://doi.org/10.1089/aid.1997.13.635

Joag, S V, Li, Z., Foresman, L., Stephens, E. B., Zhao, L. J., Adany, I., Pinson, D. M., McClure, H. M., & Narayan, O. (1996). Chimeric simian/human immunodeficiency virus that causes progressive loss of CD4+ T cells and AIDS in pig-tailed macaques. *Journal of Virology*, *70*(5), 3189–3197. https://doi.org/10.1128/jvi.70.5.3189-3197.1996

Johnson, K. A., Hessol, N. A., Kohn, R., Nguyen, T. Q., Mara, E. S., Hsu, L., Scheer, S., & Cohen, S. E. (2019). HIV Seroconversion in the Era of Pharmacologic Prevention: A Case-Control Study at a San Francisco STD Clinic. *Journal of Acquired Immune Deficiency Syndromes*, *82*(2), 159–165.

https://doi.org/10.1097/QAI.0000000000002107

Johnston, M. I., & Fauci, A. S. (2011). HIV Vaccine Development — Improving on Natural Immunity. *New England Journal of Medicine*, *365*(10), 873–875. https://doi.org/10.1056/NEJMP1107621/SUPPL_FILE/NEJMP1107621_DISCLOSURES.PDF

Kagina, B. M. N., Abel, B., Scriba, T. J., Hughes, E. J., Keyser, A., Soares, A., Gamieldien, H., Sidibana, M., Hatherill, M., Gelderbloem, S., Mahomed, H., Hawkridge, A., Hussey, G., Kaplan, G., & Hanekom, W. A. (2010). Specific T cell frequency and cytokine expression profile do not correlate with protection against tuberculosis after bacillus Calmette-Guérin vaccination of newborns. *American Journal of Respiratory and Critical Care Medicine*, *182*(8), 1073–1079. https://doi.org/10.1164/rccm.201003-0334OC

Kalsdorf, B., Scriba, T. J., Wood, K., Day, C. L., Dheda, K., Dawson, R., Hanekom, W. A., Lange, C., & Wilkinson, R. J. (2009). HIV-1 infection impairs the bronchoalveolar T-cell response to mycobacteria. *American Journal of Respiratory and Critical Care Medicine*, *180*(12), 1262–1270. https://doi.org/10.1164/rccm.200907-1011OC

Kaplan, R., Hermans, S., Caldwell, J., Jennings, K., Bekker, L. G., & Wood, R. (2018). HIV and TB co-infection in the ART era: CD4 count distributions and TB case fatality in Cape Town. *BMC Infectious Diseases*, *18*(1), 1–9. https://doi.org/10.1186/S12879-018-3256-9/TABLES/4

Keller, G., Lacaud, G., & Robertson, S. (1999). Development of the hematopoietic system in the mouse. *Experimental Hematology*, *27*, 777–787.

Kessl, J. J., Jena, N., Koh, Y., Taskent-Sezgin, H., Slaughter, A., Feng, L., De Silva, S., Wu, L., Le Grice, S. F. J., Engelman, A., Fuchs, J. R., & Kvaratskhelia, M. (2012). Multimode, cooperative mechanism of action of allosteric HIV-1 integrase inhibitors. *Journal of Biological Chemistry*, *287*(20), 16801–16811. https://doi.org/10.1074/JBC.M112.354373/ATTACHMENT/307937F4-A08E-4F79-9E66-1B8463B74095/MMC1.PDF

Kim, J., Peachman, K. K., Jobe, O., Morrison, E. B., Allam, A., Jagodzinski, L., Casares, S. A., & Rao, M. (2017). Tracking Human Immunodeficiency Virus-1 Infection in the Humanized DRAG Mouse Model. *Frontiers in Immunology*, *0*(OCT), 1405. https://doi.org/10.3389/FIMMU.2017.01405

Kinchen, J. M., & Ravichandran, K. S. (2008). Phagosome maturation: going through the acid test. *Nature Reviews Molecular Cell Biology 2008 9:10*, *9*(10), 781–795. https://doi.org/10.1038/nrm2515

Kinniburgh, D., & Russell, N. H. (1993). Comparative study of CD34-positive cells and subpopulations in human umbilical cord blood and bone marrow. *Bone Marrow Transplantation*, *12*(5), 489–494. http://www.ncbi.nlm.nih.gov/pubmed/7507766

Klatzmann, D., Champagne, E., Chamaret, S., Gruest, J., Guetard, D., Hercend, T., Gluckman, J. C., & Montagnier, L. (1984). T-lymphocyte T4 molecule behaves as

the receptor for human retrovirus LAV. *Nature*, *312*(5996), 767–768. https://doi.org/10.1038/312767A0

Klein, E., & Flynn, J. L. (1999). Mice deficient in CD4 T cells have only transiently diminished levels of IFN-gamma, yet succumb to tuberculosis SIV TB coinfection View project B cells in TB in NHP View project. *Article in The Journal of Immunology*. https://www.researchgate.net/publication/13070529

Klimas, N., Koneru, A. O. B., & Fletcher, M. A. (2008). Overview of HIV. *Psychosomatic Medicine*, *70*(5), 523–530. https://doi.org/10.1097/PSY.0B013E31817AE69F

Korber, B. T., Foley, B., Gaschen, B., & Kuiken, C. (2001). *Epidemiological and Immunological Implications of the Global Variability of HIV-1*. 1–32. https://doi.org/10.1007/978-1-59259-110-7_1

Koyanagi, Y., Miles, S., Mitsuyasu, R. T., Merrill, J. E., Vinters, H. V., & Chen, I. S. Y. (1987). Dual Infection of the Central Nervous System by AIDS Viruses with Distinct Cellular Tropisms. *Science*, *236*(4803), 819–822. https://doi.org/10.1126/SCIENCE.3646751

Koziel, H., Eichbaum, Q., Kruskal, B. A., Pinkston, P., Rogers, R. A., Armstrong, M. Y. K., Richards, F. F., Rose, R. M., & Ezekowitz, R. A. B. (1998). Reduced binding and phagocytosis of Pneumocystis carinii by alveolar macrophages from persons infected with HIV-1 correlates with mannose receptor downregulation. *Journal of*

Clinical Investigation, *102*(7), 1332–1344. https://doi.org/10.1172/JCI560

Kramnik, I., Dietrich, W. F., Demant, P., & Bloom, B. R. (2000). Genetic control of resistance to experimental infection with virulent Mycobacterium tuberculosis. *Proceedings of the National Academy of Sciences of the United States of America*, *97*(15), 8560–8565. https://doi.org/10.1073/pnas.150227197

Kumar, S. N., Prasad, T. S., Narayan, P. A., & Muruganandhan, J. (2013). Granuloma with langhans giant cells: An overview. *Journal of Oral and Maxillofacial Pathology : JOMFP*, *17*(3), 420. https://doi.org/10.4103/0973-029X.125211

Kwant-Mitchell, A., Ashkar, A. A., & Rosenthal, K. L. (2009). Mucosal Innate and Adaptive Immune Responses against Herpes Simplex Virus Type 2 in a Humanized Mouse Model. *Journal of Virology*, *83*(20), 10664. https://doi.org/10.1128/JVI.02584-08

Kwant-Mitchell, A., Pek, E. A., Rosenthal, K. L., & Ashkar, A. A. (2009). Development of Functional Human NK Cells in an Immunodeficient Mouse Model with the Ability to Provide Protection against Tumor Challenge. *PLOS ONE*, *4*(12), e8379. https://doi.org/10.1371/JOURNAL.PONE.0008379

Labarthe, L., Henriquez, S., Lambotte, O., Di Santo, J. P., Le Grand, R., Pflumio, F., Arcangeli, M. L., Legrand, N., & Bourgeois, C. (2020). Frontline Science: Exhaustion and senescence marker profiles on human T cells in BRGSF-A2 humanized mice resemble those in human samples. *Journal of Leukocyte*

Biology, *107*(1), 27–42. https://doi.org/10.1002/JLB.5HI1018-410RR

Laurence, J. (1992). *AIDS and Other Manifestations of HIV Infection. Viral cofactors in the pathogenesis of HIV disease.* . Raven Press. https://books.google.ca/books?hl=en&lr=&id=MoTubA7IDGYC&oi=fnd&pg=PA113&dq=J.+Laurence,+Viral+cofactors+in+the+pathogenesis+of+HIV+disease,+in:+G.P.+Wormser+(Ed.),+AIDS+and+other+Manifestations+of+HIV+Infection,+second+ed,+Raven+Press,+New+York,+1992,+pp.+77–83.&ots=JGwb95IaUM&sig=4Xd_xXo2I-ziqhl2m4iZ1VQMTBo#v=onepage&q&f=false

Lawn, S D, Harries, A. D., Williams, B. G., Chaisson, R. E., Losina, E., De Cock, K. M., Wood, R., & Lawn, S. D. (2011). Antiretroviral therapy and the control of HIV-associated tuberculosis. Will ART do it? NIH Public Access. *Int J Tuberc Lung Dis*, *15*(5), 571–581. https://doi.org/10.5588/ijtld.10.0483

Lawn, Stephen D., Butera, S. T., & Shinnick, T. M. (2002). Tuberculosis unleashed: the impact of human immunodeficiency virus infection on the host granulomatous response to Mycobacterium tuberculosis. *Microbes and Infection*, *4*(6), 635–646. https://doi.org/10.1016/S1286-4579(02)01582-4

Lawn, Stephen D., Harries, A. D., Williams, B. G., Chaisson, R. E., Losina, E., De Cock, K. M., & Wood, R. (2011). Antiretroviral therapy and the control of HIV-associated tuberculosis. Will ART do it? *The International Journal of Tuberculosis and Lung Disease : The Official Journal of the International Union against Tuberculosis and*

Lung Disease, *15*(5), 571. https://doi.org/10.5588/IJTLD.10.0483

Lê-Bury, G., & Niedergang, F. (2018). Defective phagocytic properties of HIV-infected macrophages: How might they be implicated in the development of invasive Salmonella Typhimurium? In *Frontiers in Immunology* (Vol. 9, Issue MAR, p. 1). Frontiers Media S.A. https://doi.org/10.3389/fimmu.2018.00531

Lee, M. W., Jang, I. K., Yoo, K. H., Sung, K. W., & Koo, H. H. (2010). Stem and progenitor cells in human umbilical cord blood. *International Journal of Hematology*, *92*(1), 45–51. https://doi.org/10.1007/s12185-010-0619-4

Lerner, T. R., Carvalho-Wodarz, C. D. S., Repnik, U., Russell, M. R. G., Borel, S., DIedrich, C. R., Rohde, M., Wainwright, H., Collinson, L. M., Wilkinson, R. J., Griffiths, G., & Gutierrez, M. G. (2017). Lymphatic endothelial cells are a replicative niche for Mycobacterium tuberculosis. *The Journal of Clinical Investigation*, *126*(3), 1093–1108. https://doi.org/10.1172/JCI83379

Li, H., Wang, X. X., Wang, B., Fu, L., Liu, G., Lu, Y., Cao, M., Huang, H., & Javid, B. (2017). Latently and uninfected healthcare workers exposed to TB make protective antibodies against Mycobacterium tuberculosis. *Proceedings of the National Academy of Sciences of the United States of America*, *114*(19), 5023–5028. https://doi.org/10.1073/pnas.1611776114

Liao, W., Lin, J.-X., & Leonard, W. J. (2011). IL-2 Family Cytokines: New Insights into the Complex Roles of IL-2 as a Broad Regulator of T helper Cell Differentiation.

Curr Opin Immunol, *23*(5), 598–604. https://doi.org/10.1016/j.coi.2011.08.003

Lin, P. L., & Flynn, J. A. L. (2015). CD8 T cells and Mycobacterium tuberculosis infection. *Seminars in Immunopathology*, *37*(3), 239. https://doi.org/10.1007/S00281-015-0490-8

Lin, P. L., Pawar, S., Myers, A., Pegu, A., Fuhrman, C., Reinhart, T. A., Capuano, S. V., Klein, E., & Flynn, J. A. L. (2006). Early Events in Mycobacterium tuberculosis Infection in Cynomolgus Macaques. *Infection and Immunity*, *74*(7), 3790. https://doi.org/10.1128/IAI.00064-06

Lin, P. L., Rutledge, T., Green, A. M., Bigbee, M., Fuhrman, C., Klein, E., & Flynn, J. L. (2012). CD4 T cell depletion exacerbates acute mycobacterium tuberculosis while reactivation of latent infection is dependent on severity of tissue depletion in cynomolgus macaques. *AIDS Research and Human Retroviruses*, *28*(12), 1693–1702. https://doi.org/10.1089/aid.2012.0028

Long, R., & Boffa, J. (2010). High HIV-TB co-infection rates in marginalized populations: evidence from Alberta in support of screening TB patients for HIV. *Canadian Journal of Public Health. Revue Canadienne de Santé Publique*, *101*(3), 202–204. https://doi.org/10.1007/bf03404374

Loré, K., & Larsson, M. (2003). The role of dendritic cells in the pathogenesis of HIV-1 infection. *Apmis*, *111*(7–8), 776–788. https://doi.org/10.1034/j.1600-0463.2003.11107809.x

Lösslein, A. K., Lohrmann, F., Scheuermann, L., Gharun, K., Neuber, J., Kolter, J., Forde, A. J., Kleimeyer, C., Poh, Y. Y., Mack, M., Triantafyllopoulou, A., Dunlap, M. D., Khader, S. A., Seidl, M., Hölscher, A., Hölscher, C., Guan, X. L., Dorhoi, A., & Henneke, P. (2021). Monocyte progenitors give rise to multinucleated giant cells. *Nature Communications*, *12*(1), 1–22. https://doi.org/10.1038/s41467-021-22103-5

M.A. Pinto, C., & R.M. Carvalho, A. (2018). Efficacy of PEP on a HIV Epidemic Model with Latent Reservoir. *SSRN Electronic Journal*. https://doi.org/10.2139/SSRN.3273675

Maecker, H. T., & Trotter, J. (2006). Flow cytometry controls, instrument setup, and the determination of positivity. *Cytometry Part A*, *69A*(9), 1037–1042. https://doi.org/10.1002/CYTO.A.20333

Maglione, P. J., Xu, J., & Chan, J. (2007). B Cells Moderate Inflammatory Progression and Enhance Bacterial Containment upon Pulmonary Challenge with Mycobacterium tuberculosis . *The Journal of Immunology*, *178*(11), 7222–7234. https://doi.org/10.4049/jimmunol.178.11.7222

Majji, S., Wijayalath, W., Shashikumar, S., Brumeanu, T. D., & Casares, S. (2018). Humanized DRAGA mice immunized with Plasmodium falciparum sporozoites and chloroquine elicit protective pre-erythrocytic immunity. *Malaria Journal*, *17*(1), 1–13. https://doi.org/10.1186/S12936-018-2264-Y/FIGURES/6

Majji, S., Wijayalath, W., Shashikumar, S., Pow-Sang, L., Villasante, E., Brumeanu, T.

D., & Casares, S. (2016). *Differential effect of HLA class-I versus class-II transgenes on human T and B cell reconstitution and function in NRG mice OPEN*. https://doi.org/10.1038/srep28093

Manches, O., Frleta, D., & Bhardwaj, N. (2013). *Dendritic cells in progression and pathology of HIV infection Promiscuous role of DC in HIV infection*. https://doi.org/10.1016/j.it.2013.10.003

Manosuthi, W., Chottanapand, S., Thongyen, S., Chaovavanich, A., & Sungkanuparph, S. (2006). Survival rate and risk factors of mortality among HIV/tuberculosis-coinfected patients with and without antiretroviral therapy. *Journal of Acquired Immune Deficiency Syndromes*, *43*(1), 42–46. https://doi.org/10.1097/01.QAI.0000230521.86964.86

Mantilla-Beniers, N. B., & Gomes, M. G. M. (2009). Mycobacterial ecology as a modulator of tuberculosis vaccine success. *Theoretical Population Biology*, *75*(2–3), 142–152. https://doi.org/10.1016/J.TPB.2009.01.006

Mariani, R., Rasala, B. A., Rutter, G., Wiegers, K., Brandt, S. M., Kra¨usslich, H.-G., Kra¨usslich, K., And, †, & Landau, N. R. (2001). Mouse-Human Heterokaryons Support Efficient Human Immunodeficiency Virus Type 1 Assembly. *JOURNAL OF VIROLOGY*, *75*(7), 3141–3151. https://doi.org/10.1128/JVI.75.7.3141-3151.2001

Marino, S., Cilfone, N. A., Mattila, J. T., Linderman, J. J., Flynn, J. L., & Kirschner, D. E. (2015). Macrophage Polarization Drives Granuloma Outcome during

Mycobacterium tuberculosis Infection. *Infection and Immunity*, *83*(1), 324. https://doi.org/10.1128/IAI.02494-14

Marsden, M. D., & Zack, J. A. (2017). Humanized Mouse Models for Human Immunodeficiency Virus Infection. *Annual Review of Virology*, *4*(1), 393–412. https://doi.org/10.1146/annurev-virology-101416-041703

Mascola, J. R., Snyder, S. W., Weislow, O. S., Belay, S. M., Belshe, R. B., Schwartz, D. H., Clements, M. Lou, Dolin, R., Graham, B. S., Gorse, G. J., Keefer, M. C., McElrath, M. J., Walker, M. C., Wagner, K. F., McNeil, J. G., McCutchan, F. E., & Burke, D. S. (1996). Immunization with Envelope Subunit Vaccine Products Elicits Neutralizing Antibodies against Laboratory-Adapted but Not Primary Isolates of Human Immunodeficiency Virus Type 1. *The Journal of Infectious Diseases*, *173*(2), 340–348. https://doi.org/10.1093/INFDIS/173.2.340

Mayito, J., Andia, I., Belay, M., Jolliffe, D. A., Kateete, D. P., Reece, S. T., & Martineau, A. R. (2019). Anatomic and cellular niches for mycobacterium tuberculosis in latent tuberculosis infection. *Journal of Infectious Diseases*, *219*(5), 685–694. https://doi.org/10.1093/infdis/jiy579

Mayumi, M., Kuritani, T., Kubagawa, H., & Cooper, M. D. (1983). IgG subclass expression by human B lymphocytes and plasma cells: B lymphocytes precommitted to IgG subclass can be preferentially induced by polyclonal mitogens with T cell help. *The Journal of Immunology*, *130*(2), 671–677. http://www.jimmunol.org/content/130/2/671

Mcdougal, J. S., Kennedy, M. S., Sligh, J. M., Cort, S. P., Mawle, A., & Nicholson, J. K. A. (1986). Binding of HTLV-III/LAV to T4+ T Cells by a Complex of the 110K Viral Protein and the T4 Molecule. *Science*, *231*(4736), 382–385. https://doi.org/10.1126/SCIENCE.3001934

McShane, H. (2005). Co-infection with HIV and TB: Double Trouble. *International Journal of STD and AIDS*, *16*(2). https://doi.org/10.1258/0956462053057576

Meditz, A. L., Haas, M. K., Folkvord, J. M., Melander, K., Young, R., McCarter, M., MaWhinney, S., Campbell, T. B., Lie, Y., Coakley, E., Levy, D. N., & Connick, E. (2011). HLA-DR+ CD38+ CD4+ T Lymphocytes Have Elevated CCR5 Expression and Produce the Majority of R5-Tropic HIV-1 RNA In Vivo. *Journal of Virology*, *85*(19), 10189. https://doi.org/10.1128/JVI.02529-10

Mehra, S., Alvarez, X., Didier, P. J., Doyle, L. A., Blanchard, J. L., Lackner, A. A., & Kaushal, D. (2013). Granuloma Correlates of Protection Against Tuberculosis and Mechanisms of Immune Modulation by Mycobacterium tuberculosis. *The Journal of Infectious Diseases*, *207*(7), 1115–1127. https://doi.org/10.1093/INFDIS/JIS778

Meijerink, H., Indrati, A. R., van Crevel, R., Joosten, I., Koenen, H., & van der Ven, A. J. A. M. (2014). The number of CCR5 expressing CD4+ T lymphocytes is lower in HIV-infected long-term non-progressors with viral control compared to normal progressors: A cross-sectional study. *BMC Infectious Diseases*, *14*(1), 683. https://doi.org/10.1186/s12879-014-0683-0

Mendoza, M., Gunasekera, D., Pratt, K. P., Qiu, Q., Casares, S., & Brumeanu, T. D. (2020). The humanized DRAGA mouse (HLA-A2. HLA-DR4. RAG1 KO. IL-2R g c KO. NOD) establishes inducible and transmissible models for influenza type A infections. *Human Vaccines & Immunotherapeutics*, *16*(9), 2222–2237. https://doi.org/10.1080/21645515.2020.1713605

Messiaen, P., Wensing, A. M. J., Fun, A., Nijhuis, M., Brusselaers, N., & Vandekerckhove, L. (2013). Clinical Use of HIV Integrase Inhibitors: A Systematic Review and Meta-Analysis. *PLOS ONE*, *8*(1), e52562. https://doi.org/10.1371/JOURNAL.PONE.0052562

Mombaerts, P., Iacomini, J., Johnson, R. S., Herrup, K., Tonegawa, S., & Papaioannou, V. E. (1992). RAG-1-deficient mice have no mature B and T lymphocytes. *Cell*, *68*(5), 869–877. https://doi.org/10.1016/0092-8674(92)90030-G

Montaner, J., Guillemi, S., & Harris, M. (2015). Therapeutic Guidelines for Antiretroviral (ARV) Treatment of Adult HIV infection. *British Columbia Centre for Acesslence in HIV/AIDS*, *September*, 410–425. http://www.cfenet.ubc.ca/sites/default/files/uploads/Guidelines/bccfe-art-guidelines-Oct_14_2015.pdf

Moore, J. P., Trkola, A., & Dragic, T. (1997). Co-receptors for HIV-1 entry. *Current Opinion in Immunology*, *9*(4), 551–562. https://doi.org/10.1016/S0952-7915(97)80110-0

Moore, R. D., & Chaisson, R. E. (1999). Natural history of HIV infection in the era of combination antiretroviral therapy. *AIDS (London, England)*, *13*(14), 1933–1942. https://doi.org/10.1097/00002030-199910010-00017

Morrison, J., Pai, M., & Hopewell, P. C. (2008). *Review Tuberculosis and latent tuberculosis infection in close contacts of people with pulmonary tuberculosis in low-income and middle-income countries: a systematic review and meta-analysis*. 359. https://doi.org/10.1016/S1473

Moyle, G. J., Wildfire, A., Mandalia, S., Mayer, H., Goodrich, J., Whitcomb, J., & Gazzard, B. G. (2005). *Epidemiology and Predictive Factors for Chemokine Receptor Use in HIV-1 Infection.* https://academic.oup.com/jid/article/191/6/866/808045

Moylett, E. H., & Shearer, W. T. (2002). HIV: Clinical manifestations. *Journal of Allergy and Clinical Immunology*, *110*(1), 3–16. https://doi.org/10.1067/MAI.2002.125978

Münk, C., Brandt, S. M., Lucero, G., & Landau, N. R. (2002). A dominant block to HIV-1 replication at reverse transcription in simian cells. *Proceedings of the National Academy of Sciences of the United States of America*, *99*(21), 13843–13848. https://doi.org/10.1073/pnas.212400099

Muñoz-Barroso, I., Durell, S., Sakaguchi, K., Appella, E., & Blumenthal, R. (1998). Dilation of the human immunodeficiency virus-1 envelope glycoprotein fusion pore revealed by the inhibitory action of a synthetic peptide from gp41. *Journal of Cell*

Biology, *140*(2), 315–323. https://doi.org/10.1083/jcb.140.2.315

Muñoz-Barroso, I., Salzwedel, K., Hunter, E., & Blumenthal, R. (1999). Role of the Membrane-Proximal Domain in the Initial Stages of Human Immunodeficiency Virus Type 1 Envelope Glycoprotein-Mediated Membrane Fusion. *Journal of Virology*, *73*(7), 6089–6092. https://doi.org/10.1128/jvi.73.7.6089-6092.1999

Murray, L. W., Satti, I., Meyerowitz, J., Jones, M., Willberg, C. B., Ussher, J. E., Goedhals, D., Hurst, J., Phillips, R. E., McShane, H., van Vuuren, C., & Frater, J. (2018). Human immunodeficiency virus infection impairs Th1 and Th17 mycobacterium tuberculosis–specific T-Cell responses. *Journal of Infectious Diseases*, *217*(11), 1782–1792. https://doi.org/10.1093/infdis/jiy052

Mwandumba, H. C., Russell, D. G., Nyirenda, M. H., Anderson, J., White, S. A., Molyneux, M. E., & Squire, S. B. (2004). Mycobacterium tuberculosis Resides in Nonacidified Vacuoles in Endocytically Competent Alveolar Macrophages from Patients with Tuberculosis and HIV Infection . *The Journal of Immunology*, *172*(7), 4592–4598. https://doi.org/10.4049/jimmunol.172.7.4592

Naif, H. M. (2013). Pathogenesis of HIV infection. *Infectious Disease Reports*, *5*(SUPPL.1), 26–30. https://doi.org/10.4081/idr.2013.s1.e6

Namale, P. E., Abdullahi, L. H., Fine, S., Kamkuemah, M., Wilkinson, R. J., & Meintjes, G. (2015). Paradoxical TB-IRIS in HIV-infected adults: A systematic review and meta-analysis. In *Future Microbiology* (Vol. 10, Issue 6, pp. 1077–1099). Future

Medicine Ltd. https://doi.org/10.2217/fmb.15.9

Naqvi, K. F., Huante, M. B., Saito, T., Chauhan, S., Walker, A., Lisinicchia, J., Gelman, B., & Endsley, J. J. (2018). Targeting the inflammasome as host directed therapy for Mycobacterium tuberculosis and HIV co-infection. *The Journal of Immunology*, *200*(1 Supplement).

Nguyen, P. V., Wessels, J. M., Mueller, K., Vahedi, F., Anipindi, V., Verschoor, C. P., Chew, M., Deshiere, A., Karniychuk, U., Mazzulli, T., Tremblay, M. J., Ashkar, A. A., & Kaushic, C. (2017). Frequency of Human CD45+ Target Cells is a Key Determinant of Intravaginal HIV-1 Infection in Humanized Mice. *Scientific Reports*, *7*(1). https://doi.org/10.1038/s41598-017-15630-z

Nicas, M., Nazaroff, W. W., & Hubbard, A. (2005). Toward understanding the risk of secondary airborne infection: Emission of respirable pathogens. *Journal of Occupational and Environmental Hygiene*, *2*(3), 143–154. https://doi.org/10.1080/15459620590918466

Nusbaum, R., Huante, M., Sutjita, P., Calderon, V., Vijayakumar, S., Aronson, J., Hunter, R., Actor, J., Cirillo, J., Valbuena, G., & Endsley, J. (2015). HIV-1 promotes neutrophil infiltration and lung damage in humanized mice co-infected with Mycobacterium tuberculosis (HUM1P.266). *The Journal of Immunology*, *194*(1 Supplement).

Nusbaum, R. J., Calderon, V. E., Huante, M. B., Sutjita, P., Vijayakumar, S., Lancaster,

K. L., Hunter, R. L., Actor, J. K., Cirillo, J. D., Aronson, J., Gelman, B. B., Lisinicchia, J. G., Valbuena, G., & Endsley, J. J. (2016). Pulmonary Tuberculosis in Humanized Mice Infected with HIV-1. *Scientific Reports*, *6*. https://doi.org/10.1038/srep21522

Ocheretyaner, E. R., Yusuff, J., & Park, T. E. (2019). Immunologic and virologic responses to antiretroviral therapy in treatment-naïve, HIV-infected elderly patients. *International Journal of STD and AIDS*, *30*(13), 1304–1310. https://doi.org/10.1177/0956462419872857

Okwundu, C. I., Uthman, O. A., & Okoromah, C. A. (2012). Antiretroviral pre-exposure prophylaxis (PrEP) for preventing HIV in high-risk individuals. *Cochrane Database of Systematic Reviews*, *7*. https://doi.org/10.1002/14651858.CD007189.PUB3/MEDIA/CDSR/CD007189/IMAGE_N/NCD007189-CMP-003-02.PNG

Ottop, F. M., Assob, J. C. N., Robinson Enow, M. B. U., & Ngowe, M. N. (2020). Trimestral Evaluation of the Impact of Highly Active Antiretroviral Therapy on the Viral Load, Liver and Kidney Function Tests of Hiv Pregnant Women in the East Region of Cameroon. *European Journal of Biomedical*, *7*(10), 520–525. www.ejbps.com520

Pastore, C., Ramos, A., & Mosier, D. E. (2004). Intrinsic Obstacles to Human Immunodeficiency Virus Type 1 Coreceptor Switching. *Journal of Virology*, *78*(14), 7565. https://doi.org/10.1128/JVI.78.14.7565-7574.2004

Pawlowski, A., Jansson, M., Sköld, M., Rottenberg, M. E., & Källenius, G. (2012). Tuberculosis and HIV co-infection. *PLoS Pathogens*, *8*(2), 1–7. https://doi.org/10.1371/journal.ppat.1002464

Pearson, T., Shultz, L. D., Miller, D., King, M., Laning, J., Fodor, W., Cuthbert, A., Burzenski, L., Gott, B., Lyons, B., Foreman, O., Rossini, A. A., & Greiner, D. L. (2008). Non-obese diabetic-recombination activating gene-1 (NOD-Rag1 null) interleukin (IL)-2 receptor common gamma chain (IL2rγnull) null mice: A radioresistant model for human lymphohaematopoietic engraftment. *Clinical and Experimental Immunology*, *154*(2), 270–284. https://doi.org/10.1111/j.1365-2249.2008.03753.x

Penn, M. L., Grivel, J.-C., Schramm, B., Goldsmith, M. A., & Margolis, L. (1999). CXCR4 utilization is sufficient to trigger CD4 T cell depletion in HIV-1-infected human lymphoid tissue. *National Institutes of Health*, *96*, 663–668. www.pnas.org.

Pethe, K., Swenson, D. L., Alonso, S., Anderson, J., Wang, C., & Russell, D. G. (2004). *Isolation of Mycobacterium tuberculosis mutants defective in the arrest of phagosome maturation*. *101*(37). www.pnas.orgcgidoi10.1073pnas.0401657101

PHAC. (2017). Tuberculosis: Monitoring. *Government of Canada*. https://www.canada.ca/en/public-health/services/diseases/tuberculosis/surveillance.html#a1

PHAC. (2018). Estimates of HIV incidence, prevalence and Canada's progress on

meeting the 90-90-90 HIV targets. *Government of Canada*. https://www.canada.ca/en/public-health/services/publications/diseases-conditions/summary-estimates-hiv-incidence-prevalence-canadas-progress-90-90-90.html#s8

Phuah, J., Wong, E. A., Gideon, H. P., Maiello, P., Coleman, M. T., Hendricks, M. R., Ruden, R., Cirrincione, L. R., Chan, J., Lin, P. L., & Flynn, J. A. L. (2016). Effects of B Cell Depletion on Early Mycobacterium tuberculosis Infection in Cynomolgus Macaques. *Infection and Immunity*, *84*(5), 1301. https://doi.org/10.1128/IAI.00083-16

Pieper, K., Grimbacher, B., & Eibel, H. (2013). B-cell biology and development. *Journal of Allergy and Clinical Immunology*, *131*(4), 959–971. https://doi.org/10.1016/j.jaci.2013.01.046

Pinto, C. M. A., Ana, A. R., Baleanu, D., & Srivastava, H. M. (2019). Efficacy of the Post-Exposure Prophylaxis and of the HIV Latent Reservoir in HIV Infection. *Mathematics 2019, Vol. 7, Page 515*, *7*(6), 515. https://doi.org/10.3390/MATH7060515

Plotkin, S. A. (2010). Correlates of Protection Induced by Vaccination. *CLINICAL AND VACCINE IMMUNOLOGY*, *17*(7), 1055–1065. https://doi.org/10.1128/CVI.00131-10

Podack, E. R., DING-E YOUNGt, J., & COHNt, Z. A. (1985). Isolation and biochemical

and functional characterization of perforin 1 from cytolytic T-cell granules (T lymphocytes/cell-mediated cytolysis/polymerization/transmembrane channels/patch-clamp). *Proc. Nati. Acad. Sci. USA*, *82*, 8629–8633.

Pollom, E., Dang, K. K., Potter, E. L., Gorelick, R. J., Burch, C. L., Weeks, K. M., & Swanstrom, R. (2013). Comparison of SIV and HIV-1 Genomic RNA Structures Reveals Impact of Sequence Evolution on Conserved and Non-Conserved Structural Motifs. *PLOS Pathogens*, *9*(4), e1003294. https://doi.org/10.1371/JOURNAL.PPAT.1003294

Ponnighaus, J. M., Msosa, E., Gruer, P. J. K., Liomba, N. G., Fine, P. E. M., Sterne, J. A. C., Wilson, R. J., Bliss, L., Jenkins, P. A., & Lucas, S. B. (1992). Efficacy of BCG vaccine against leprosy and tuberculosis in northern Malawi. *The Lancet*, *339*(8794), 636–639. https://doi.org/10.1016/0140-6736(92)90794-4

Quispe Calla, N. E., Vicetti Miguel, R. D., Glick, M. E., Kwiek, J. J., Gabriel, J. M., & Cherpes, T. L. (2018). Exogenous oestrogen inhibits genital transmission of cell-associated HIV-1 in DMPA-treated humanized mice. *Journal of the International AIDS Society*, *21*(1), e25063. https://doi.org/10.1002/jia2.25063

Ralls, K., Frankham, R., & Ballou, J. D. (2013). Inbreeding and Outbreeding. *Encyclopedia of Biodiversity: Second Edition*, *4*, 245–252. https://doi.org/10.1016/B978-0-12-384719-5.00073-3

Reddy, P., Birkett, R., & Mestan, K. (2020). Hyperoxia-induced lung engraftment of

human cord blood monocytes in a humanized mouse model of bronchopulmonary dysplasia. *Ann & Robert H Lurie Children's Hospital of Chicago/ Northwestern University Feinberg School of Medicine/ Neonatology*.

Reeves, J. D., Gallo, S. A., Ahmad, N., Miamidian, J. L., Harvey, P. E., Sharron, M., Pö, S., Sfakianos, J. N., Derdeyn, C. A., Blumenthal, R., Hunter, E., & Doms, R. W. (2002). Sensitivity of HIV-1 to entry inhibitors correlates with envelopecoreceptor affinity, receptor density, and fusion kinetics. *National Institutes of Health, 256*. www.pnas.orgcgidoi10.1073pnas.252469399

Reimann, K. A., Li, J. T., Veazey, R., Halloran, M., Park, I.-W., Karlsson, G. B., Sodroski, J., & Letvin, N. L. (1996). A Chimeric Simian/Human Immunodeficiency Virus Expressing a Primary Patient Human Immunodeficiency Virus Type 1 Isolate env Causes an AIDS-Like Disease after In Vivo Passage in Rhesus Monkeys. *JOURNAL OF VIROLOGY*, *70*(10), 6922–6928.

Reimann, K. A., Watson, A., Dailey, P. J., Lin, W., Lord, C. I., Steenbeke, T. D., Parker, R. A., Axthelm, M. K., & Karlsson, G. B. (1999). Viral burden and disease progression in rhesus monkeys infected with chimeric simian-human immunodeficiency viruses. *Virology*, *256*(1), 15–21. https://doi.org/10.1006/viro.1999.9632

Riou, C., Bunjun, R., Müller, T. L., Kiravu, A., Ginbot, Z., Oni, T., Goliath, R., Wilkinson, R. J., & Burgers, W. A. (2016). Selective reduction of IFN-γ single positive mycobacteria-specific CD4+ T cells in HIV-1 infected individuals with

latent tuberculosis infection. *Tuberculosis*, *101*, 25–30. https://doi.org/10.1016/j.tube.2016.07.018

Salinger, D. H., Subramoney, V., Everitt, D., & Nedelman, J. R. (2019). *Population Pharmacokinetics of the Antituberculosis Agent Pretomanid*. https://doi.org/10.1128/AAC

Sarzotti-Kelsoe, M., Bailer, R. T., Turk, E., Lin, C. li, Bilska, M., Greene, K. M., Gao, H., Todd, C. A., Ozaki, D. A., Seaman, M. S., Mascola, J. R., & Montefiori, D. C. (2014). Optimization and validation of the TZM-bl assay for standardized assessments of neutralizing antibodies against HIV-1. In *Journal of Immunological Methods* (Vol. 409, pp. 131–146). Elsevier. https://doi.org/10.1016/j.jim.2013.11.022

Scanga, C. A., Mohan, V. P., Yu, K., Joseph, H., Tanaka, K., Chan, J., & Flynn, J. A. L. (2000). Depletion of CD4+ T cells causes reactivation of murine persistent tuberculosis despite continued expression of interferon γ and nitric oxide synthase 2. *Journal of Experimental Medicine*, *192*(3), 347–358. https://doi.org/10.1084/jem.192.3.347

Scarlatti, G., Tresoldi, E., Bjorndal, A., Fredriksson, R., Colognesi, C., Hong Kui Deng, Malnati, M. S., Plebani, A., Siccardi, A. G., Littman, D. R., Fenyo, E. M., & Lusso, P. (1997). In vivo evolution of HIV-1 co-receptor usage and sensitivity to chemokine-mediated suppression. *Nature Medicine 1997 3:11*, *3*(11), 1259–1265. https://doi.org/10.1038/nm1197-1259

Schenten, D., & Medzhitov, R. (2011). The Control of Adaptive Immune Responses by the Innate Immune System. *Advances in Immunology*, *109*, 87–124. https://doi.org/10.1016/B978-0-12-387664-5.00003-0

Schiff, A. E., Linder, A. H., Luhembo, S. N., Banning, S., Deymier, M. J., Diefenbach, T. J., Dickey, A. K., Tsibris, A. M., Balazs, A. B., Cho, J. L., Medoff, B. D., Walzl, G., Wilkinson, R. J., Burgers, W. A., Corleis, B., & Kwon, D. S. (2021). T cell-tropic HIV efficiently infects alveolar macrophages through contact with infected CD4+ T cells. *Scientific Reports*, *11*(1), 3890. https://doi.org/10.1038/s41598-021-82066-x

Scholl, P. R., & Geha, R. S. (1994). MHC class II signaling in B-cell activation. *Immunology Today*, *15*(9), 418–422. https://doi.org/10.1016/0167-5699(94)90271-2

Schweighardt, B., Roy, A.-M., Meiklejohn, D. A., Grace, E. J., Moretto, W. J., Heymann, J. J., & Nixon, D. F. (2004). R5 Human Immunodeficiency Virus Type 1 (HIV-1) Replicates More Efficiently in Primary CD4+ T-Cell Cultures Than X4 HIV-1. *Journal of Virology*, *78*(17), 9164–9173. https://doi.org/10.1128/jvi.78.17.9164-9173.2004

Sharma, A., Wu, W., Sung, B., Huang, J., Tsao, T., Li, X., Gomi, R., Tsuji, M., & Worgall, S. (2016). Respiratory Syncytial Virus (RSV) Pulmonary Infection in Humanized Mice Induces Human Anti-RSV Immune Responses and Pathology. *Journal of Virology*, *90*(10), 5068. https://doi.org/10.1128/JVI.00259-16

Shaw, G. M., & Hunter, E. (2012). HIV transmission. *Cold Spring Harbor Perspectives*

in Medicine, *2*(11). https://doi.org/10.1101/cshperspect.a006965

Shehu-Xhilaga, M., Crowe, S. M., & Mak, J. (2001). Maintenance of the Gag/Gag-Pol Ratio Is Important for Human Immunodeficiency Virus Type 1 RNA Dimerization and Viral Infectivity. *Journal of Virology*, *75*(4), 1834–1841. https://doi.org/10.1128/jvi.75.4.1834-1841.2001

Shi, L., Jiang, Q., Bushkin, Y., Subbian, S., & Tyagi, S. (2019). *Biphasic Dynamics of Macrophage Immunometabolism during Mycobacterium tuberculosis Infection*. https://doi.org/10.1128/mBio

Shultz, L. D., Brehm, M. A., Victor Garcia-Martinez, J., & Greiner, D. L. (2012). Humanized mice for immune system investigation: Progress, promise and challenge. *Nature Reviews. Immunology*, *12*(11), 786. /pmc/articles/PMC3749872/

Shultz, L. D., Lyons, B. L., Burzenski, L. M., Gott, B., Chen, X., Chaleff, S., Kotb, M., Gillies, S. D., King, M., Mangada, J., Greiner, D. L., & Handgretinger, R. (2005). Human Lymphoid and Myeloid Cell Development in NOD/LtSz- scid IL2R γ null Mice Engrafted with Mobilized Human Hemopoietic Stem Cells . *The Journal of Immunology*, *174*(10), 6477–6489. https://doi.org/10.4049/jimmunol.174.10.6477

Shultz, L. D., Saito, Y., Najima, Y., Tanaka, S., Ochi, T., Tomizawa, M., Doi, T., Sone, A., Suzuki, N., Fujiwara, H., Yasukawa, M., & Ishikawa, F. (2010). Generation of functional human T-cell subsets with HLA-restricted immune responses in HLA class I expressing NOD/SCID/IL2rγnull humanized mice. *Proceedings of the*

National Academy of Sciences of the United States of America, *107*(29), 13022–13027. https://doi.org/10.1073/pnas.1000475107

Singh, A. K., & Gupta, U. D. (2018). Animal models of tuberculosis: Lesson learnt. *Indian Journal of Medical Research*, *147*(May), 456–463. https://doi.org/10.4103/ijmr.IJMR_554_18

Singh, S. K., Andersson, A. M., Ellegård, R., Lindestam Arlehamn, C. S., Sette, A., Larsson, M., Stendahl, O., & Blomgran, R. (2016). HIV Interferes with Mycobacterium tuberculosis Antigen Presentation in Human Dendritic Cells. *American Journal of Pathology*, *186*(12), 3083–3093. https://doi.org/10.1016/j.ajpath.2016.08.003

Singh, S. K., Larsson, M., Schön, T., Stendahl, O., & Blomgran, R. (2019). HIV Interferes with the Dendritic Cell–T Cell Axis of Macrophage Activation by Shifting Mycobacterium tuberculosis –Specific CD4 T Cells into a Dysfunctional Phenotype . *The Journal of Immunology*, *202*(3), 816–826. https://doi.org/10.4049/jimmunol.1800523

Skelton, J. K., Ortega-Prieto, A. M., & Dorner, M. (2018). A Hitchhiker's guide to humanized mice: new pathways to studying viral infections. In *Immunology* (Vol. 154, Issue 1, pp. 50–61). Blackwell Publishing Ltd. https://doi.org/10.1111/imm.12906

Skelton, J. K., Ortega-Prieto, A. M., Kaye, S., Manuel Jimenez-Guardeño, J., Turner, J.,

Malim, M. H., Towers, G. J., & Dorner, M. (2019). *Kinetics of Early Innate Immune Activation during HIV-1 Infection of Humanized Mice*. https://doi.org/10.1128/JVI

Song, Y., Gbyli, R., Fu, X., & Halene, S. (2020). Functional analysis of human hematopoietic stem cells in vivo in humanized mice. *Methods in Molecular Biology*, *2097*, 273–289. https://doi.org/10.1007/978-1-0716-0203-4_18

Sonntag, K., Eckert, F., Welker, C., Müller, H., Müller, F., Zips, D., Sipos, B., Klein, R., Blank, G., Feuchtinger, T., Schumm, M., Handgretinger, R., & Schilbach, K. (2015). Chronic graft-versus-host-disease in CD34+-humanized NSG mice is associated with human susceptibility HLA haplotypes for autoimmune disease. *Journal of Autoimmunity*, *62*, 55–66. https://doi.org/10.1016/j.jaut.2015.06.006

Stafford, J. L., Neumann, N. F., & Belosevic, M. (2002). Macrophage-mediated innate host defense against protozoan parasites. In *Critical Reviews in Microbiology* (Vol. 28, Issue 3, pp. 187–248). Informa Healthcare. https://doi.org/10.1080/1040-840291046731

Stephens, E. B., Joag, S. V., Sheffer, D., Liu, Z. Q., Zhao, L., Mukherjee, S., Foresman, L., Adany, I., Li, Z., Pinson, D., & Narayan, O. (1996). Initial characterization of viral sequences from a SHIV-inoculated pig-tailed macaque that developed AIDS. *Journal of Medical Primatology*, *25*(3), 175–185. https://doi.org/10.1111/J.1600-0684.1996.TB00014.X

Sun-Wada, G. H., Tabata, H., Kawamura, N., Aoyama, M., & Wada, Y. (2009). Direct

recruitment of H+-ATPase from lysosomes for phagosomal acidification. *Journal of Cell Science*, *122*(14), 2504–2513. https://doi.org/10.1242/JCS.050443

Sun, Z., Denton, P. W., Estes, J. D., Othieno, F. A., Wei, B. L., Wege, A. K., Melkus, M. W., Padgett-Thomas, A., Zupancic, M., Haase, A. T., & Garcia, J. V. (2007). Intrarectal transmission, systemic infection, and CD4+ T cell depletion in humanized mice infected with HIV-1. *Journal of Experimental Medicine*, *204*(4), 705–714. https://doi.org/10.1084/jem.20062411

Sutherland, I., & Springett, V. H. (1987). Effectiveness of BCG vaccination in england and wales in 1983. *Tubercle*, *68*(2), 81–92. https://doi.org/10.1016/0041-3879(87)90023-7

Szántó, S., Bárdos, T., Szabó, Z., David, C. S., Buzás, E. I., Mikecz, K., & Glant, T. T. (2004). Induction of arthritis in HLA–DR4–humanized and HLA–DQ8–humanized mice by human cartilage proteoglycan aggrecan but only in the presence of an appropriate (non-MHC) genetic background. *Arthritis & Rheumatism*, *50*(6), 1984–1995. https://doi.org/10.1002/ART.20285

Taft, R. A., Davisson, M., & Wiles, M. V. (2006). Know thy mouse. *Trends in Genetics*, *22*(12), 649–653. https://doi.org/10.1016/j.tig.2006.09.010

Takatsu', K. (1997). *Cytokines Involved in B-Cell Differentiation and Their Sites of Action (44119)*. 2151. https://doi.org/10.5010

Taneja, V., & David, C. S. (2010). Role of HLA class II genes in susceptibility/resistance

to inflammatory arthritis: studies with humanized mice. *Immunological Reviews*, *233*(1), 62–78. https://doi.org/10.1111/J.0105-2896.2009.00858.X

Tersmette, M., De Goede, R. E. Y., Lange, J. M. A., De Wolf, F., Eeftink-Schattenkerk, J. K. M., Schellekens, P. T. A., Coutinho, R. A., Goudsmit, J., Huisman, J. G., & Miedema, F. (1989). ASSOCIATION BETWEEN BIOLOGICAL PROPERTIES OF HUMAN IMMUNODEFICIENCY VIRUS VARIANTS AND RISK FOR AIDS AND AIDS MORTALITY. *The Lancet*, *333*(8645), 983–985. https://doi.org/10.1016/S0140-6736(89)92628-7

Thongcharoen, P., Suriyanon, V., Paris, R. M., Khamboonruang, C., De Souza, M. S., Ratto-Kim, S., Karnasuta, C., Polonis, V. R., Baglyos, L., Habib, R. El, Gurunathan, S., Barnett, S., Brown, A. E., Birx, D. L., McNeil, J. G., & Kim, J. H. (2007). A phase 1/2 comparative vaccine trial of the safety and immunogenicity of a CRF01_AE (subtype E) candidate vaccine: ALVAC-HIV (vCP1521) prime with oligomeric gp160 (92TH023/LAI-DID) or bivalent gp120 (CM235/SF2) boost. *Journal of Acquired Immune Deficiency Syndromes*, *46*(1), 48–55. https://doi.org/10.1097/QAI.0B013E3181354BD7

Toossi, Z., & Ellner, J. J. (1998). The role of TGFβ in the pathogenesis of human tuberculosis. In *Clinical Immunology and Immunopathology* (Vol. 87, Issue 2, pp. 107–114). Academic Press Inc. https://doi.org/10.1006/clin.1998.4528

Trottier, B., Lake, J. E., Logue, K., Brinson, C., Santiago, L., Brennan, C., Koteff, J. A., Wynne, B., Hopking, J., Granier, C., & Aboud, M. (2017).

Dolutegravir/abacavir/lamivudine versus current ART in virally suppressed patients (STRIIVING): a 48-week, randomized, non-inferiority, open-label, Phase IIIb study. *Antiviral Therapy*, *22*(4), 295–305. https://doi.org/10.3851/IMP3166

Turner, C. T., Brown, J., Shaw, E., Uddin, I., Tsaliki, E., Roe, J. K., Pollara, G., Sun, Y., Heather, J. M., Lipman, M., Chain, B., & Noursadeghi, M. (2021). Persistent T Cell Repertoire Perturbation and T Cell Activation in HIV After Long Term Treatment. *Frontiers in Immunology*, *12*. https://doi.org/10.3389/fimmu.2021.634489

Tweed, C. D., Dawson, R., Burger, D. A., Conradie, A., Crook, A. M., Mendel, C. M., Conradie, F., Diacon, A. H., Ntinginya, N. E., Everitt, D. E., Haraka, F., Li, M., van Niekerk, C. H., Okwera, A., Rassool, M. S., Reither, K., Sebe, M. A., Staples, S., Variava, E., & Spigelman, M. (2019). Bedaquiline, moxifloxacin, pretomanid, and pyrazinamide during the first 8 weeks of treatment of patients with drug-susceptible or drug-resistant pulmonary tuberculosis: a multicentre, open-label, partially randomised, phase 2b trial. *The Lancet Respiratory Medicine*, *7*(12), 1048–1058. https://doi.org/10.1016/S2213-2600(19)30366-2

Uittenbogaart, C. H., Anisman, D. J., Jamieson, B. D., Kitchen, S., Schmid, I., Zack, J. A., & Hays, E. F. (1996). Differential tropism of HIV-1 isolates for distinct thymocyte subsets in vitro. *AIDS (London, England)*, *10*(7). https://doi.org/10.1097/00002030-199606001-00001

UNAIDS. (2020). *Prevailing against pandemics by putting people at the centre: World AIDS Day Report 2020.*

https://www.unaids.org/en/resources/documents/2020/prevailing-against-pandemics

Uppal, S. S., Tewari, S. C., Verma, S., & Dhot, P. S. (2004). Comparison of CD4 and CD8 lymphocyte counts in HIV-negative pulmonary TB patients with those in normal blood donors and the effect of antitubercular treatment: Hospital-based flow cytometric study. *Cytometry*, *61B*(1), 20–26. https://doi.org/10.1002/cyto.b.20018

Vanshylla, K., Held, K., Eser, T. M., Gruell, H., Kleipass, F., Stumpf, R., Jain, K., Weiland, D., Münch, J., Grüttner, B., Geldmacher, C., & Klein, F. (2021). Cd34t+ humanized mouse model to study mucosal hiv-1 transmission and prevention. *Vaccines*, *9*(3), 1–16. https://doi.org/10.3390/vaccines9030198

Veazey, R. S., Mansfield, K. G., Tham, I. C., Carville, A. C., Shvetz, D. E., Forand, A. E., & Lackner, A. A. (2000). Dynamics of CCR5 Expression by CD4+ T Cells in Lymphoid Tissues during Simian Immunodeficiency Virus Infection. *Journal of Virology*, *74*(23), 11001–11007. https://doi.org/10.1128/jvi.74.23.11001-11007.2000

Venturini, E., Lodi, L., Francolino, I., Ricci, S., Chiappini, E., de Martino, M., & Galli, L. (2019). Cd3, cd4, cd8, cd19 and cd16/cd56 positive cells in tuberculosis infection and disease: Peculiar features in children. *International Journal of Immunopathology and Pharmacology*, *33*, 205873841984024. https://doi.org/10.1177/2058738419840241

Verma, B., & Wesa, A. (2020). Establishment of Humanized Mice from Peripheral Blood Mononuclear Cells or Cord Blood CD34+ Hematopoietic Stem Cells for Immune-

Oncology Studies Evaluating New Therapeutic Agents. *Current Protocols in Pharmacology*, *89*(1), e77. https://doi.org/10.1002/cpph.77

Verrall, A. J., Alisjahbana, B., Apriani, L., Novianty, N., Nurani, A. C., Van Laarhoven, A., Ussher, J. E., Indrati, A., Ruslami, R., Netea, M. G., Sharples, K., Van Crevel, R., & Hill, P. C. (2020). Early Clearance of Mycobacterium tuberculosis: The INFECT Case Contact Cohort Study in Indonesia. *The Journal of Infectious Diseases*, *221*(8), 1351–1360. https://doi.org/10.1093/INFDIS/JIZ168

Verrall, A. J., G. Netea, M., Alisjahbana, B., Hill, P. C., & van Crevel, R. (2014). Early clearance of Mycobacterium tuberculosis: A new frontier in prevention. *Immunology*, *141*(4), 506–513. https://doi.org/10.1111/imm.12223

Via, L. E., England, K., Weiner, D. M., Schimel, D., Zimmerman, M. D., Dayao, E., Chen, R. Y., Dodd, L. E., Richardson, M., Robbins, K. K., Cai, Y., Hammoud, D., Herscovitch, P., Dartois, V., Flynn, J. L., Barry, C. E., & III. (2015). A Sterilizing Tuberculosis Treatment Regimen Is Associated with Faster Clearance of Bacteria in Cavitary Lesions in Marmosets. *Antimicrobial Agents and Chemotherapy*, *59*(7), 4181. https://doi.org/10.1128/AAC.00115-15

Vierboom, M. P. M., Dijkman, K., Sombroek, C. C., Hofman, S. O., Boot, C., Vervenne, R. A. W., Haanstra, K. G., van der Sande, M., van Emst, L., Domínguez-Andrés, J., Moorlag, S. J. C. F. M., Kocken, C. H. M., Thole, J., Rodríguez, E., Puentes, E., Martens, J. H. A., van Crevel, R., Netea, M. G., Aguilo, N., … Verreck, F. A. W. (2021). Stronger induction of trained immunity by mucosal BCG or MTBVAC

vaccination compared to standard intradermal vaccination. *Cell Reports Medicine*, *2*(1). https://doi.org/10.1016/j.xcrm.2020.100185

Volk, V., Schneider, A., Spineli, L. M., Grosshennig, A., & Stripecke, R. (2016). *The gender gap: discrepant human T-cell reconstitution after cord blood stem cell transplantation in humanized female and male mice*. https://doi.org/10.1038/bmt.2015.290

Vordermeier, H. M., Venkataprasad, N., Harris, D. P., & Ivanyi, J. (1996). Increase of tuberculous infection in the organs of B cell-deficient mice. *Clinical & Experimental Immunology*, *106*(2), 312–316. https://doi.org/10.1046/J.1365-2249.1996.D01-845.X

Vudattu, N. K., Waldron-Lynch, F., Truman, L. A., Deng, S., Preston-Hurlburt, P., Torres, R., Raycroft, M. T., Mamula, M. J., & Herold, K. C. (2014). Humanized Mice as a Model for Aberrant Responses in Human T Cell Immunotherapy. *The Journal of Immunology*, *193*(2), 587–596. https://doi.org/10.4049/jimmunol.1302455

Walter, N. D., Born, S. E. M., Robertson, G. T., Reichlen, M., Dide-Agossou, C., Ektnitphong, V. A., Rossmassler, K., Ramey, M. E., Bauman, A. A., Ozols, V., Bearrows, S. C., Schoolnik, G., Dolganov, G., Garcia, B., Musisi, E., Worodria, W., Huang, L., Davis, J. L., Nguyen, N. V., … Voskuil, M. I. (2021). Mycobacterium tuberculosis precursor rRNA as a measure of treatment-shortening activity of drugs and regimens. *Nature Communications 2021 12:1*, *12*(1), 1–11. https://doi.org/10.1038/s41467-021-22833-6

Wang, S., Wu, J., Chen, J., Gao, Y., Zhang, S., Zhou, Z., Huang, H., Shao, L., Jin, J., Zhang, Y., & Zhang, W. (2018). Evaluation of Mycobacterium tuberculosis-specific antibody responses for the discrimination of active and latent tuberculosis infection. *International Journal of Infectious Diseases*, *70*, 1–9. https://doi.org/10.1016/j.ijid.2018.01.007

Warner, D. F., & Mizrahi, V. (2007). The survival kit of Mycobacterium tuberculosis. In *Nature Medicine* (Vol. 13, Issue 3, pp. 282–284). Nature Publishing Group. https://doi.org/10.1038/nm0307-282

Weiss, L., Donkova-Petrini, V., Caccavelli, L., Le Balbo, M., Dric Carbonneil, C., & Levy, Y. (2004). *Human immunodeficiency virus-driven expansion of CD4 CD25 regulatory T cells, which suppress HIV-specific CD4 T-cell responses in HIV-infected patients*. https://doi.org/10.1182/blood-2004-01-0365

Wessels, J. M., Nguyen, P. V., Vitali, D., Mueller, K., Vahedi, F., Felker, A. M., Dupont, H. A., Bagri, P., Verschoor, C. P., Deshiere, A., Mazzulli, T., Tremblay, M. J., Ashkar, A. A., & Kaushic, C. (2021). Depot medroxyprogesterone acetate (DMPA) enhances susceptibility and increases the window of vulnerability to HIV-1 in humanized mice. *Scientific Reports*, *11*(1), 3894. https://doi.org/10.1038/s41598-021-83242-9

West, E. E., Youngblood, B., Tan, W. G., Jin, H. T., Araki, K., Alexe, G., Konieczny, B. T., Calpe, S., Freeman, G. J., Terhorst, C., Haining, W. N., & Ahmed, R. (2011). Tight Regulation of Memory CD8+ T Cells Limits Their Effectiveness during

Sustained High Viral Load. *Immunity*, *35*(2), 285–298. https://doi.org/10.1016/J.IMMUNI.2011.05.017

WHO. (2010). *COMMERCIAL SERODIAGNOSTIC TESTS FOR DIAGNOSIS OF TUBERCULOSIS: EXPERT GROUP MEETING REPORT*. file:///C:/Users/acer/Downloads/WHO_HTM_TB_2011.14_eng.pdf

WHO. (2018). Weekly epidemiological record Relevé épidémiologique hebdomadaire. *WHO Position Paper*. http://www.who.int/immunization/sage/

WHO. (2019). Update of recommendations on first- and second-line antiretroviral regimens. Geneva, Switzerland:World Health Organization; *Who*, *July*, 3. http://www.who.int/hiv/pub/arv/arv-update-2019-policy/en/%0Afile:///C:/Users/Harrison/Downloads/WHO-CDS-HIV-19.15-eng.pdf

WHO. (2020a). *HIV/AIDS Facts Sheet.* https://www.who.int/news-room/fact-sheets/detail/hiv-aids

WHO. (2020b). *Tuberculosis Facts Sheet*. https://www.who.int/news-room/fact-sheets/detail/tuberculosis

WHO. (2021). *Global Tuberculosis Report 2021: TB Research and Innovation*. *7*.

Wolber, F. M., Leonard, E., Michael, S., Orschell-Traycoff, C. M., Yoder, M. C., & Srour, E. F. (2002). Roles of spleen and liver in development of the murine hematopoietic system. *Experimental Hematology*, *30*(9), 1010–1019. https://doi.org/10.1016/S0301-472X(02)00881-0

Wolf, A. J., Desvignes, L., Linas, B., Banaiee, N., Tamura, T., Takatsu, K., & Ernst, J. D. (2008). Initiation of the adaptive immune response to Mycobacterium tuberculosis depends on antigen production in the local lymph node, not the lungs. *Journal of Experimental Medicine*, *205*(1), 105–115. https://doi.org/10.1084/jem.20071367

Wolff, M. J., Giganti, M. J., Cortes, C. P., Cahn, P., Grinsztejn, B., Pape, J. W., Padgett, D., Sierra-Madero, J., Gotuzzo, E., Duda, S. N., McGowan, C. C., & Shepherd, B. E. (2017). A decade of HAART in Latin America: Long term outcomes among the first wave of HIV patients to receive combination therapy. *PLoS ONE*, *12*(6), e0179769. https://doi.org/10.1371/journal.pone.0179769

Wu, L., & KewalRamani, V. N. (2006). Dendritic-cell interactions with HIV: Infection and viral dissemination. *Nature Reviews Immunology*, *6*(11), 859–868. https://doi.org/10.1038/nri1960

Yao, Y., Lai, R., Afkhami, S., Haddadi, S., Zganiacz, A., Vahedi, F., Ashkar, A. A., Kaushic, C., Jeyanathan, M., & Xing, Z. (2017). Enhancement of Antituberculosis Immunity in a Humanized Model System by a Novel Virus-Vectored Respiratory Mucosal Vaccine. *Journal of Infectious Diseases*, *216*(1), 135–145. https://doi.org/10.1093/infdis/jix252

Yin, Y., Qin, J., Dai, Y., Zeng, F., Pei, H., & Wang, J. (2015). The CD4+/CD8+ ratio in pulmonary tuberculosis: Systematic and meta-analysis article. In *Iranian Journal of Public Health* (Vol. 44, Issue 2, pp. 185–193). Iranian Journal of Public Health. http://ijph.tums.ac.ir

Yu, J.-J., Goluguri, T., Guentzel, M. N., Chambers, J. P., Murthy, A. K., Klose, K. E., Forsthuber, T. G., & Arulanandam, B. P. (2010). Francisella tularensis T-Cell Antigen Identification Using Humanized HLA-DR4 Transgenic Mice. *CLINICAL AND VACCINE IMMUNOLOGY*, *17*(2), 215–222. https://doi.org/10.1128/CVI.00361-09

Yu, Y. R. A., Hotten, D. F., Malakhau, Y., Volker, E., Ghio, A. J., Noble, P. W., Kraft, M., Hollingsworth, J. W., Gunn, M. D., & Tighe, R. M. (2016). Flow cytometric analysis of myeloid cells in human blood, bronchoalveolar lavage, and lung tissues. *American Journal of Respiratory Cell and Molecular Biology*, *54*(1), 13–24. https://doi.org/10.1165/rcmb.2015-0146OC

Zennou, V., Mammano, F., Paulous, S., Mathez, D., & Clavel, F. (1998). Loss of Viral Fitness Associated with Multiple Gag and Gag-Pol Processing Defects in Human Immunodeficiency Virus Type 1 Variants Selected for Resistance to Protease Inhibitors In Vivo. *Journal of Virology*, *72*(4), 3300. https://doi.org/10.1128/jvi.72.4.3300-3306.1998

Zevin, A. S., McKinnon, L., Burgener, A., & Klatt, N. R. (2016). Microbial translocation and microbiome dysbiosis in HIV-associated immune activation. *Current Opinion in HIV and AIDS*, *11*(2), 182–190. https://doi.org/10.1097/COH.0000000000000234

Zhao, J., Siddiqui, S., Shang, S., Bian, Y., Bagchi, S., He, Y., & Wang, C.-R. (2015). *Mycolic acid-specific T cells protect against Mycobacterium tuberculosis infection in a humanized transgenic mouse model*. https://doi.org/10.7554/eLife.08525.001

Zheng, J., Liu, Y., Liu, Y., Liu, M., Xiang, Z., Lam, K. T., Lewis, D. B., Lau, Y. L., & Tu, W. (2013). Human CD8+ regulatory T cells inhibit GVHD and preserve general immunity in humanized mice. *Science Translational Medicine*, *5*(168). https://doi.org/10.1126/SCITRANSLMED.3004943/SUPPL_FILE/5-168RA9_SM.PDF

Zhu, T., Mo, H., Wang, N., Nam, D. S., Cao, Y., Koup, R. A., & Ho, D. D. (1993). Genotypic and Phenotypic Characterization of HIV-1 Patients with Primary Infection. *Science*, *261*(5125), 1179–1181. https://doi.org/10.1126/SCIENCE.8356453

Zicari, S., Sessa, L., Cotugno, N., Ruggiero, A., Morrocchi, E., Concato, C., Rocca, S., Zangari, P., Manno, E. C., & Palma, P. (2019). Immune Activation, Inflammation, and Non-AIDS Co-Morbidities in HIV-Infected Patients under Long-Term ART. *Viruses 2019, Vol. 11, Page 200*, *11*(3), 200. https://doi.org/10.3390/V11030200

Zwahlen, M., & Egger, M. (2006). *Progression and mortality of untreated HIV-positive individuals living in resource-limited settings: Update of literature review and evidence synthesis UNAIDS Obligation HQ/05/422204*. http://www.epidem.org